The Abdus Salam International Centre for Theoretical Physics

2443-26

Winter College on Optics: Trends in Laser Development and Multidisciplinary Applications to Science and Industry

4 - 15 February 2013

Phase retrieval techniques

M. Kujawinska
WUT
Poland

Winter College on Optics, ICTP, February 2013

Phase retrieval techniques

Malgorzata Kujawinska

Warsaw University of Technology, Poland
m.kujawinska@mchtr.pw.edu.pl

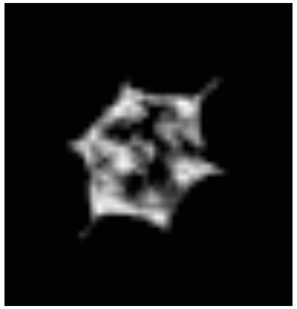

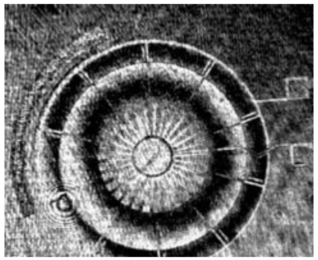

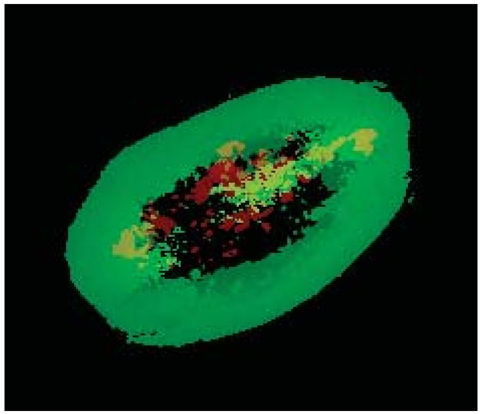


Political Map of Europe
YourEuropeMap.com
is sponsored by
pocket-talk.org
Your Free Travel Dictionaries!
ICELAND
NORWAY
SWEDEN
FINLAND
RUSSIA
ESTONIA
LATVIA
LITHUANIA
DENMARK
IRELAND
UNITED KINGDOM
BELORUSSIA
KAZAKHSTAN
THE NETHERLANDS
GERMANY
POLAND
BELGIUM
UKRAINE
CZECH REPUBLIC
SLOVAKIA
MOLDAVIA
FRANCE
AUSTRIA
HUNGARY
SWITZERLAND
ROMANIA
GEORGIA
AZERBAIJAN
SLOVENIA
CROATIA
ARMENIA
ITALY
BOSNIA & HER.
SERBIA
IRAN
BULGARIA
KOSOVO
MACE-DONIA
TURKEY
PORTUGAL
SPAIN
ALBANIA
GREECE
SYRIA
IRAQ
CYPRUS
ALGERIA
TUNESIA

Warsaw University of Technology

Localization

Warsaw

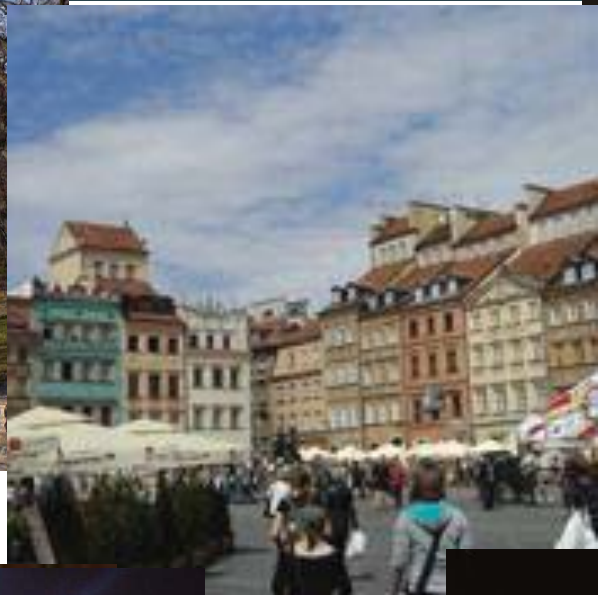

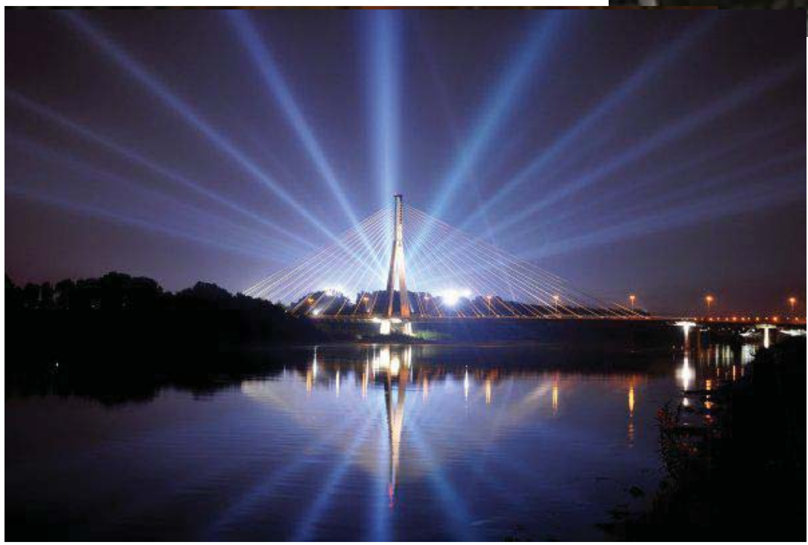

Warsaw University of Technology

www.pw.edu.pl

Warsaw University of Technology

- Biggest technical university in Polan
- 2000 acad. teachers,30000 students,
- 20 faculties

Photonics at
Faculty of Mechatronics

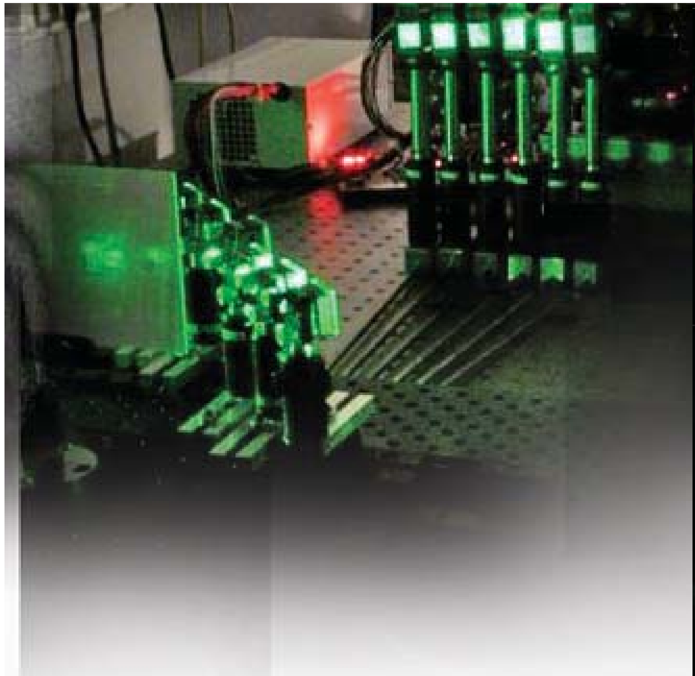

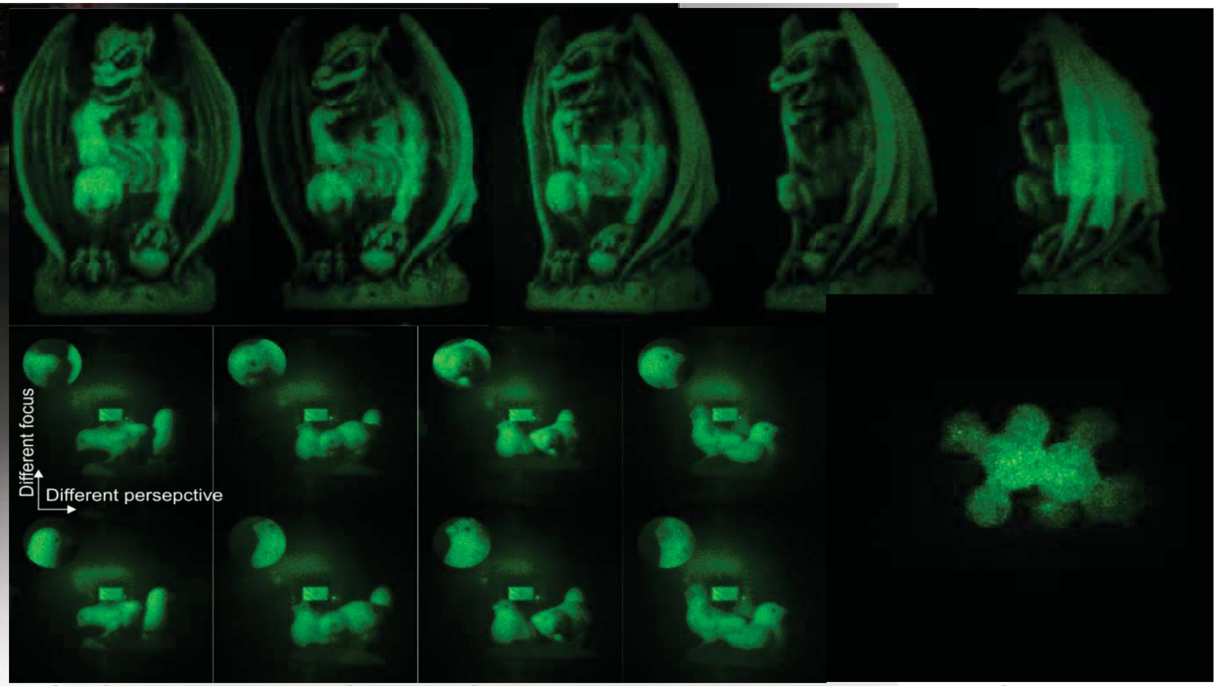

TRUE 3D DIGITAL HOLOGRAPHIC DISPLAY AND VIDEO OF REAL WORLD OBJECTS

- design and development holographic displays
- opto-numerical image data processing
- DH interferometry and remote full 3D measurements

Photonics at
Faculty of Mechatronics

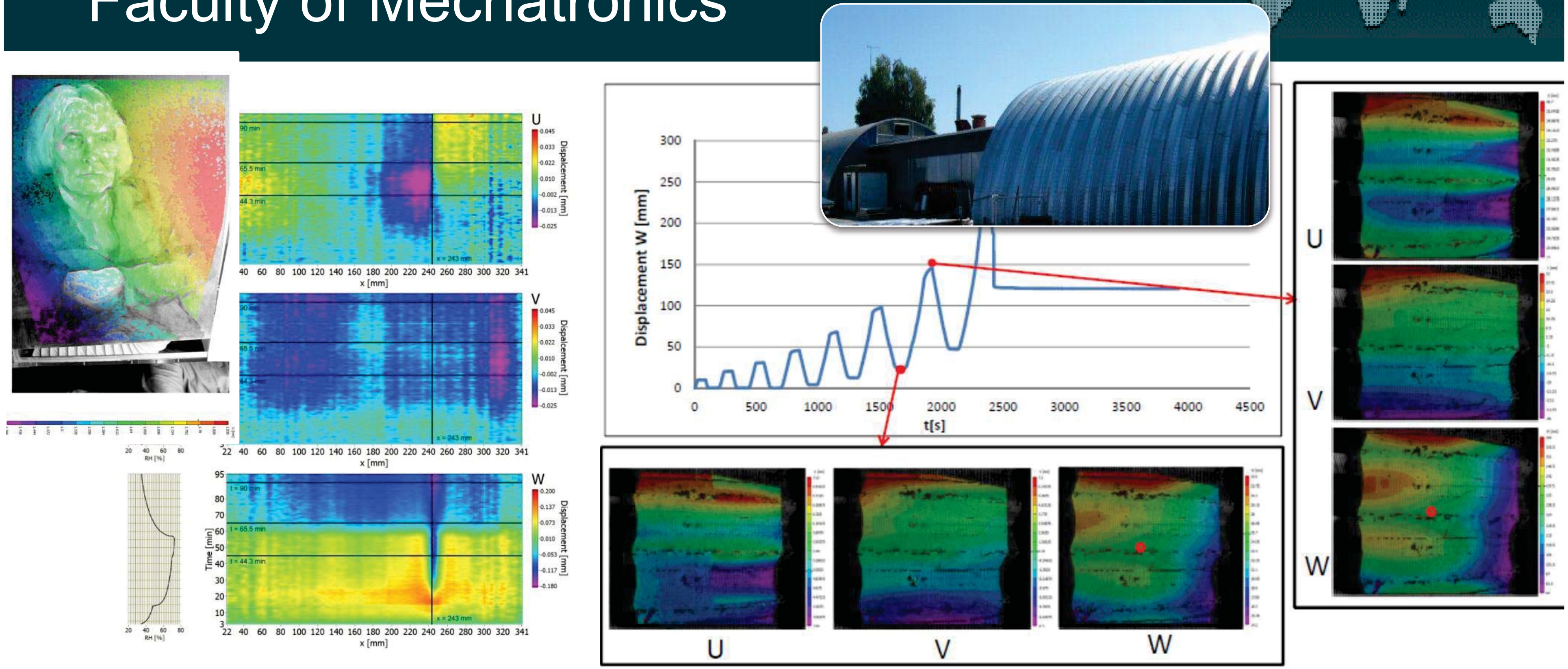

FULL-FIELD MEASUREMENT & CHARACTERIZATION

- design and development of systems based on noncoherent light methods
- engineering and art structures health monitoring

Photonics at
Faculty of Mechatronics

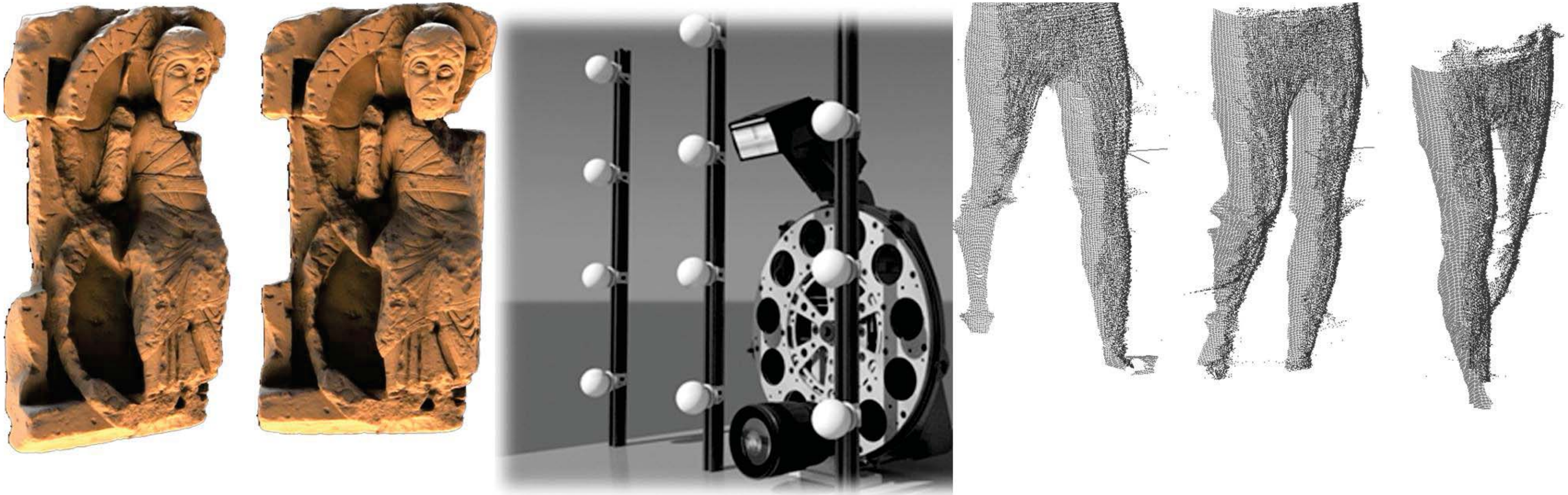

3D/4D MEASUREMENT

- development of structured light measurement system
- precise 3D and 4D (3D + time) measurement
- development of algorithms for automated 3D/4D data processing

Archiving cultural heritage objects

4D data capture
- medical applications

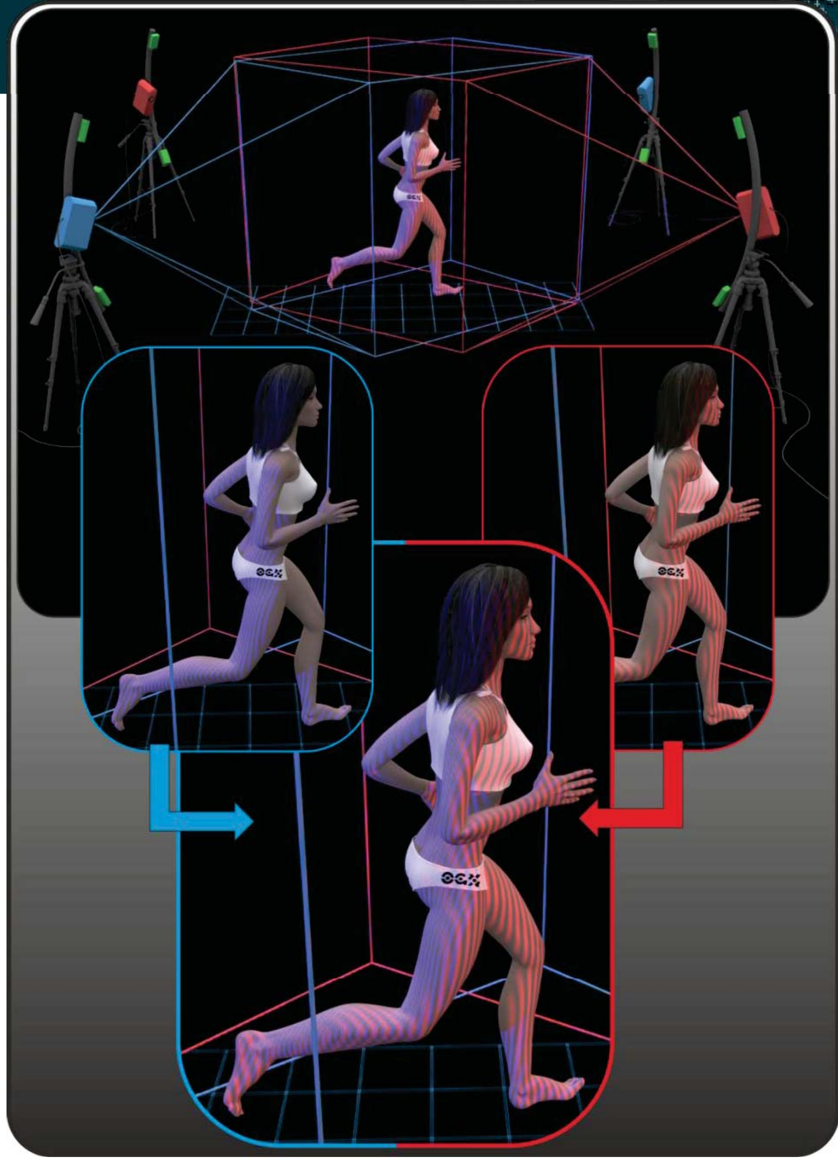

■Multidirectional measurement of static shape as well as dynamic surface coordinates

■Parameters:

- **measurement volume**: 2m x 2m x 1,5m
- **measurement uncertainty**: 0,4mm (static), 1mm (dynamic)
- **measurement frequency**: 60Hz.

■Resulting data:

■- **4D coordinates** (x, y, z, t),

■- **movement parameters** (angles, corssections, etc).

Static and active MEMS/MOEMS studies

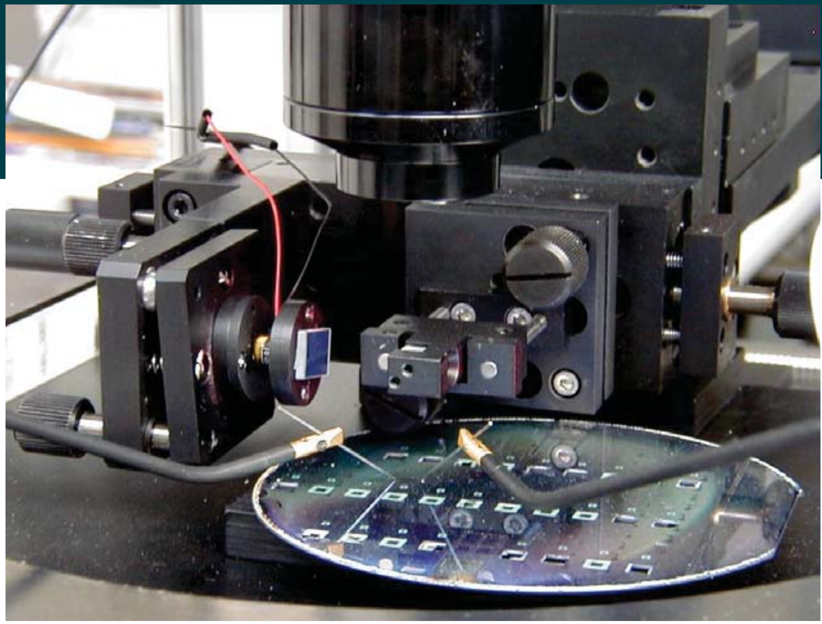

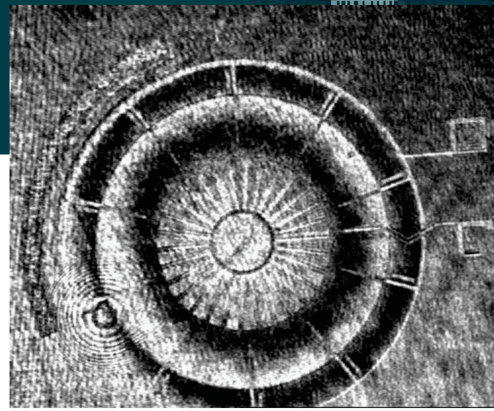

Shape

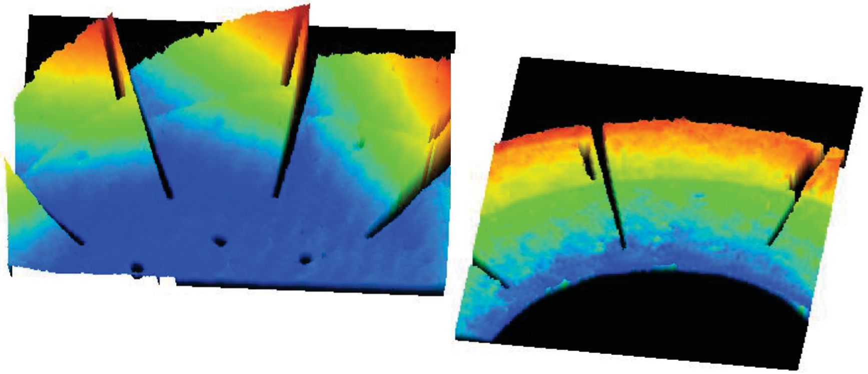

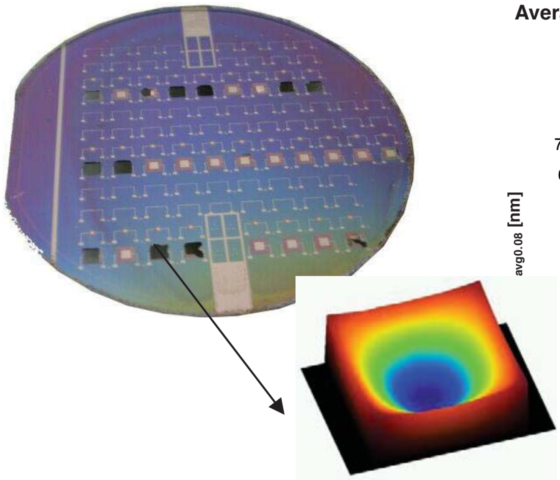

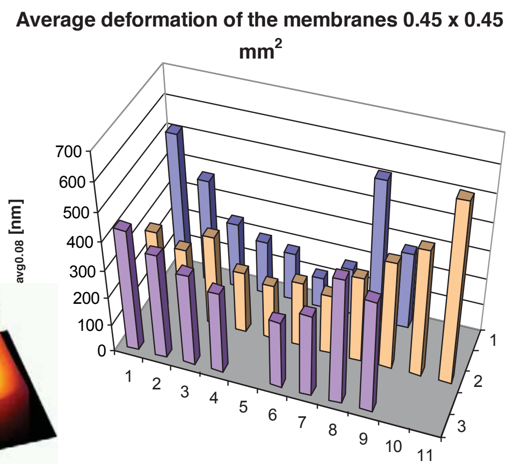

Vibration Enhanced TAI

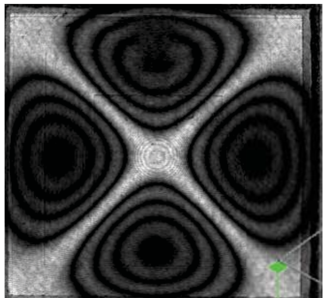

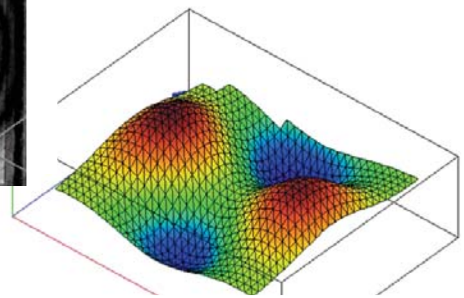

Phase microscopy and tomography – new approach to 3D measurements of biological and technological structures

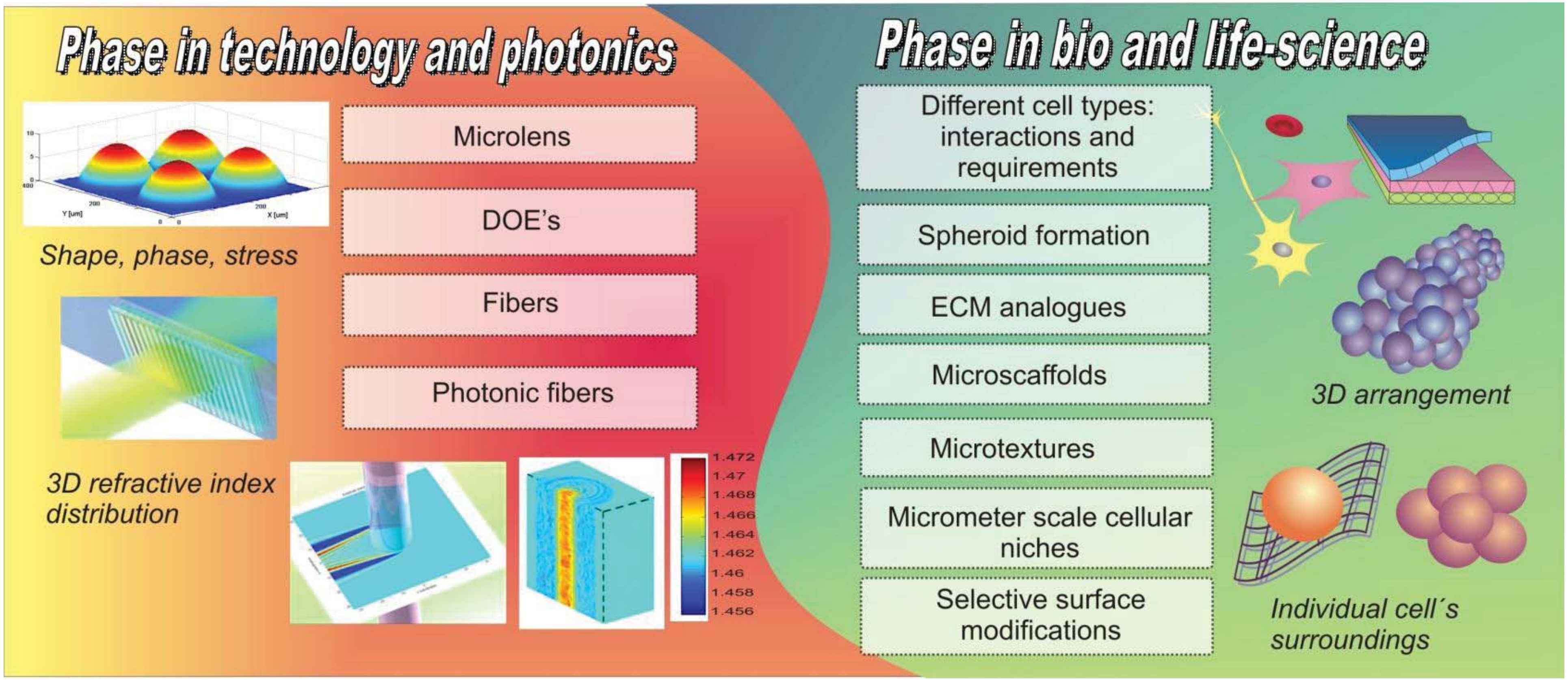

Recent challenges for Full-Field Optical Metrology

- Provide convenient tool for nanomaterials and microsystems (technical and biological) characterization with extended resolution capabilities
- Provide experimental data for Computer Aided Engineering (CAE) incl. industrial measurement, reliability analysis and outdoor structures monitoring
- Provide extended range of 3D (x,y,z)/4D(x,y,x;t) data with the automatic path of their processing for new engineering/biomedical/multimedia applications.

*General trend to transfer from 2D (x,y) imaging into **3D (x,y,z)** and from point measurement/monitoring into **4D (x,y,z;t) (u,v,w,t)** measurement/visualization*

Measurement Process

MP = code the information (complex amplitude) in intensity data +
+ capture the data + decode/reconstruct the information

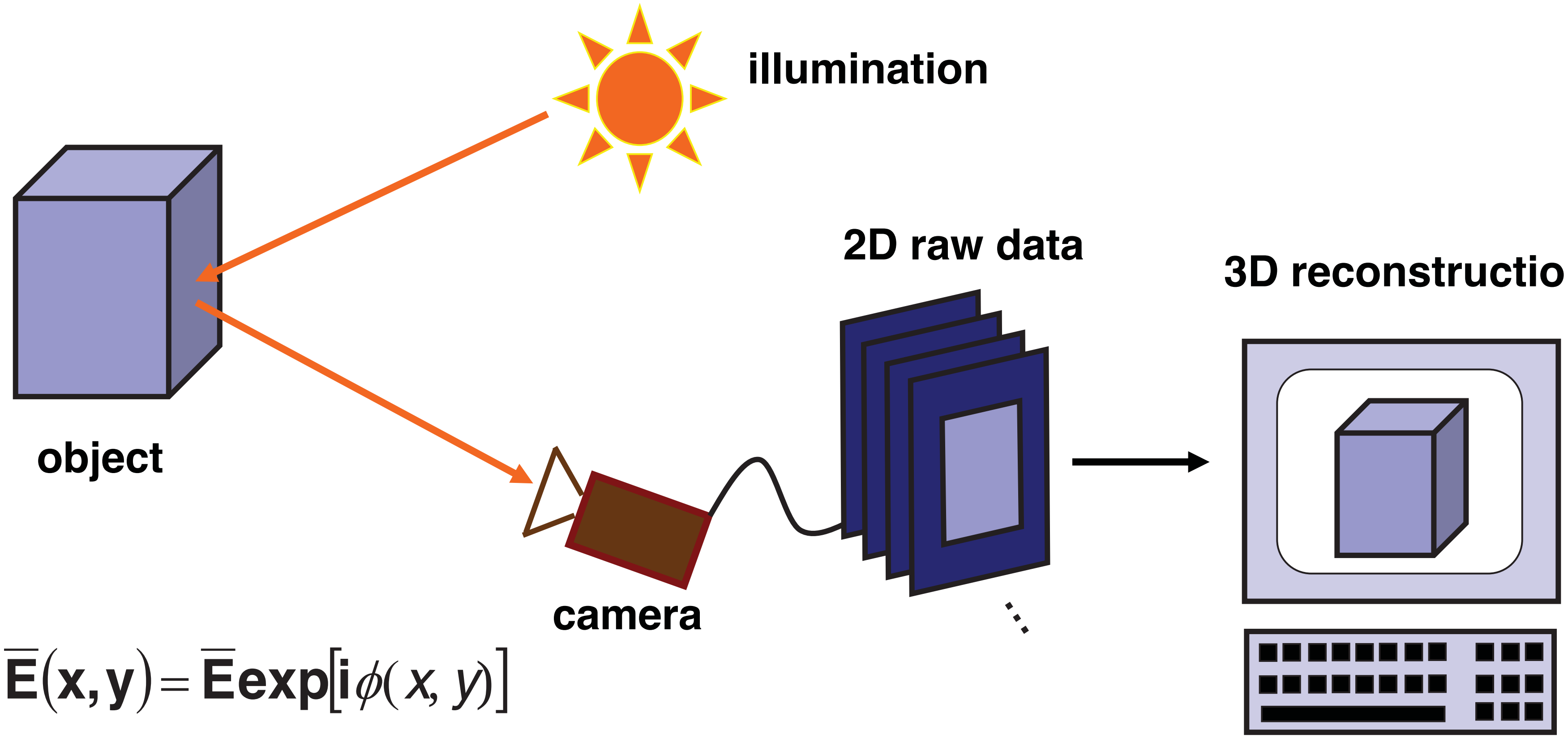

$$\bar{\mathbf{E}}(\mathbf{x},\mathbf{y}) = \bar{\mathbf{E}}\exp[\mathbf{i}\phi(x, y)]$$

Detectors capture intensity data only.
Phase has to be coded

Coherent and noncoherent light based measurements methods

Assumption:

Output of coding: Fringe pattern/interferogram
Hologram
Specklegram/correlogram

Coherent methods of coding based on:

- **interferometry**
- **holography**

Noncoherent methods of coding based on:

- **grid/grating methods**
- **moire methods (mechanical interference)**
- **digital correlation methods**

Measurement tasks

PRIMARY MEASUREMENT TASKS

- shape/distance (geometrical properties incl. roughness)
- optical properties (wavefront aberrations)
- in-plane displacements (u, v)
- out-of-plane displacement (w)
- strains
- dynamic (vibration) characteristic (frequency, amplitude, phase)

RELATED MEASUREMENT TASKS

- material constants: E, ν, thermal coef., ...
- stress
- defect detection, quality assessment (NDT)
- figures of merit (MTF,…….)

Full-field coding of information

Coherent versus noncoherent methods

Full-field optical metrology

Noncoherent

Methods based on photogrammetry and/or image correlation

IBM – image/intensity based methods

PMM – Phase Measuring Methods

Grid/moiré (mechanical interferometry)

$$T_u(r) = \sum a_n \exp\left[in\left(\frac{2\pi}{p}\bar{r}\right)\right]$$

$$T_d(r) = \sum a_n \exp\left\{ in\left[\frac{2\pi}{p}(\bar{r} - u(\bar{r}))\right]\right\}$$

↓ or

$$I = I_i \, T_u \, T_d$$

↓ filtering

$$I_m(\bar{r}) = a_0 + a_1 \cos\left[\alpha \frac{2\pi u(\bar{r})}{p}\right]$$

$u(\bar{r})$ – grid projection, $\bar{r}(r_x, r_y)$

α - depends on the method and geometry

Coherent

PMM

Interferometric

$E_0(r,t) = E_0 \exp\{i[\phi_1(\bar{r}) - \omega_1 t]\}$ - refrence

$E_R(r,t) = E_{R0} \exp\{i[\phi_2(\bar{r}) - \omega_2 t]\}$ - object

↓

$I = (E_0 + E_R)(E_0 + E_R)^*$

↓

$I \cong a_0 + a_1 \cos\delta(\bar{r})$

or

$I \cong I_0 \left| M[\delta(\bar{r})] \right|$

$\delta = \phi_1 - \phi_2$ - phase difference

M - the characteristic function (depends on registration technique and object movement)

INFORMATION CODED INTO INTERFEROGRAMS AND FRINGE PATTERNS

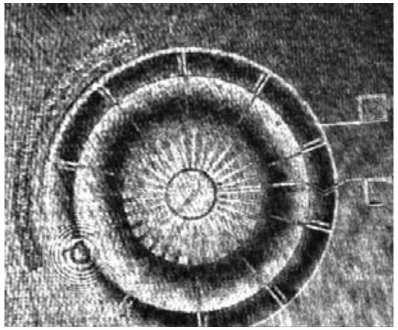

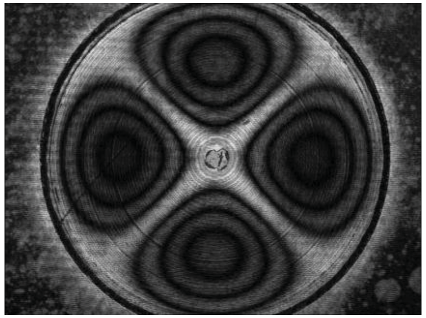

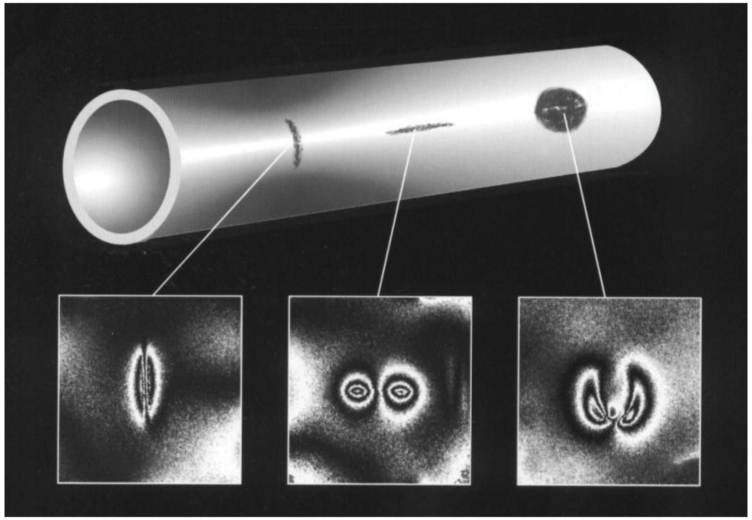

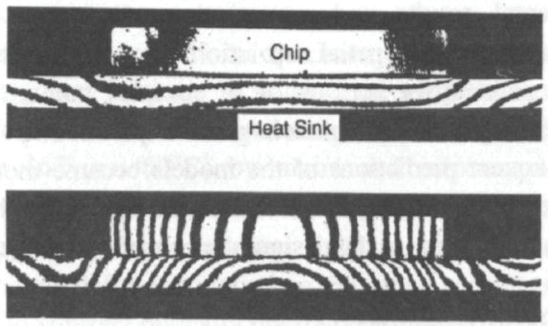

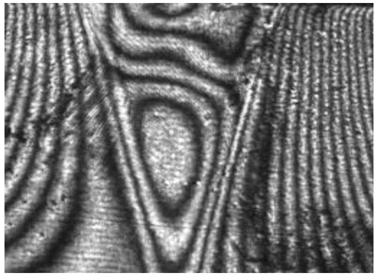

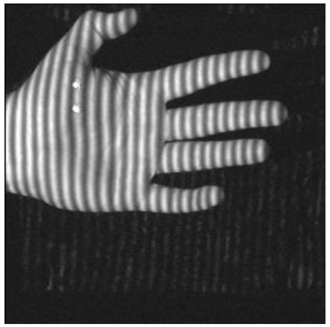

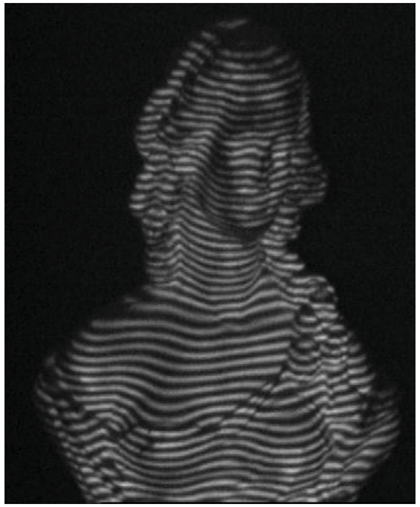

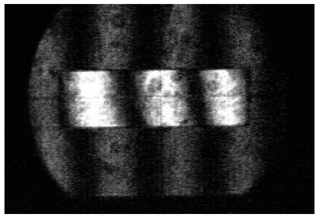

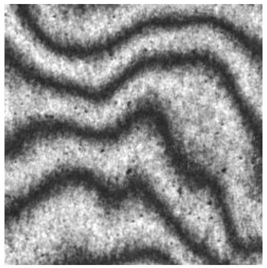

Optical coding - sensitiviy vector

PHYSICAL PHENOMENON

MEASUREMENT TASK

$M(\bar{r})$

LASER INTERFEROMETRY

INTERFEROGRAM

INTERFEROGRAM ANALYSIS

$$\mathbf{I(x,y) = a(x,y) + b(x,y)\cos\phi(x,y)}$$

$$\boldsymbol{\varphi}(\bar{\mathbf{r}}) = \bar{\mathbf{S}}(\bar{\mathbf{r}}) \cdot \mathbf{M}(\bar{\mathbf{r}})$$

S(r)- sensitivity vector, M(r) – measurand,

a(P), b(P) –directional vectors of illumination and observation

$$\mathbf{S}(P) = 2\pi/\lambda(\mathbf{b}(P) - \mathbf{a}(P))$$

THE SAME RULES REFER TO NONCOHERENT FRINGE BASED METHODS

Phase detection

- Optical methods provide fringe patterns (holography, interferometry, moiré, speckle) or line patterns (grid method).
- An image by itself is not a measurement, it is an intensity recording, following: $I(\varphi) = A\left[1 + \gamma\,\mathrm{frgn}\left(\varphi\right)\right]$
- The parameter of interest is the phase

  but nowdays the modulation can be of interest as well e.g.

  - Bessel fringes decoding for vibration parameters analysis
  - fringes obtained in white light interferometry

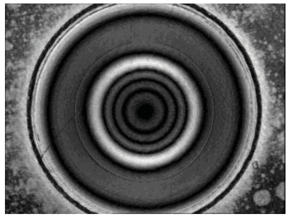

- Phase detection is the calculation of the phase field from the intensity field

Information coded into Fringe Patterns

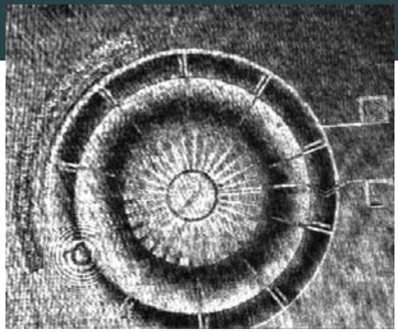

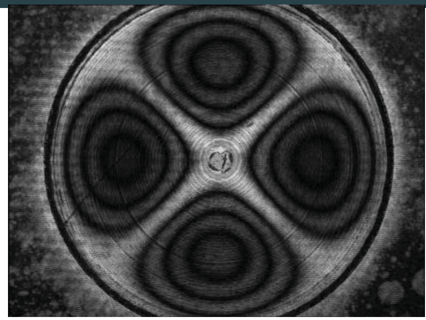

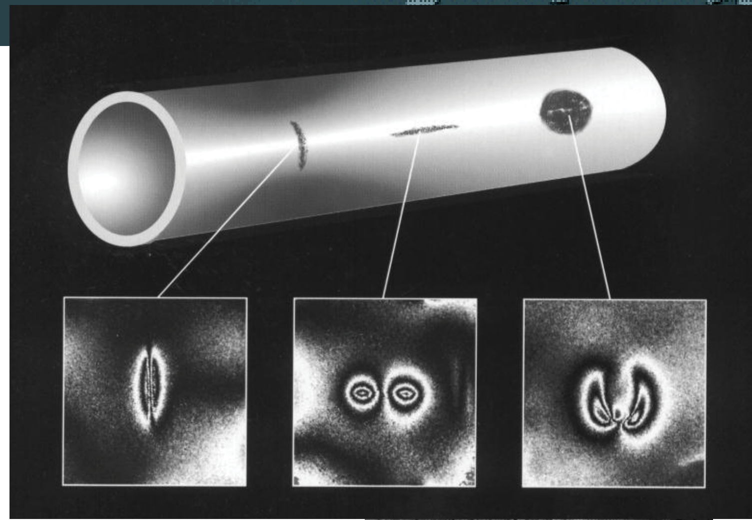

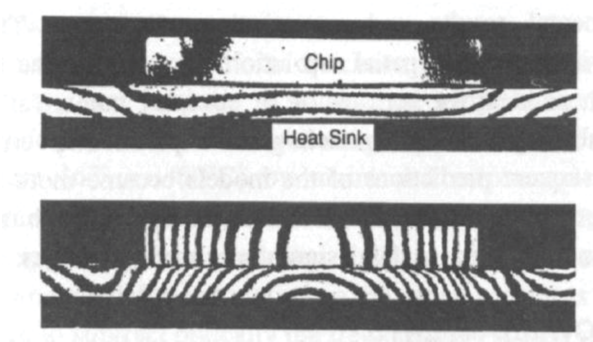

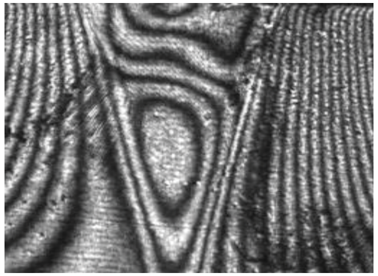

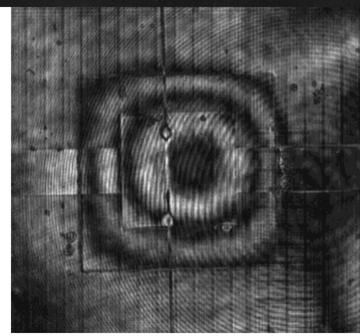

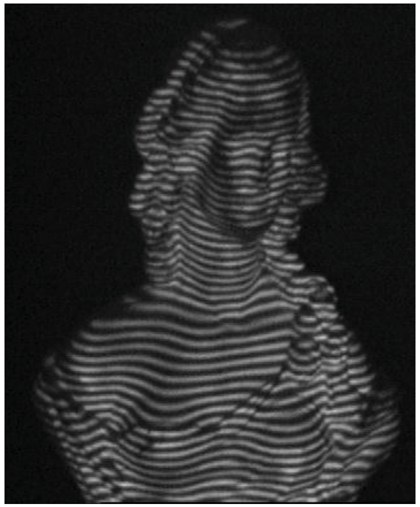

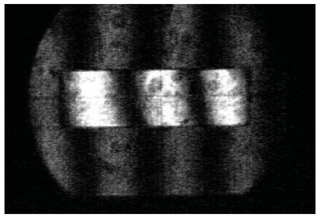

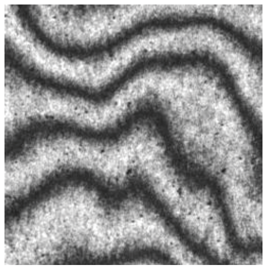

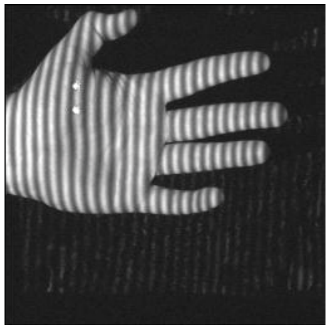

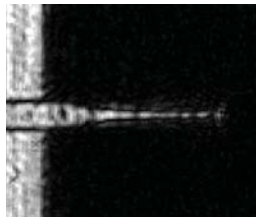

Fringe pattern analysis

Goal: **full reconversion of the original feature(s) represented by FP i.e. solving an inverse problem**

basic FP: $I(x,y) = a(x,y) + b(x,y) \cos \phi(x,y)$

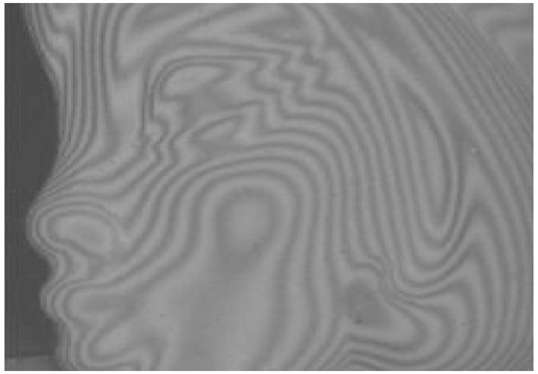

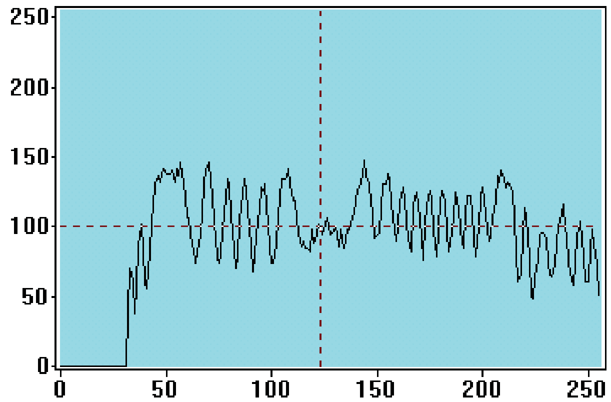

difficulties:

- **ill posed problem due to unknown a, b, ϕ**
- **the sign ambiguity problem $\cos(\phi) = \cos(-\phi)$**
- **the mod 2π problem ($\cos(\phi) = \cos(\phi + 2N\pi)$)**

Extended definition of FP (object complexity)

static event:

$$I(x, y) = a_0(x, y) + \sum_{n=1}^{\infty} a_n(x, y)\cos[n\varphi(x, y)] + n(x, y)$$

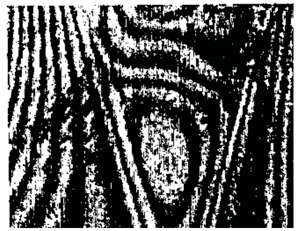

dynamic event:

$$I(x, y; t) = a_0(x, y; t) + \sum_{n=1}^{\infty} a_n(x, y; t)\cos[n\varphi(x, y; t)] + n(x, y; t)$$

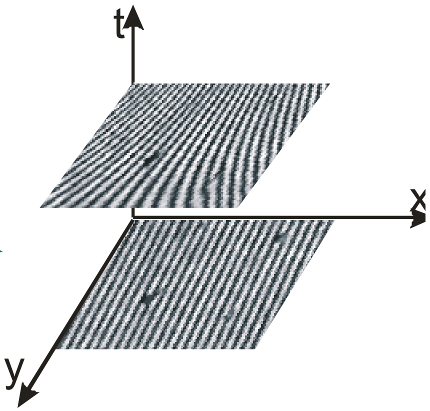

multiplexed events:

$$I(x, y) = \left(\sum_{k=1}^{K} \text{or} \prod_{k=1}^{K}\right)\left(a(x, y) + \sum_{n=1}^{\infty} a_{kn}(x, y)\cos[n\varphi_k(x, y)]\right) + n(x, y)$$

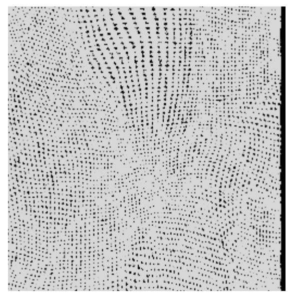

difficulties:

- **noise, nonlinearities**
- **features variable in time**
- **demultiplexing**

Fringe pattern analysis methods

Intensity (passive) methods – single interferogram processed and analysed without modifications based on conventional digital image analysis methods
Problems of sign and mod 2π solved with „a priori" knowledge
(still used for archive interferogram analysis, not used in commercial measurement systems)

Phase (active) methods – require modifications (design) of fringe pattern through changes of phase acc. equation

$$I(x,y,t) = a(x,y) + b(x,y)\cos[2\pi(f_{ox}x + f_{oy}y) + \nu_o t) + \alpha(t) + \varphi(x,y)]$$

where f_{0x}, f_{0y} are spatial carrier frequencis
ν_0 is temporal carrier frequency (running fringes)
α is additionally introduced phase shift

For different phase methods one of these phase values is introduced

Intensity methods – fringe localization

Fringe extrema localization (skeletoning, fringe tracking).
Require strong initial image preprocessing to allow efficient segmentation

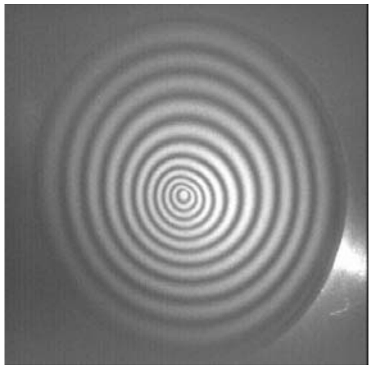

Image preprocessing

Segmentation

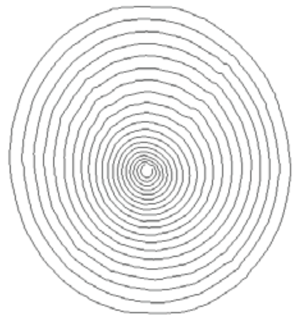

Skeletoning and fringe numbering

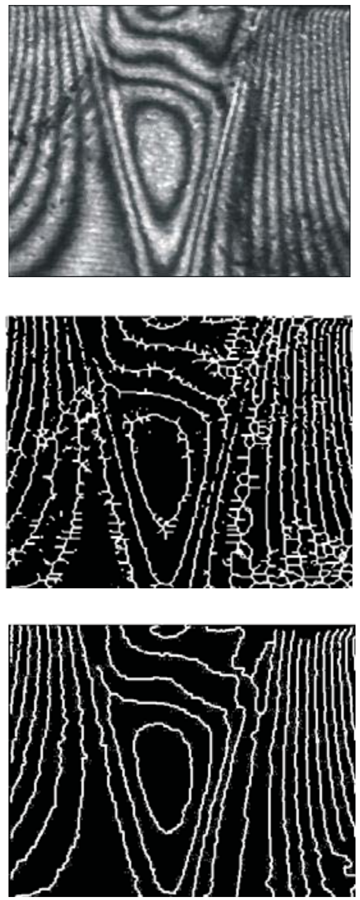

„a priori” knowledge required, difficult to automate analysis, noneven sampling, low accuracy (<fringe/10)

Now: new approaches with regularization methods

Intensity methods – RPT method

Regularized phase-tracking method RPT

Assumptions:

- **agreement between model and experiment**
- **initial knowledge about spatial variations of searched function**

Cost function U_T given by:

$$U_T = \sum_{(x,y \in N_{x,y})} U_{x,y}\left(\phi_0, f_x, f_y\right)$$

where

$$U(x,y) = \sum_{(\in,\eta)\in N_{x,y}\cap S} \left\{ \left[I'(\in,\eta) - \cos p(x,y,\in,\eta) \right]^2 - \lambda \left[\phi_0(\in,\eta) - p(x,y,\in,\eta) \right]^2 m(\in,\eta) \right\}$$

$$p(x,y,\in,\eta) = \phi_0(x,y) + 2\pi f_x(x,y)(x-\varepsilon) + 2\pi f_y(x,y)(y-\eta)$$

λ – regularization parameter controlling the smoothness of phase, N_{xy}- neighbourhood

has to be minimized by estimated function $\phi(x,y)$

Intensity methods - RPT

Possibility to reconstruct phase from a single fringe pattern without its modification

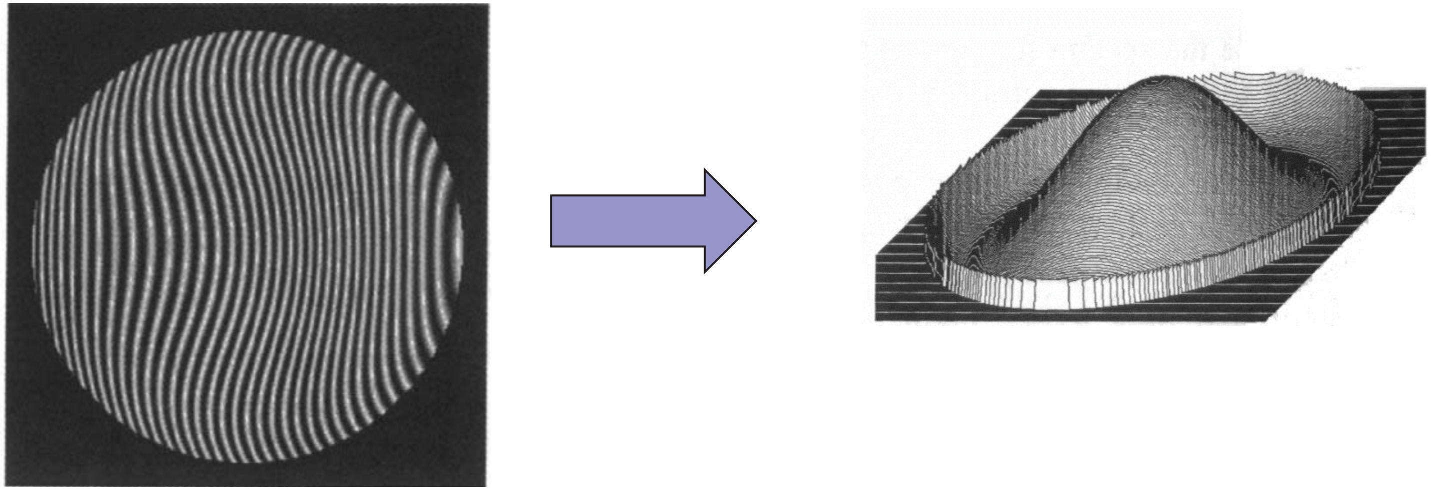

Result of direct phase reconstruction from interferogram by RPT method.

However strong restrictions on reconstructed phase, long processing, local minima of cost function and high sensitivity to noise in fringe pattern. RPT is not used in commercial systems.

Phase based fringe pattern analysis methods

$$I(x,y,t) = a(x,y) + b(x,y)\cos[2\pi[(f_{ox}x + f_{oy}y) + \nu_o(t)] + \alpha(t) + \varphi(x,y)]$$

Required controlled modifications of phase in FP:

$\nu_0(t)$ – introduces temporal heterodyning (running fringes) – electronic signal analysis (future specialized CMOS) by heterodyning method

$\alpha(t)$ – introduces controled phase shifts – Temporal Phase Shifting (Stepping) Method (TPS)

f_{0x}, f_{0y} – introduces controlled number of carrier fringes in FP – Fourier Transform Method and Spatial Carrier Phase Shifting Method

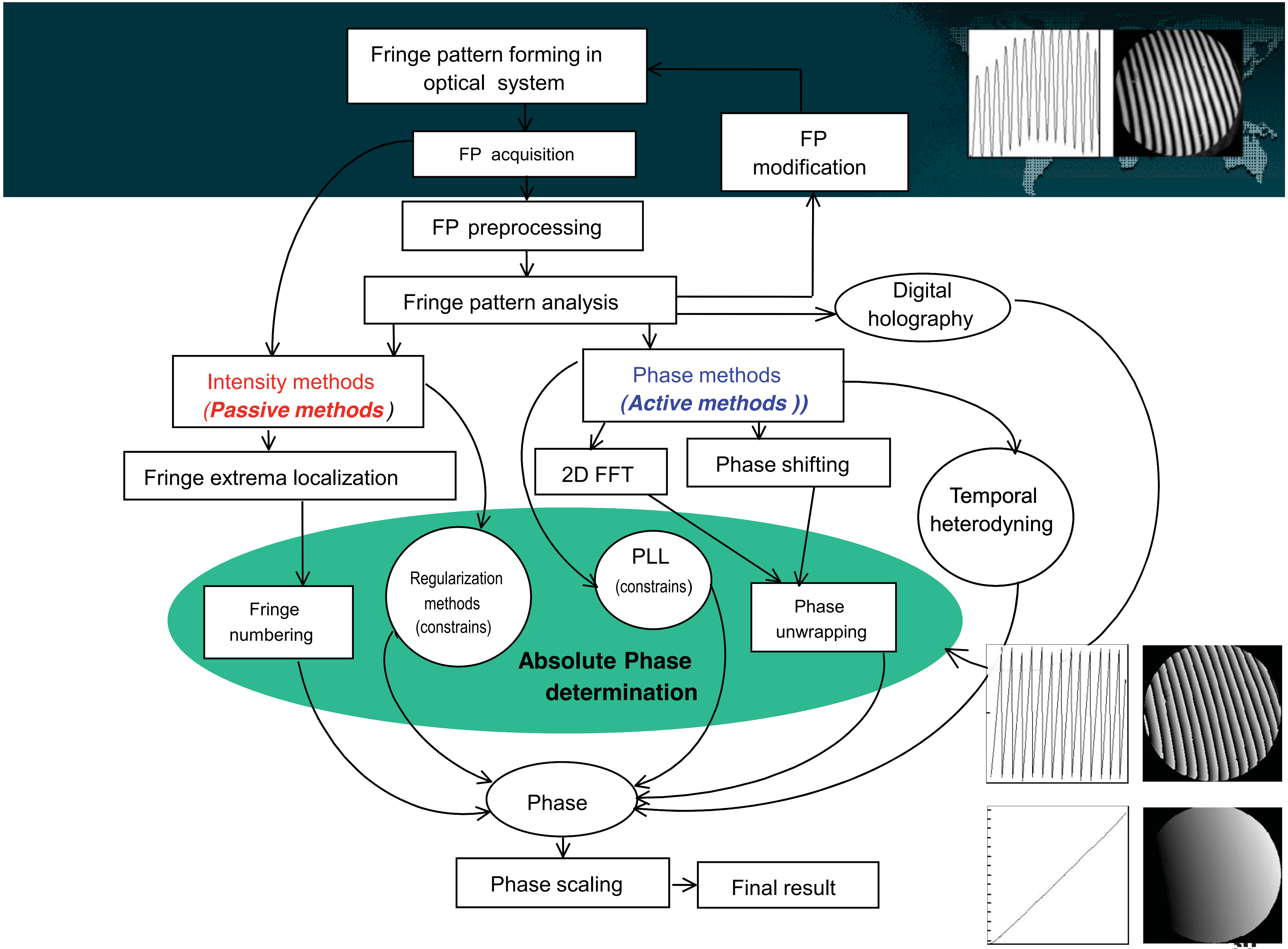

Fringe pattern forming in optical system
FP acquisition
FP modification
FP preprocessing
Fringe pattern analysis
Digital holography
Intensity methods
(Passive methods)
Phase methods
(Active methods))
Fringe extrema localization
2D FFT
Phase shifting
Temporal heterodyning
Regularization methods (constrains)
PLL (constrains)
Fringe numbering
Phase unwrapping
Absolute Phase determination
Phase
Phase scaling
Final result

Automatic fringe pattern analysis

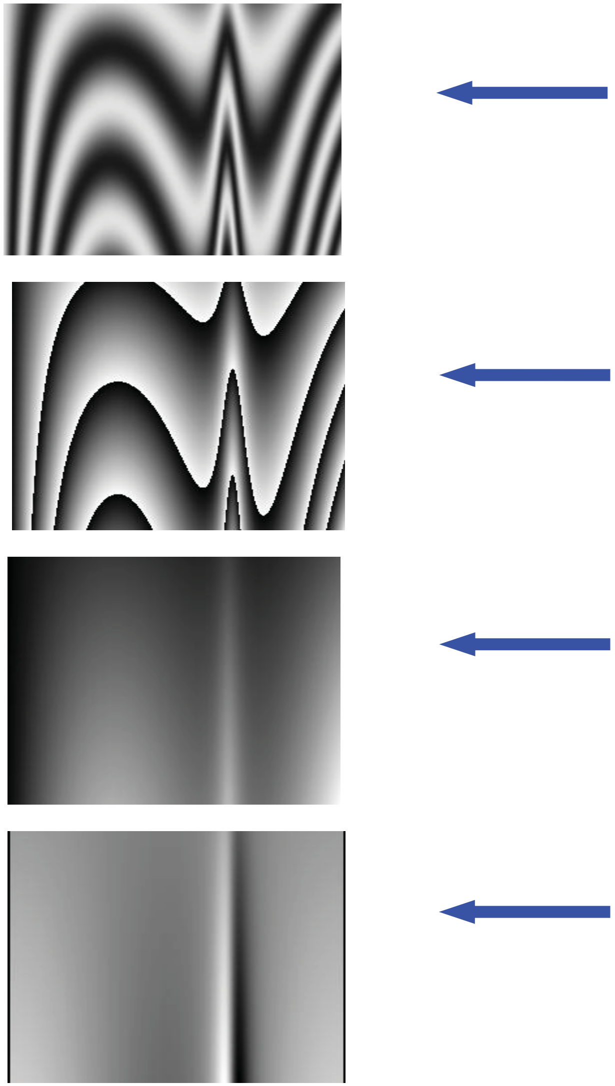

Phenomenon / Method
HI, ESPI, GI, FP

↓

Interferogram Acquisition

↓

Phase Measuring Methods
temporal | spatial

↓

Phase mod 2π

↓

Phase unwrapping

↓

Scalling
displacement: u, v, w

↓

Results midifications

↓

Strains / material constants
$\varepsilon_x, \varepsilon_y, \gamma_{xy}, \nu, E$

Fringe pattern analysis strategies

- Temporal strategy
  Many images are required
  One independent measurement per pixel (unless spatial smoothing)
  - Temporal phase stepping or phase shifting
- Spatial strategies:
  Only one image is required
  The spatial resolution is low (not one independent measurement per pixel)
  - Intensity methods (interpolation, fringe tracking, fringe multiplication…)
  - Fourier transform method (extraction of the analytic signal when a carrier is present)
  - Spatial phase stepping and spatial carrier phase shifting method
  - Algorithms based on a wavelet transform

Phase shifting methods: temporal phase shifting

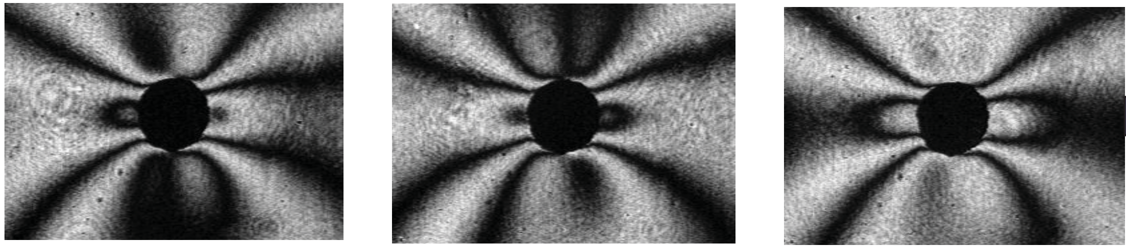

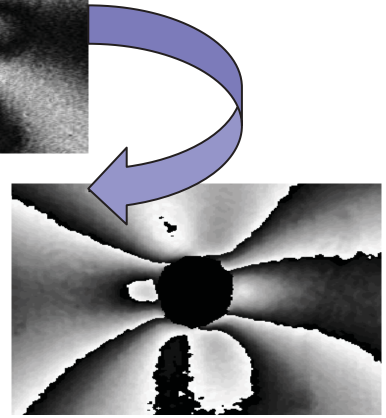

$$\overline{\Phi}(x, y) = \mathrm{arctg}\left[\frac{\sum_{i=1}^{N} a_i I_i(x, y)}{\sum_{i=1}^{N} b_i I_i(x, y)}\right]$$

where i = 0, ..N-1 for N-frame algorithms

The phase shifting algorithm is defined by:

- number of images/frames,
- phase shift introduced in images,
- the values of coefficients a and b (Fourier coefficients described by FFT of signal)

Means of temporal phase shifting

- How to add a known constant phase to the intensity?

- Interferometric systems:
  - Mirror on piezo transducer
  - Rotating glass plate
  - Rotation of a polarizer
  - Using fibre optics phase shifter (FO at PZT cylinder)

- Profilometry by structured light, deflectometry, moiré:
  - Translation of a grid or grating
  - Electronic moire (translation of virtual grid)

Temporal Phase Shifting Method

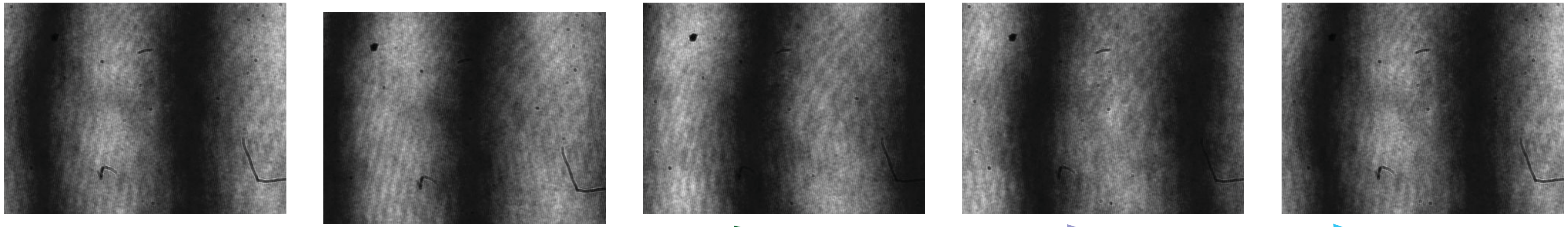

Five fringe patterns shifted in phase by 90º

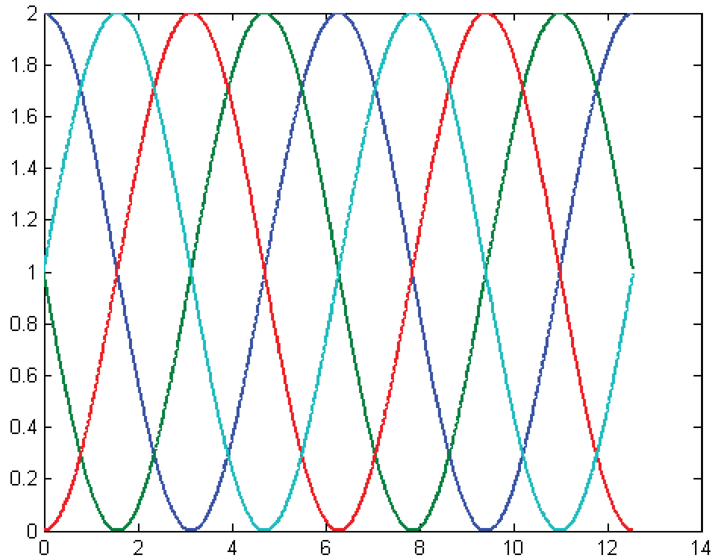

$\delta_{1;5}$ = 0º; 360º

δ_2 = 90º;

δ_3 = 180º;

δ_4 = 270º;

Extracting the phase

- The fringe profile is:

$$I(\phi) = A\left[1 + \gamma\,\mathrm{frgn}\,(\phi)\right]$$

- The recorded intensities are:

$$I_k = I(\phi + k\delta)$$

- When *N* samples are taken with a phase shift of 2π/*N*, the phase of the first Fourier component is the argument of the first coefficient of the DFT of the intensities => *N*-bucket algorithm

$$m_n = \sum_{k=0}^{N-1} I_k \exp(-i\,2\pi kn/N)$$

$$\phi = \arg(m_1) = -\,\arctan\left[\frac{\sum_{k=0}^{N-1} I_k \sin(2\pi k/N)}{\sum_{k=0}^{N-1} I_k \cos(2\pi k/N)}\right]$$

Temporal phase shifting (TPS)

Modes of phase shifted image capture

Phase stepping

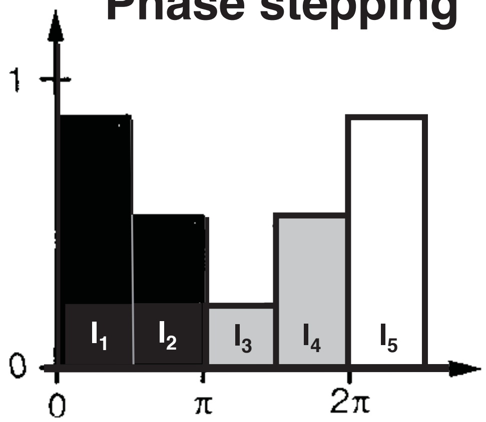

Integrated bucket technique (phase shifting)

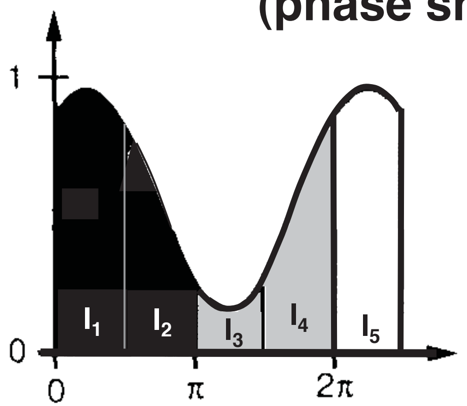

if $\alpha_i = \frac{i2\pi}{N}$ where $i = 1,........N$ **then**

$$\varphi(x,y) = \arctan\frac{\sum I_i(x,y)\sin\alpha_i}{\sum I_i(x,y)\cos\alpha_i}$$

For $\Delta\alpha=2\pi/3$ 3-image algorithm

$$\overline{\Phi} = \mathrm{arctg}\left[\sqrt{3}\,\frac{I_1 - I_3}{2I_2 - I_1 - I_3}\right]$$

For $\Delta\alpha=\pi/2$ 4-image algorithm

$$\overline{\Phi} = \mathrm{arctg}\left[\frac{I_4 - I_2}{I_1 - I_3}\right]$$

;

For $\Delta\alpha=\pi/2$ 5-image algorithm

$$\overline{\Phi} = \arctan\left[\frac{2(I_2 - I_4)}{2I_3 - I_1 - I_5}\right]$$

Sources of errors in TPS

1. nonconstant phase shift $\delta = \frac{2\pi}{N}(1+\epsilon)$

2. nonsinusoidal fringes (higher harmonics in fringe profile)

3. nonconstant values of background a(x,y) & modulation b(x,y)

4. random noise (speckle, white detector noise...)

$$\sigma_\phi^2 = \frac{2\sigma_1^2}{\eta N a_1^2}$$

where σ_1 is standard deviation of intensity function
η is the value 0.8-1

Solutions:

Ad1. M= N+1 images algorithms (first and last images should be the same)
Ad2. For q- harmonics in fringe profile number of images N>q+1
Ad1+2. M=2N-2 images

Spatial Carrier Phase Shifting

$$I_i(x,y) = a(x,y) + b(x,y)\cos[\phi(x,y) + 2\pi f_{0x}(x+i)]$$

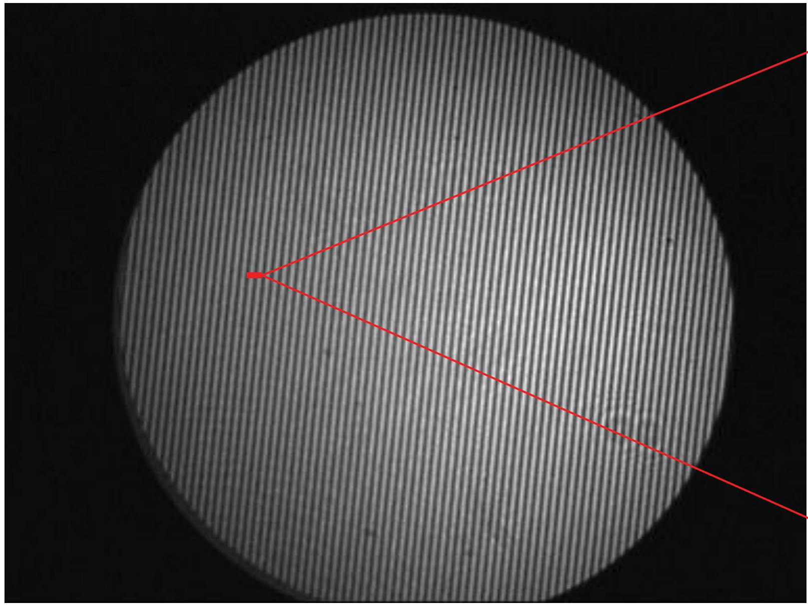

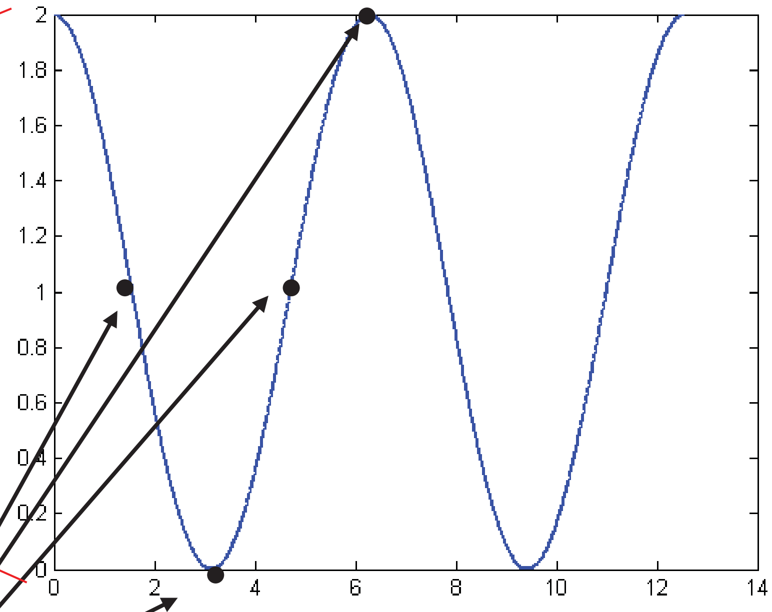

Assumption:
Phase is constant in the sampling window

Sampling points

SCPS
Analysis based on a single fringe pattern

Spatial Carrier Phase Shifting

Spatial carrier given by number of fringes in FP domain f_0 = P/N
where P- number of sampling points in FP domain (depend on detector resolution,
N- number of sampling points for one fringe (2π)

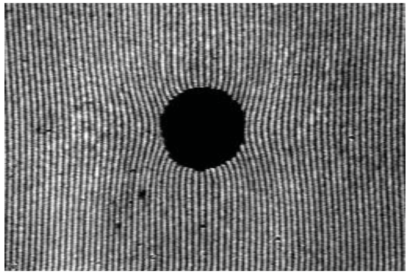

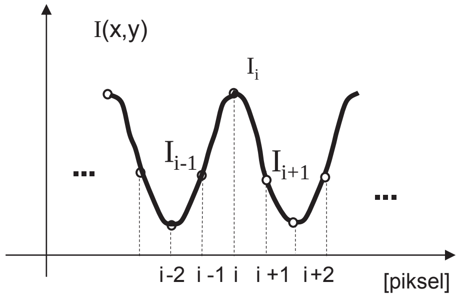

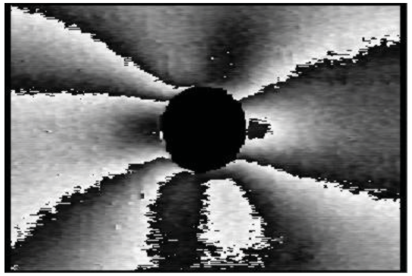

N-point algorithms

For α= π/2 and M+1

$$\phi'' = (x, y) = \mathrm{arctg}\left[\frac{2\{I(x-1, y) - I(x+1, y)\}}{2I(x, y) - I(x-2, y) - I(x+2, y)}\right], \quad \phi'(x, y) = \phi''(x, y) - x\frac{\pi}{2}$$

$$\phi(x, y) = \mathrm{arctg}\frac{\sin\phi'(x, y)}{\cos\phi'(x, y)}$$

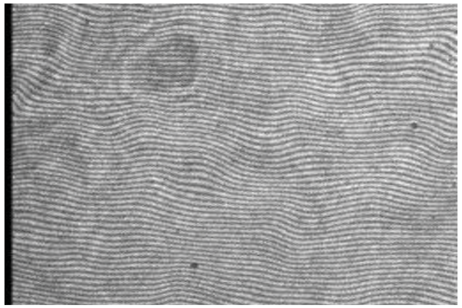

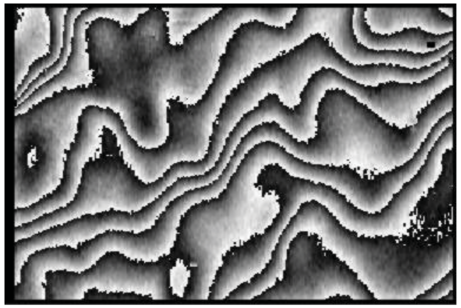

Spatial carrier in x or in y directions

TPS and SCPS comparison

- TPS

☺ High accuracy phase retrival (fringe/50),

☺ Phase retrival independently in each point (no error propagation),

☺ Analysis of arbitrary shape of fringes (including closed)

☹ Require capturing a few phase shifted FP (static object/conditions).

- SCPS

☹ Lower accuracy phase retrieval (fringe/20)

☹ Phase retrieval under assumption of constant phase in sampling window,

☹ Analysis of linearized fringes with high carrier frequency

☺ Analysis based on a single image (analysis of dynamic events)

TPS and SCPS are widely used in commercial optical measurement instrumentation

Fourier Transform Method

$$I(x,y,t) = \sum a_n(x,y)\cos[2\pi\ n\ (f_{ox}x + f_{oy}y) + \varphi_n(x,y)]$$

spatial heterodyning – adding carrier frequencies f_{ox} or f_{oy}

Condition: $f_0 > \max(\text{grad}\ \phi)$
if higher harmonics present they cannot overlapp +1st diffraction (information order)

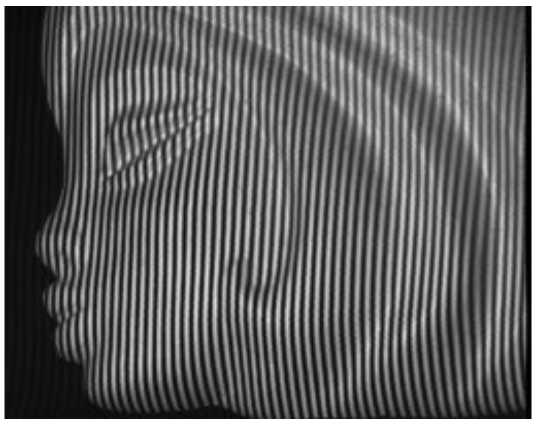

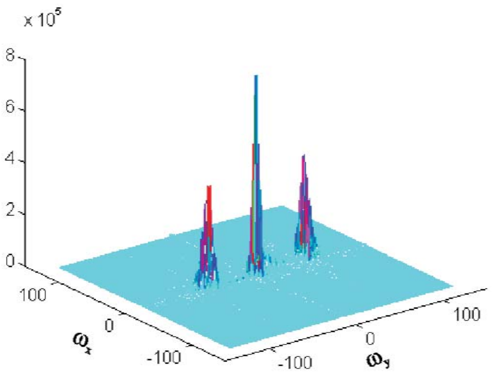

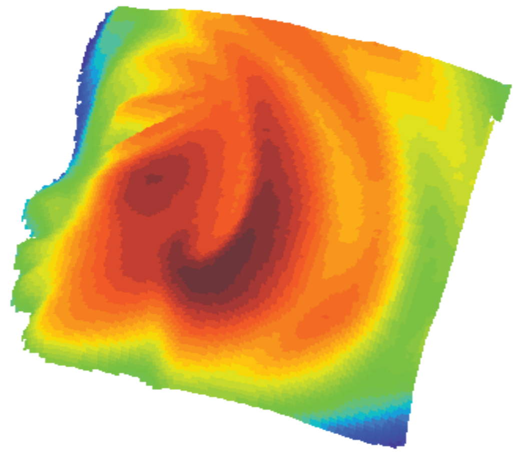

Analytic signal (FT) method

- The intensity is a phase modulation of the carrier:

$$
\begin{aligned}
I(\boldsymbol{r}) &= A\left\{1+\gamma\cos\left[2\pi \boldsymbol{f}_0.\boldsymbol{r}+\phi(\boldsymbol{r})\right]\right\} \\
&= A+\frac{A\gamma}{2}\exp(i\,2\pi \boldsymbol{f}_0.\boldsymbol{r})\exp[i\,\phi(\boldsymbol{r})]+\frac{A\gamma}{2}\exp(-i\,2\pi \boldsymbol{f}_0.\boldsymbol{r})\exp[-i\,\phi(\boldsymbol{r})] \\
&= A+C(\boldsymbol{r})\exp(i\,2\pi \boldsymbol{f}_0.\boldsymbol{r})+C^*(\boldsymbol{r})\exp(-i\,2\pi \boldsymbol{f}_0.\boldsymbol{r}),
\end{aligned}
$$

with $C(\boldsymbol{r})=\dfrac{A\gamma}{2}\exp[i\,\phi(\boldsymbol{r})]$

- Fourier transform:

$$
\begin{aligned}
\widehat{I}(\boldsymbol{f}) = &\; A\delta(\boldsymbol{f})+\widehat{C}(\boldsymbol{f}-\boldsymbol{f}_0)+\widehat{C^*}(\boldsymbol{f}+\boldsymbol{f}_0) \\
= &\; A\delta(\boldsymbol{f})+\widehat{C}(\boldsymbol{f}-\boldsymbol{f}_0)+\widehat{C}^{\,*}(-\boldsymbol{f}-\boldsymbol{f}_0)
\end{aligned}
$$

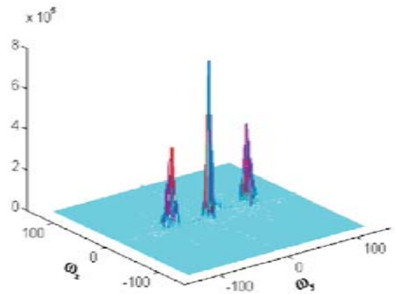

Filtering in the Fourier plane

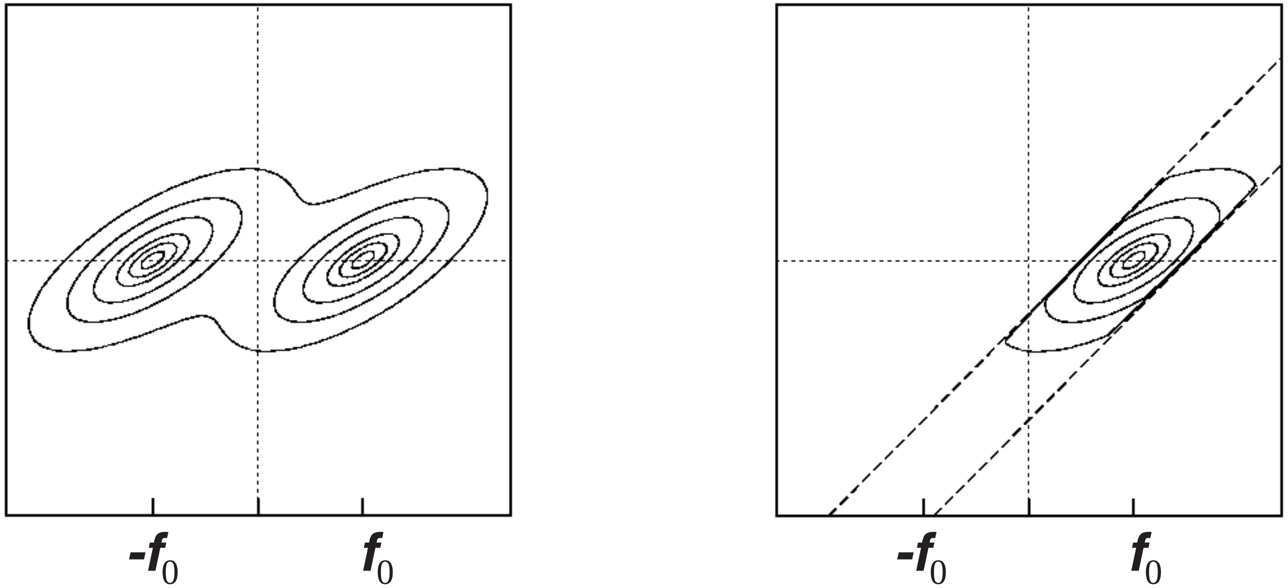

- The negative frequencies in the Fourier plane are cancelled

- The argument of $C(\boldsymbol{r})$ can then be extracted

$$C(\boldsymbol{r})\exp(i\,2\pi\boldsymbol{f}_0.\boldsymbol{r})$$

Two-dimensional information

- When two orthogonal carriers are used and when the signal contains harmonics:

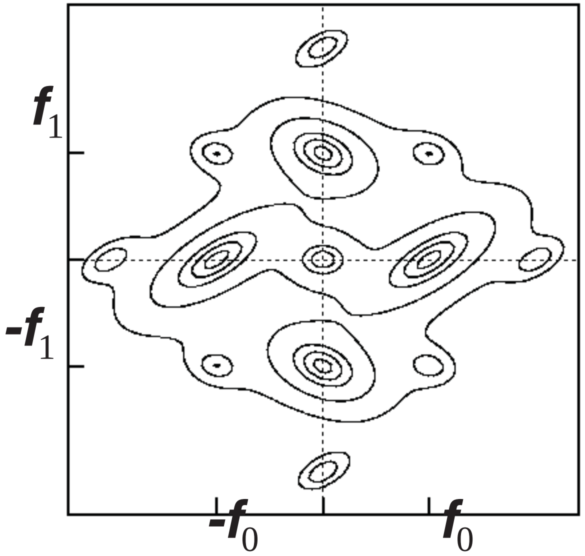

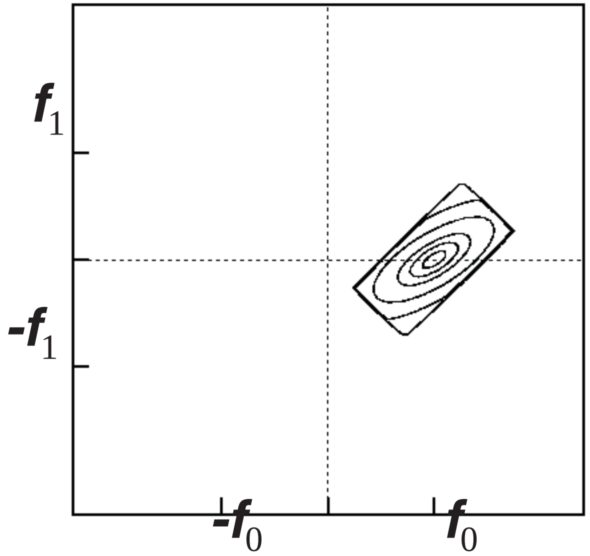

- => Difficult to fully automate

$$\phi(x,y) = \arctan \frac{\mathrm{Im}[c(x,y)]}{\mathrm{Re}[c(x,y)]}$$

Sources of errors in FTM

1. Wrong filtration (size of the filter) in Fourier space
2. FFT errors   i. alliasing   ii. domain truncation and discontinuities

3. Influence of background and high order terms if they overlapp with information bandwidth

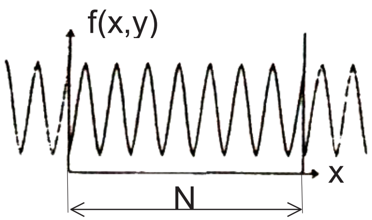

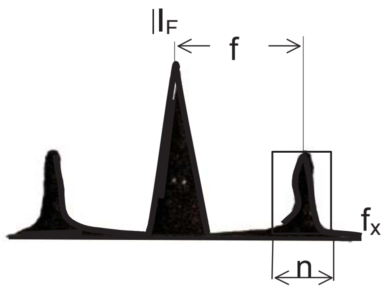

Significant errors at domain edges

Solutions: fringes extrapolation or multiplication by Hamming or Han window

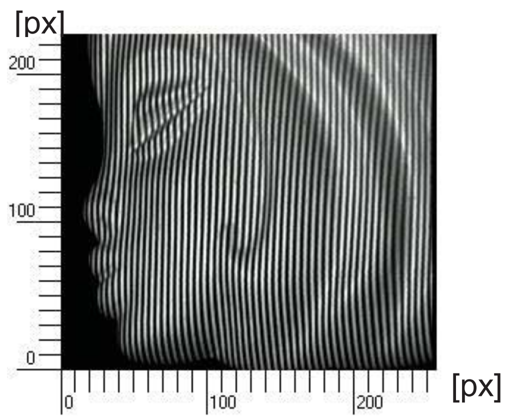

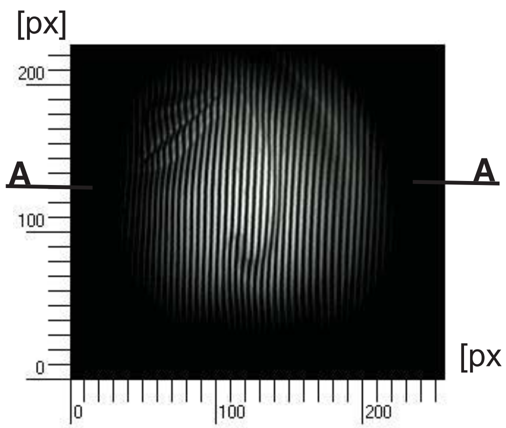

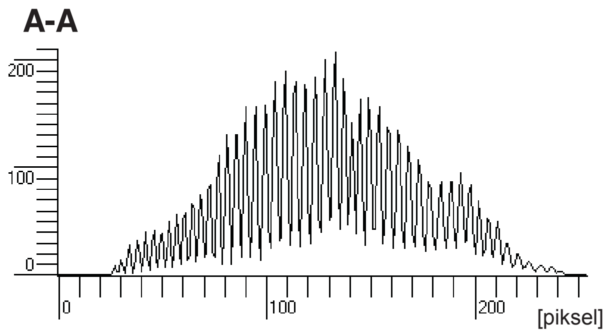

FTM – (+/-)

- **Advantages**

  - analysis based on a single image – dynamic events analysis,

  - filtration of background and high frequency errors

- **Disadvantages**

  - difficult to automate (selection of location of filtering window,

  - possibility to introduce significant local phase errors due to truncation of information frequencies,

  - significant errors at edges.

FTM is not widely used in commercial FPA systems

Comparison FTM and SCPS

- Spatial phase-stepping
  - The phase error can be evaluated everywhere with analytic formulae
  - The tuning requirement is more stringent : more than 15 % mismatch between the real and ideal sampling frequencies will result in phase oscillations

- Analytic (Fourier transform) signal method
  - Edge effects
  - The phase error cannot be evaluated
  - The tuning requirement is less stringent. If the cutoff frequencies are $\boldsymbol{f}_0/2$ and $2\boldsymbol{f}_0$, the fringe frequency can vary in a large range (400 % of the minimal value). This conclusion may be amended if there are a large amount of harmonics.

Decoding of fringe pattern modulation

Examples of information encoding in the intensity modulation distribution:

- time average interferometry for vibration studies

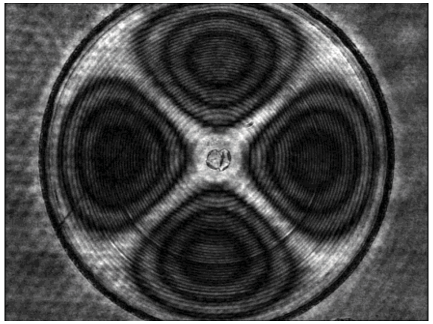

- white light interferometry

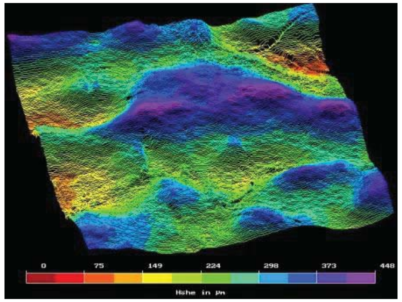

- modulation transfer function measurement

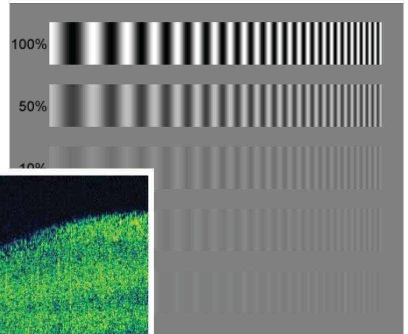

- optical coherence tomography

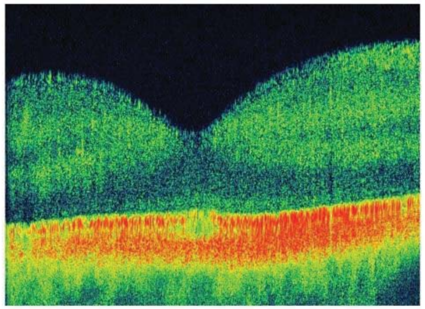

- additive type moire

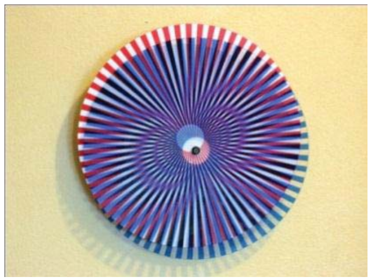

Absolute phase determination

Phase ambiguity problem

$$\cos\phi(x,y) = \cos[s\phi(x,y) + \tilde{N}(x,y)2\pi]$$

$$s \in [-1,1],\ \tilde{N}\ \text{additive integer}$$

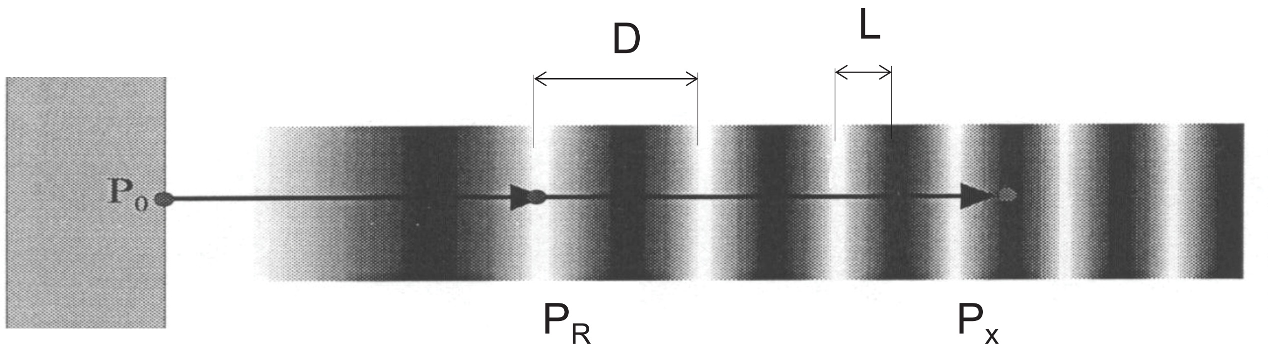

$$\phi(P_x) = N2\pi = [N_R + \tilde{N} + \hat{N}]2\pi$$

$$N_R - \text{known} \qquad \tilde{N} = \frac{1}{2\pi}\phi \bmod (2\pi)$$

$\hat{N}$ – integer obtained by unwrapping procedure

Numerical unwrapping procedures

Goal of phase unwrapping procedure: convert phase fringes into continous phase function

Sequential unwrapping by searching for discontinuities   dϕ/dx ≤ π [rad/piksel]

Determination of a step-like function

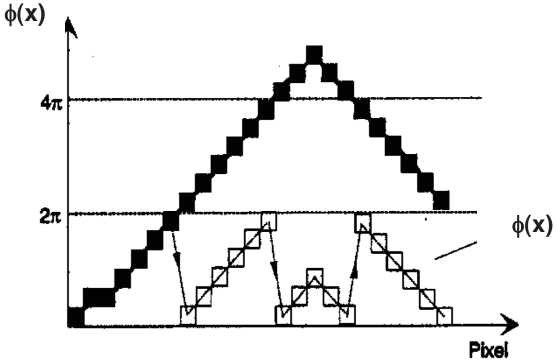

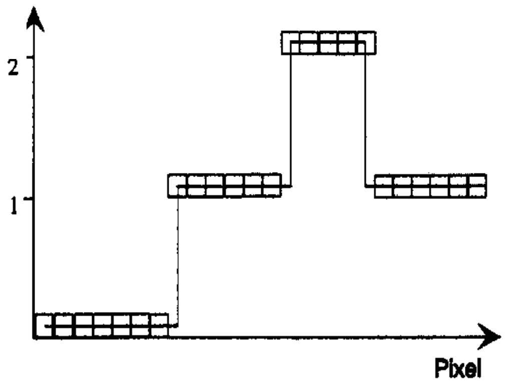

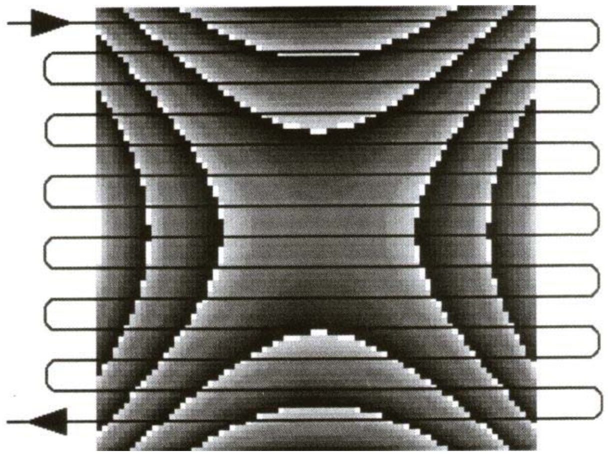

Line-by-line unwrapping

Problems in unwrapping procedures

- Problems due to:

  - noise, domain and physical discontinuities,

  - low phase fringe contrast....

Example:
phase fringes obtained from ESPI

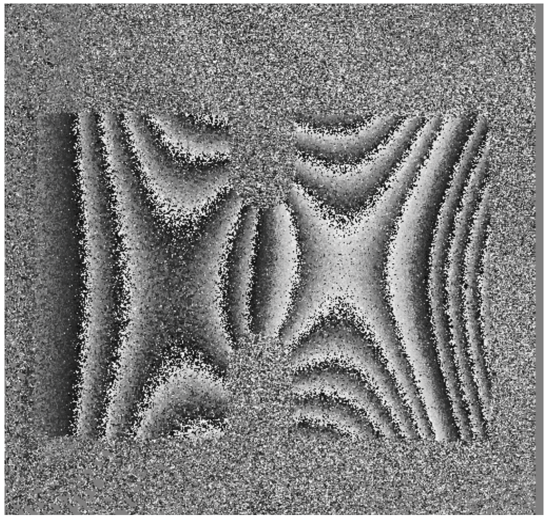

Result of line-by-line unwrapping

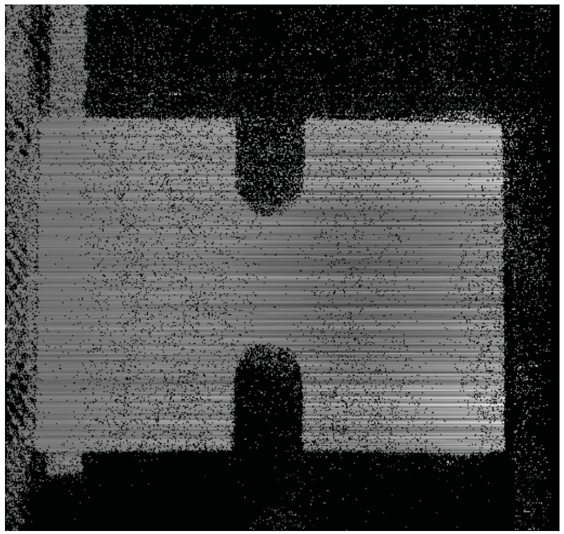

Two basic unwrapping approaches

Path-following

$$\Phi_u(i) = \sum_{i'=1}^{i} \Delta\Phi_w(i')$$

Global optimisation: minimise

$$S = \sum_{i=1}^{N-1} \{[\Phi_u(i) - \Phi_u(i-1)] - \Delta\Phi_w(i)\}^p$$

$p = 2 \Rightarrow$ Least squares unwrapping

In 1-D, both approaches give the same result

+ temporal unwrapping

2-D unwrapping (path following): Example

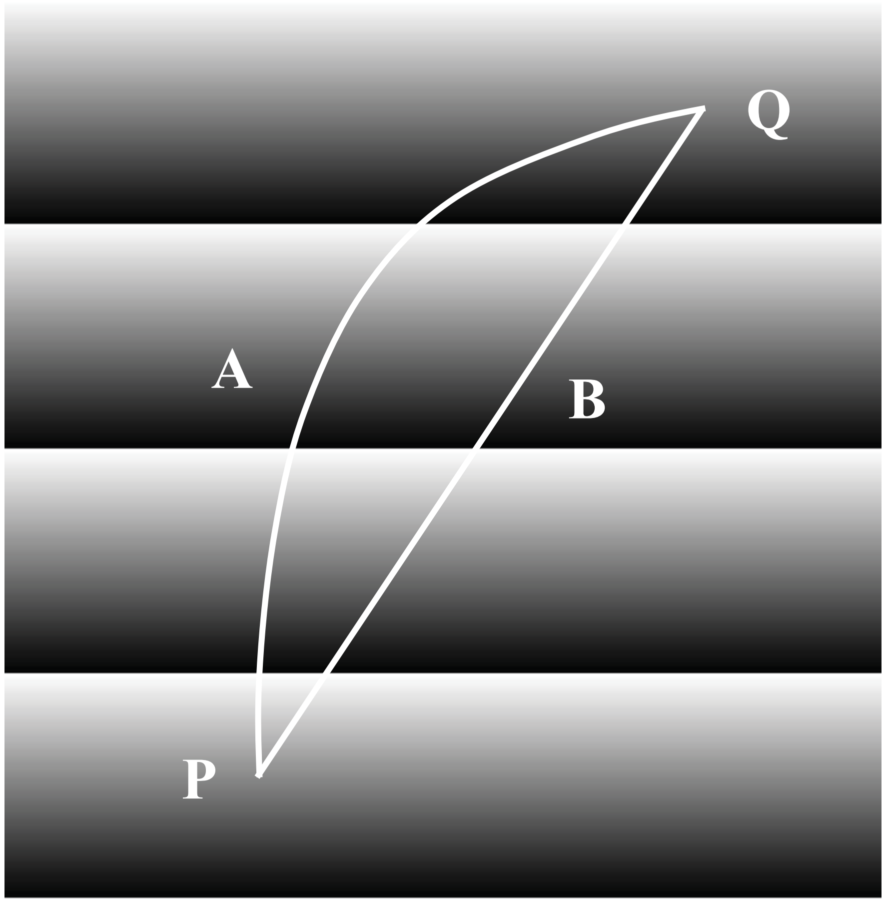

- Noise-free phase map
- Unwrap from P to Q
- Path A: 6π to be added to phase at Q
- Path B: 6π to be added to phase at Q

2-D unwrapping: example 2

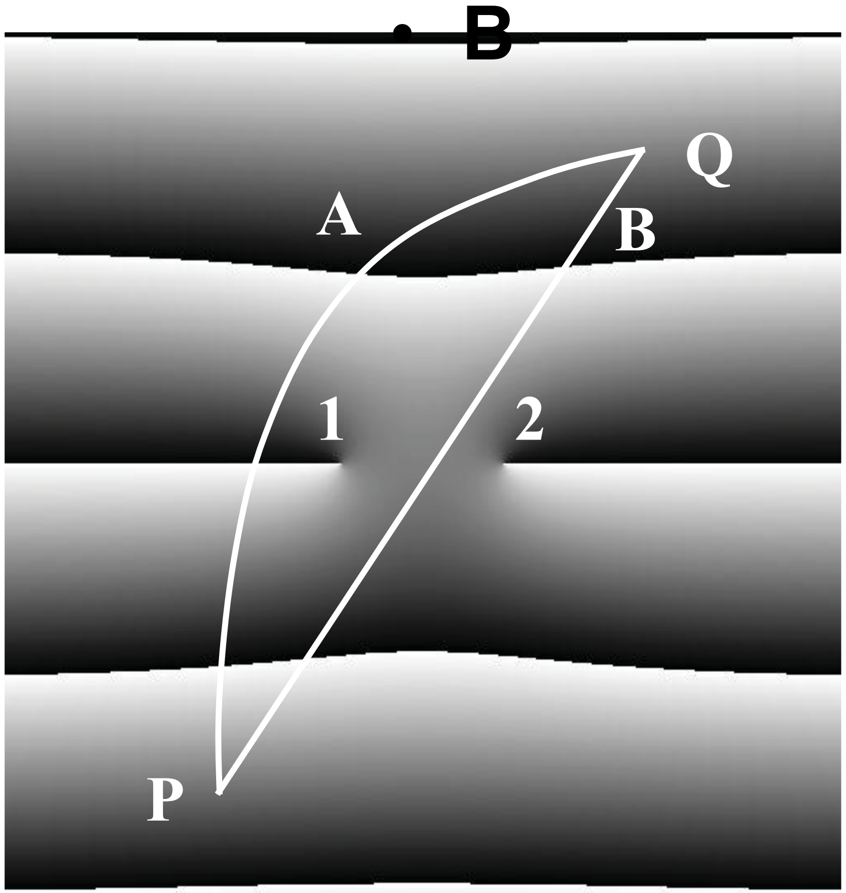

- Noisy phase map
- Unwrap from P to Q
- Path A: 6π to be added to phase at Q

BUT:

- Path B: 4π to be added to phase at Q

Path dependence is at the root of all 2-D phase unwrapping problems

"Discontinuity sources" 1 and 2 can be detected by unwrapping around closed loops of 2 x 2 pixels

Detection of discontinuity sources

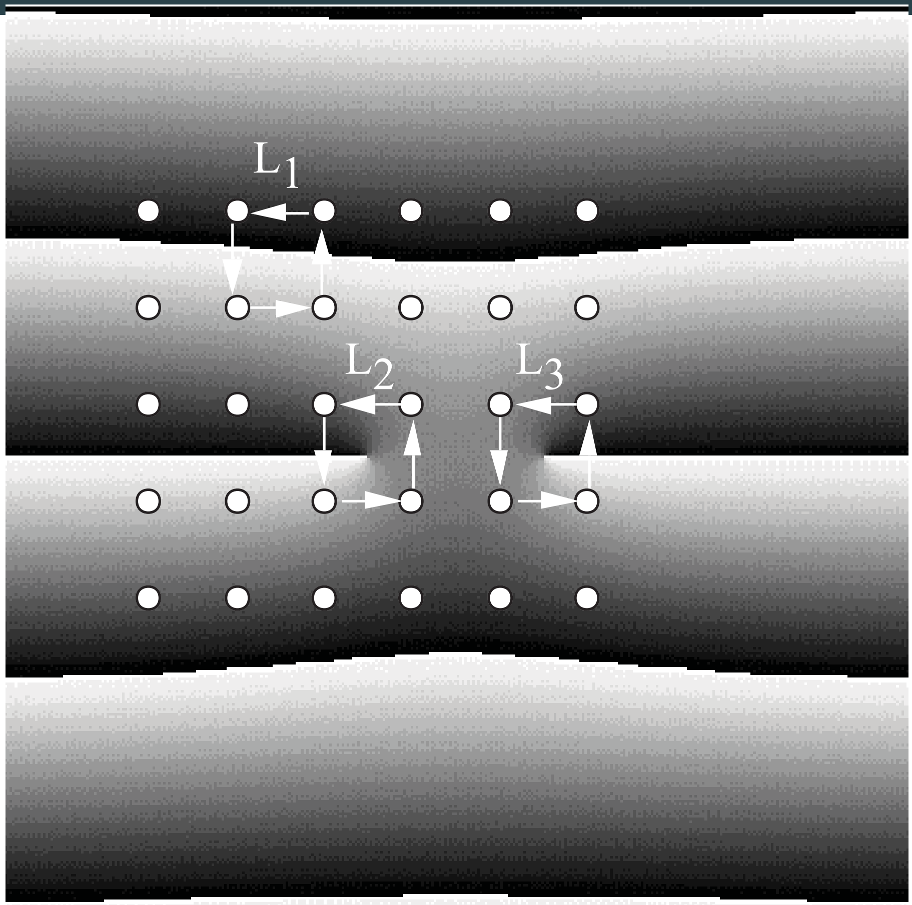

- Unwrap round 2 x 2 pixel squares starting at each pixel in the image
- Total number of 2π phase jumps, d, round the closed loop is zero except for a loop enclosing a discontinuity source

E.g.:

- Loop L_1: d = 0
- Loop L_2: d = 1
- Loop L_3: d = -1

Path-following unwrapping in 2-D

- Approach 1: try to avoid the regions of the phase map containing the discontinuity sources, e.g. using modulation information

  Robinson and Williams; Opt. Commun. **57** 26-30(1986)

  Kwon; Proc. SPIE **816** 196-211 (1987)

  Vrooman and Maas; Appl. Opt. **30** 1636-41 (1989)

  Takeda and Abe, Opt. Eng. **35** 2345-2351 (1996)

- Approach 2: place branch cuts between the +1 and –1 discontinuity sources to act as barriers to unwrapping. All possible unwrapping routes then give the same phase map

  Goldstein et al.; Radio Science **23** 713-720 (1988)

  Huntley; Appl. Opt. **28** 3268-70 (1989)

  Barr et al.; Opt. Eng. **30** 1405-14 (1991)

Cut-line method

Commercially used

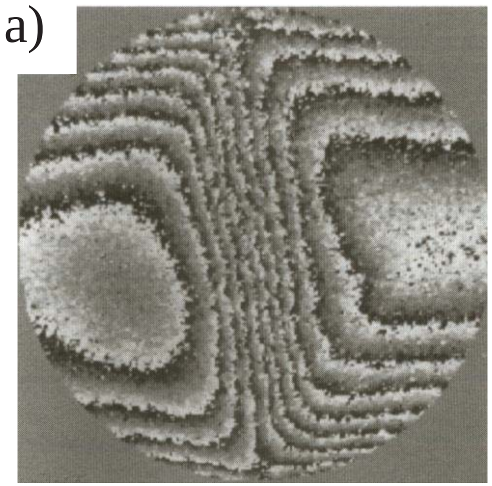

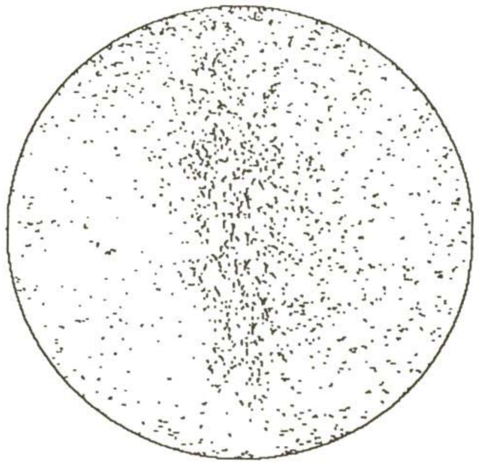

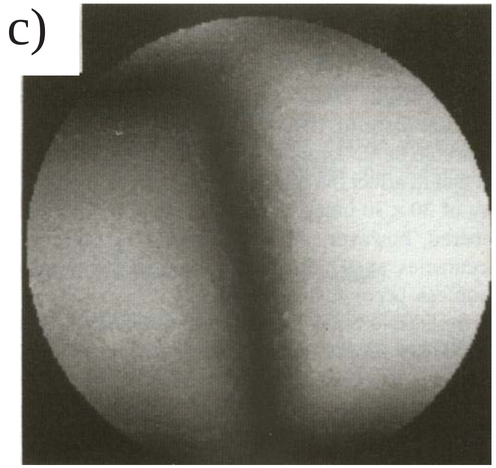

Phase fringes (from ESPI)

Cut-lines

Unwrapped phase

Numerical unwrapping – path dependent

Pixel queueing method (incl. Cut-lines method), which forms the queue of the nonprocessed pixels based on checking the quality of their neighbourhood

Minimum/maximum spanning tree method based on building up a reliable unwrapping path by checking the local gradient of phase or local modulation of signal

Commercially widely used

Sectioning by regions - unwrapping with simple algorithms (e.g. line-by-line) in the predefined regions and latter combining these regions)

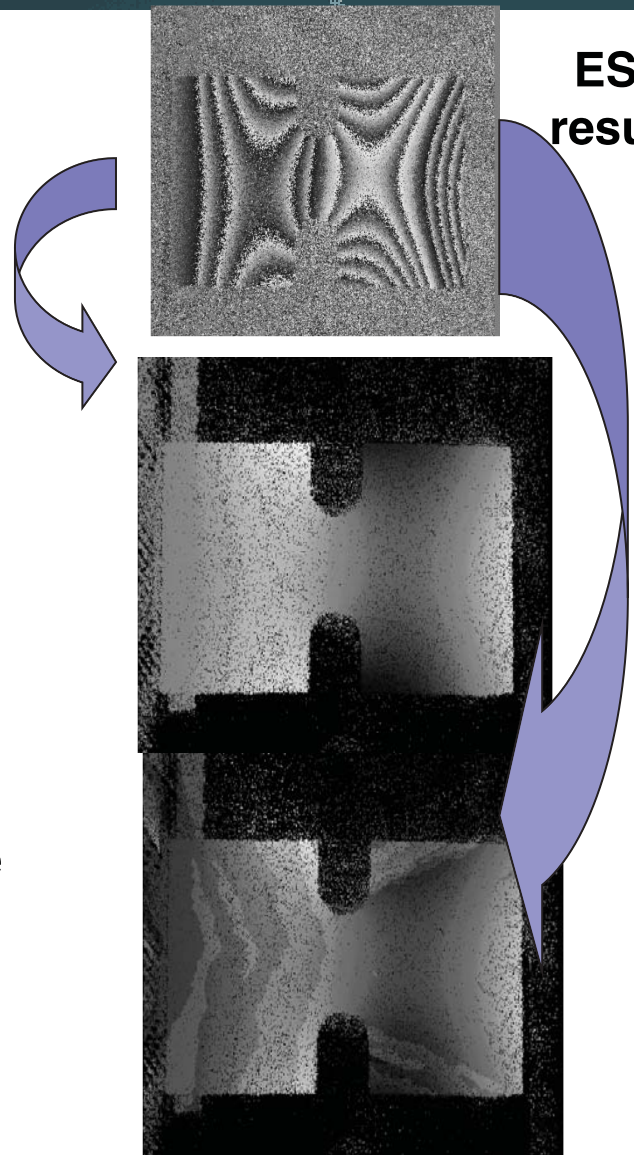

ESPI results

Path independent phase unwrapping
Unweighted least-squares phase unwrapping

- In two dimensions, choose the $\Phi_u(i,j)$ values that minimise S:

$$S = \sum_{i=1}^{N-1} \sum_{j=1}^{N-1} \{[\Phi_u(i,j) - \Phi_u(i-1,j)] - \Delta\Phi_w^{(x)}(i,j)\}^p$$

$$+ \sum_{i=1}^{N-1} \sum_{j=1}^{N-1} \{[\Phi_u(i,j) - \Phi_u(i,j-1)] - \Delta\Phi_w^{(y)}(i,j)\}^p$$

- Problem reduces to finding a solution to discretized Poisson equation
- Cosine transform provides one efficient solution method
  - Ghiglia and Romero, JOSA **11** 107-117 (1994)
- Problems:
  - Smoothes the data
  - Systematic under-estimation of phase gradients

Path independent phase unwrapping: Temporal phase unwrapping

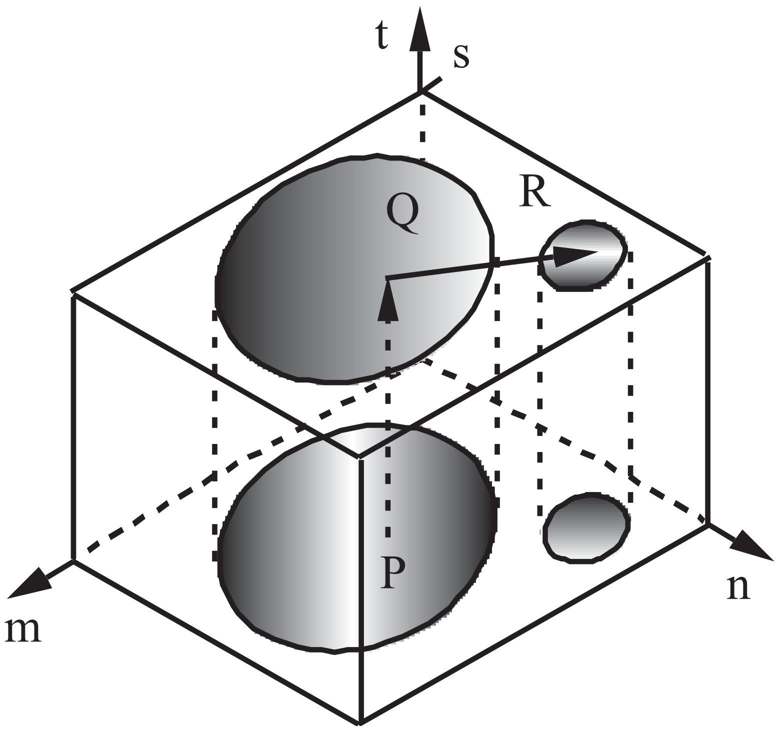

- Measure wrapped phase as a function of time, t
- Form a three-dimensional phase distribution, $\Phi(m,n,t)$
- Unwrap along the time axis (e.g. PQ) rather than spatially (e.g. QR)
- Avoids spatial propagation of unwrapping errors

BUT

- Large quantity of data to process

Temporal phase unwrapping

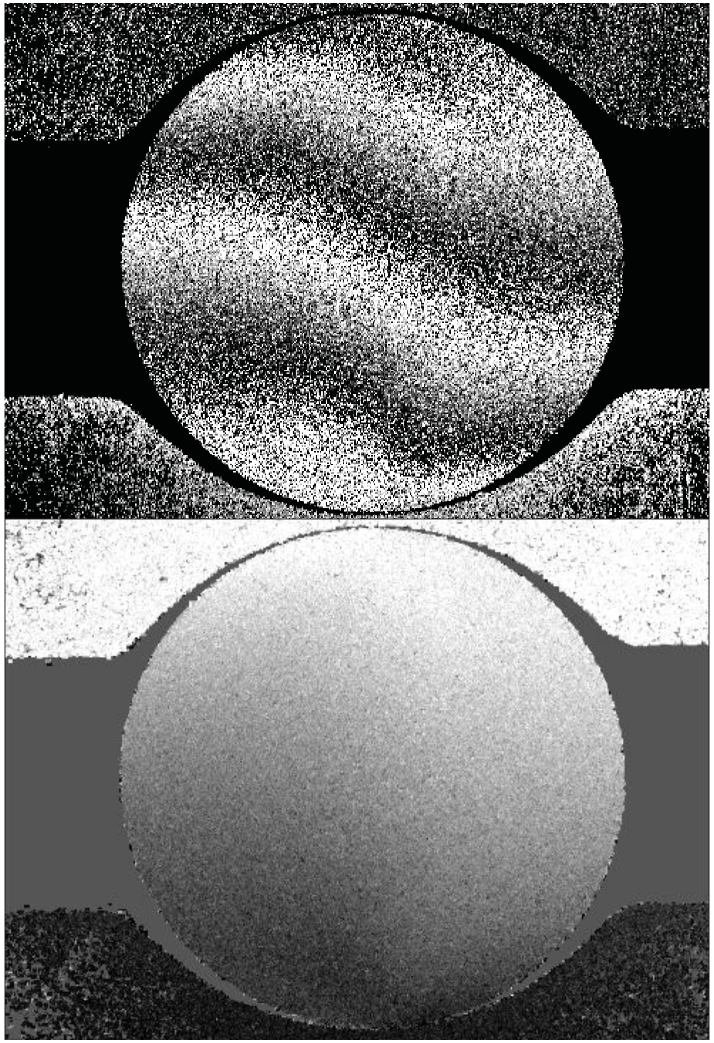

- Wrapped phase map from an in-plane speckle interferometer
- Total phase change between first and last in a sequence of 22 phase measurements
- Boundaries and noise prevent successful unwrapping
- Result of temporal unwrapping through the 22 intermediate phase maps
- Fully automated analysis: no data smoothing or specification of boundary positions required

Further solutions for absolute phase problems

In the case of physical discontinuity between regions or severl objects in the field of view the obtained phase values will be nonconsistent.

Solution :
Modification of system parameters

$$\left[\tilde{N}_m^n + \hat{N}\right]2\pi = \frac{2\pi}{\lambda} S^n(P_m) + N_R^n(P_R)2\pi$$

$$n = 1,\ldots..N \qquad m = 1,\ldots..M$$

Solving system for NM > 3M + N equation

- concept of synthetic wavelength
- concept of hierarchical measurement

Methods for the generation of synthetic wavelength

Method	Parameter	Synthetic wavelength
Symmetrical rotation of two grids	Rotation angle γ	$\Lambda^{(k)} = \frac{D}{2\sin\gamma^{(k)}}$
Variation of spatial frequencies of two grids	Difference of spatial frequencies (periods) $\Delta = D_1 - D_2$	$\Lambda = \frac{D^2}{\Delta D}$
Variation of the wavelength of the illumination beam	Difference of wavelengths $\Delta\lambda = \lambda_1 - \lambda_2$	$\Lambda = \frac{\lambda^2}{\Delta\lambda}$
Variation of the angle separation of the illumination sources where	Angle separation α	$\Lambda^{(k)} = \frac{\lambda}{2\sin\left(\alpha^{(k)}/2\right)}$

Wavelength scanning interferometry → white light interferometry

White light interferometry + PSM = wide range and high precission

Structured light method: Fringe and Gray code projection metod for 3D shape measurement

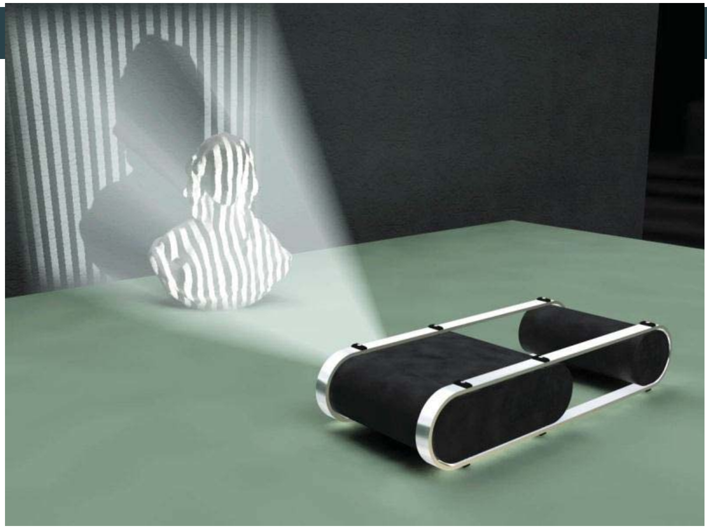

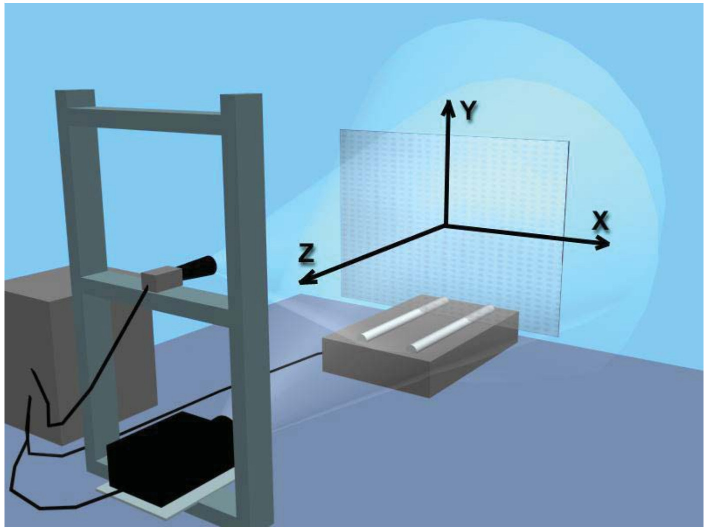

$$\Phi(i,j)\mathrm{mod}(2\pi) + N(i,j)*2\pi = \Phi(i,j)$$

Calibration

$$(i,j,\Phi) \rightarrow (x,y,z)$$

New challanges in 3D content capture

- Adding atributes to measured objects
- Automatization of measurement and processing

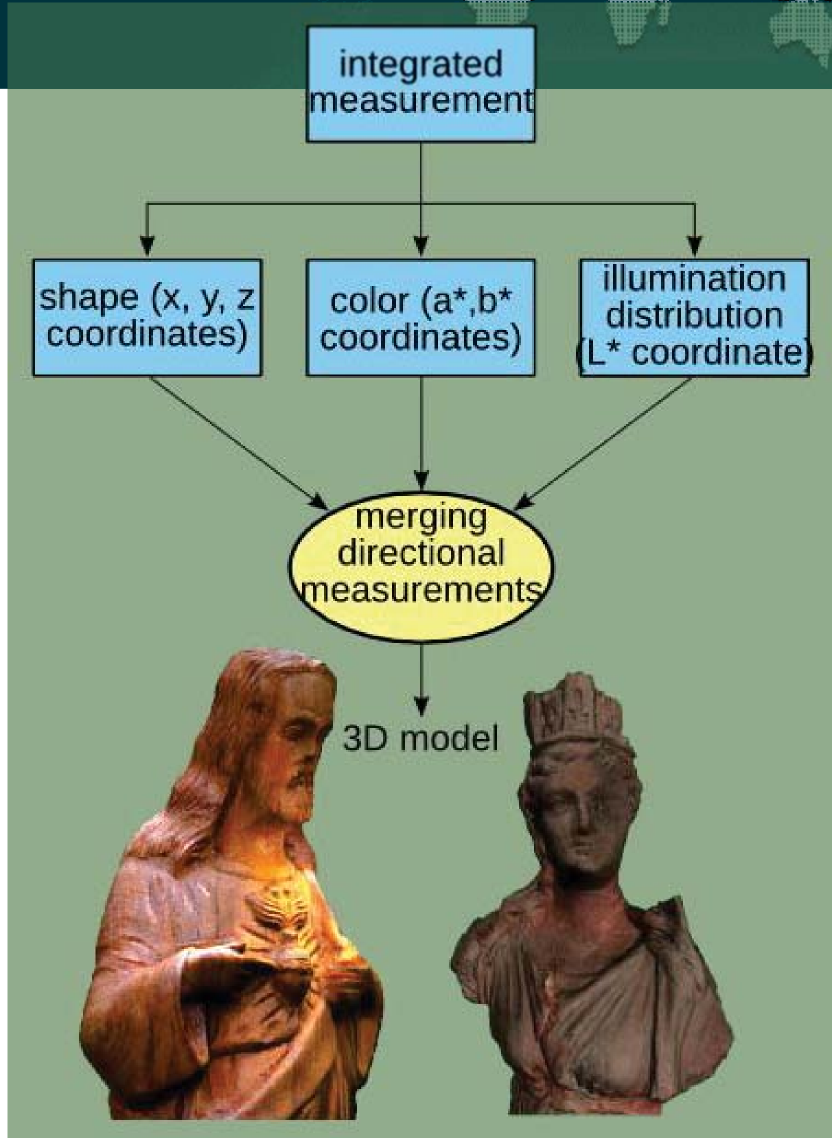

OGX I Automated

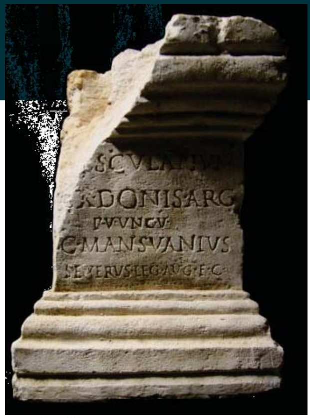

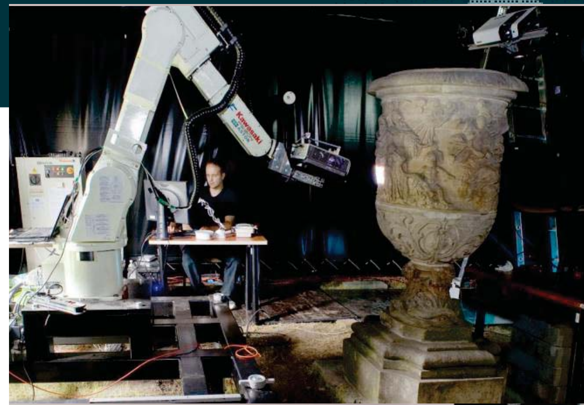

4D data capture - medical applications

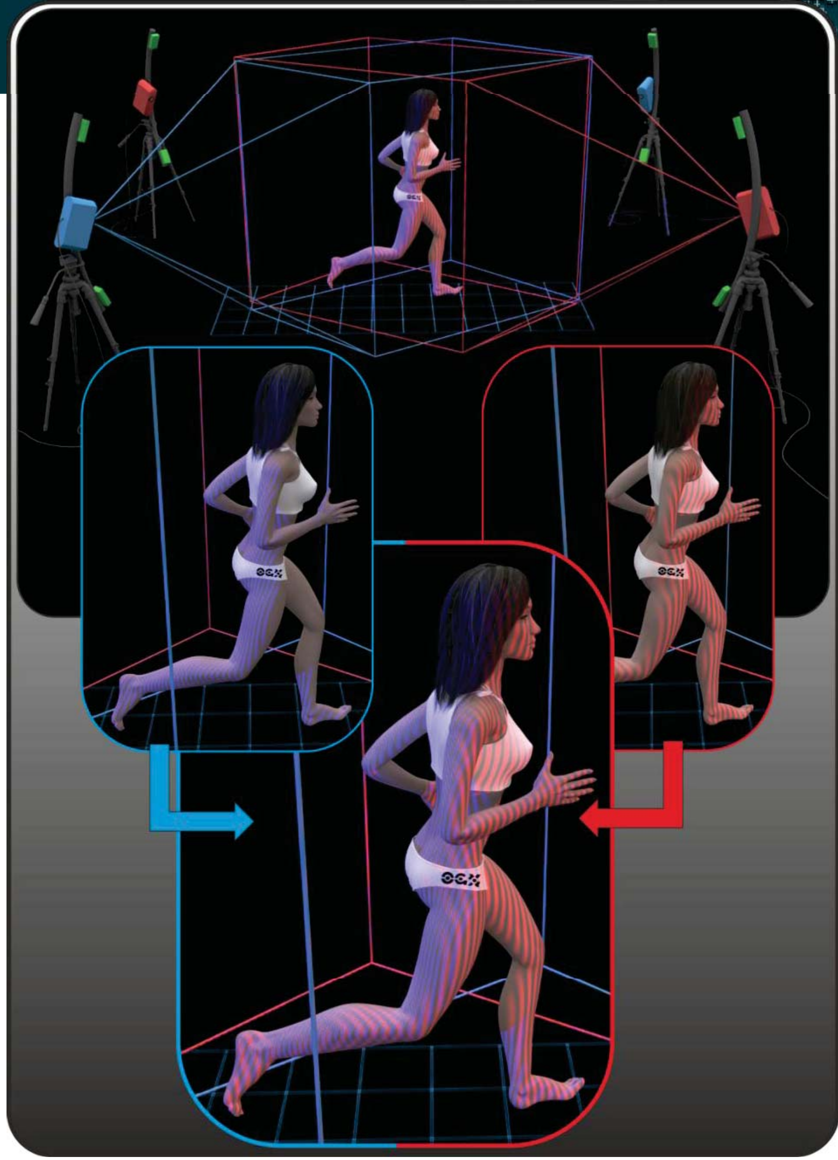

- Multidirectional measurement of static shape as well as dynamic surface coordinates

- Parameters:
  - **measurement volume**: 2m x 2m x 1,5m
  - **measurement uncertainty**: 0,4mm (static), 1mm (dynamic)
  - **measurement frequency**: 60Hz.

- Resulting data:
  - **4D coordinates** (x, y, z, t),
  - **movement parameters** (angles, corssections, etc).

Phase retrieval from speckle photography

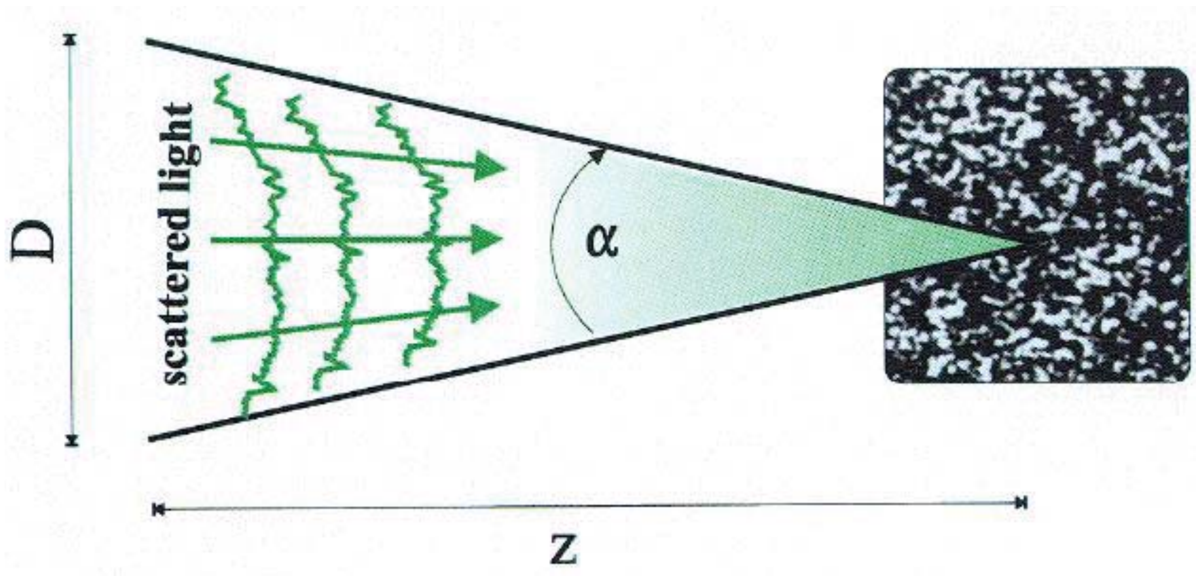

Mean speckle diameter: $d_{speckle} = 2.44\ \lambda\ z/D$

D : diameter of illuminated area … objective speckle
D : diameter of imaging lens … subjective speckle

So we can control the speckle size !!!!!

Speckle photography

Two speckle fields (representing the object states before and after deformtion) are incoherently superimposed to give information about in plane displacement

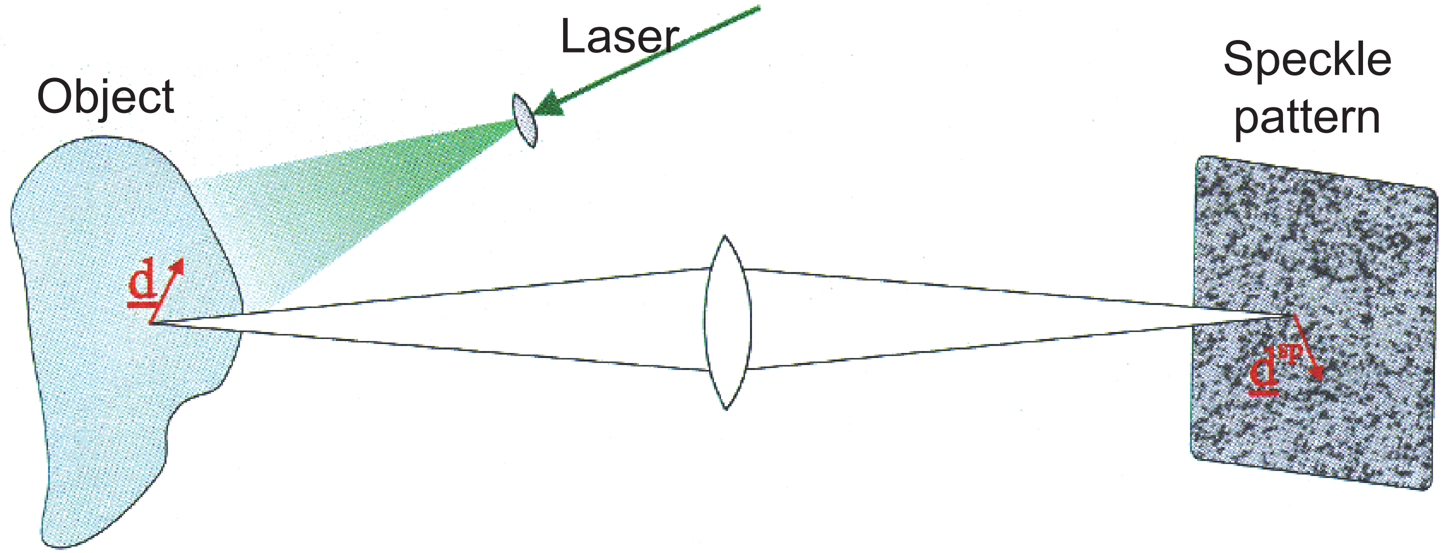

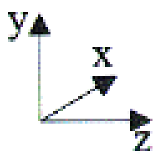

$$d_x = -1/m\ d_x^{sp}$$
$$d_y = -1/m\ d_y^{sp}$$

m- magnification

Measuring:
speckle displacement d^{sp}

a) Young's fringes
b) digital correlation

Optical methods of speckle pattern analysis

The specklegram + double exposure negative
The specklegram acts like the two apertures in Young's double Aperture interferogram

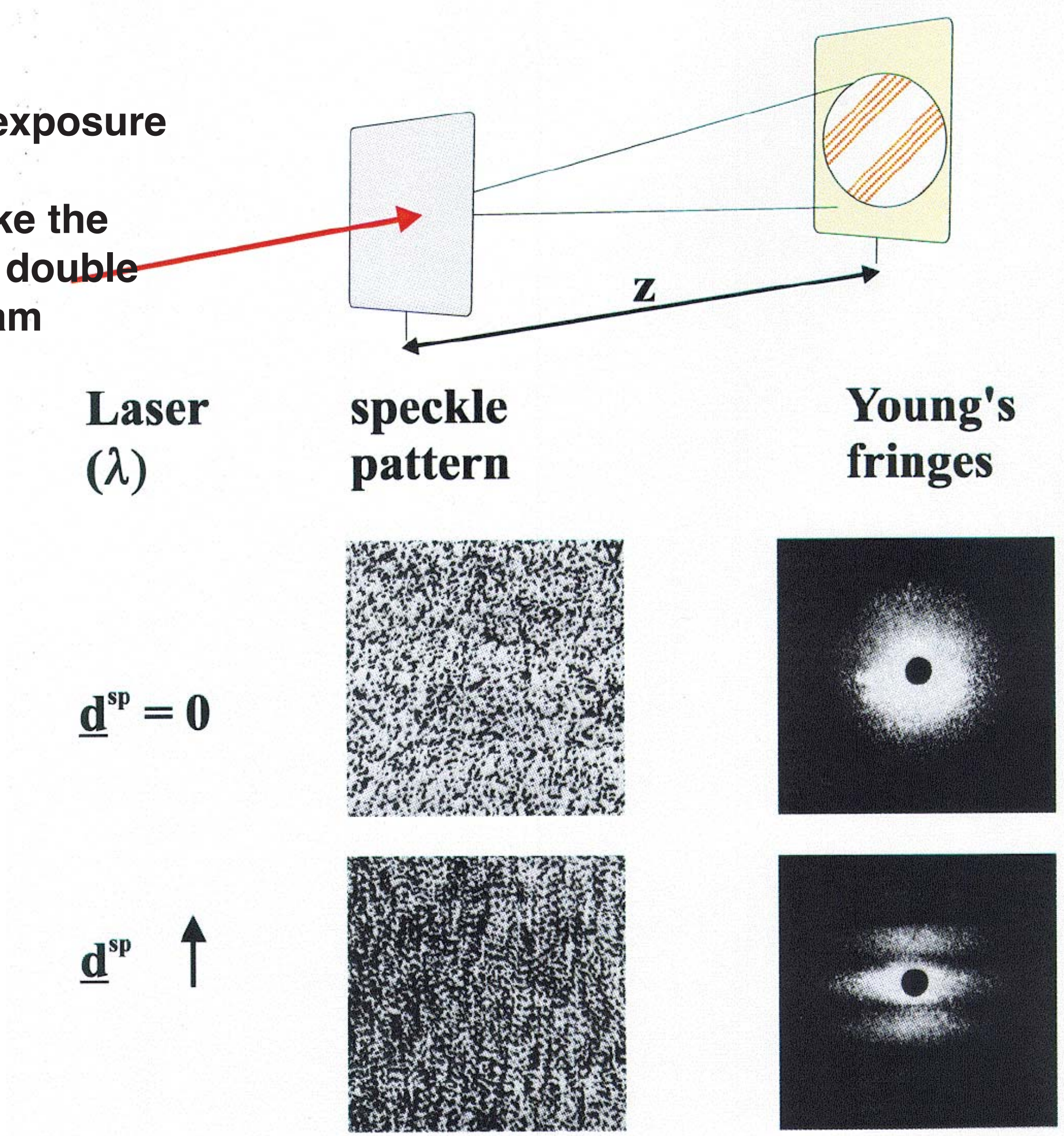

Point by point analysis

$$|d_x| = \frac{\lambda z}{m s_x}$$

$$|d_y| = \frac{\lambda z}{m s_y}$$

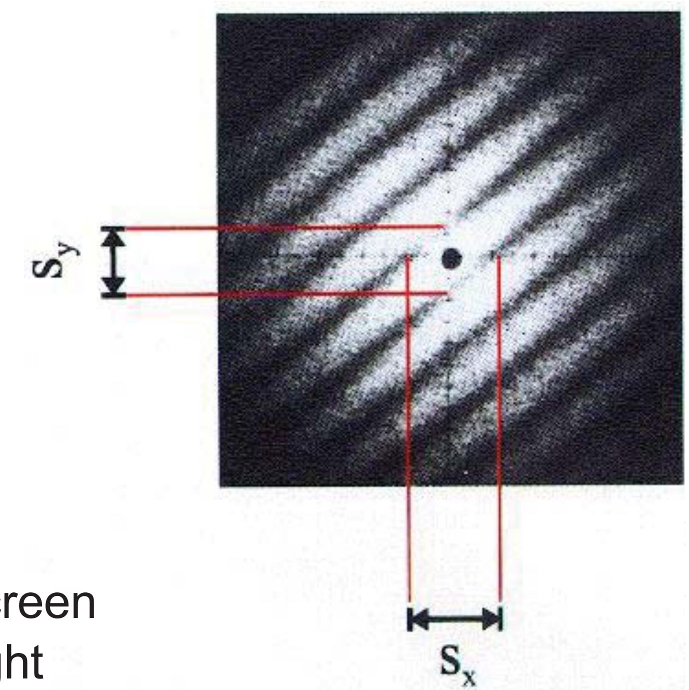

m … magnification
z … distance specklegram-screen
λ … wavelength of laser light

The orientation of the fringes is perpendicular to the direction of in-plane displacement

Speckle photography – optical analysis

1. Point-wise analysis system

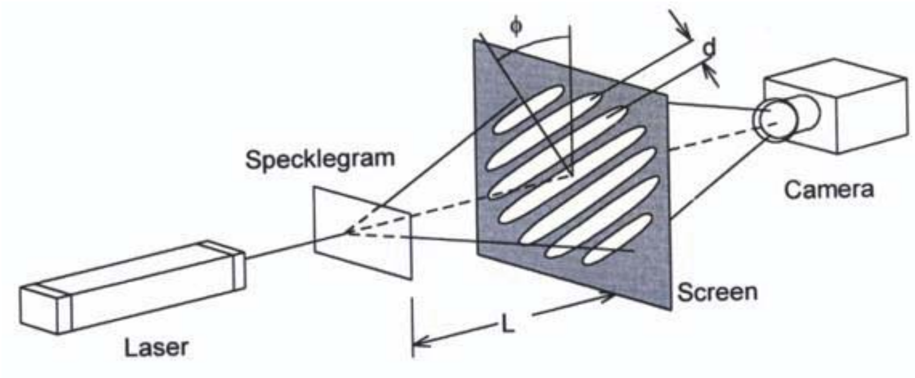

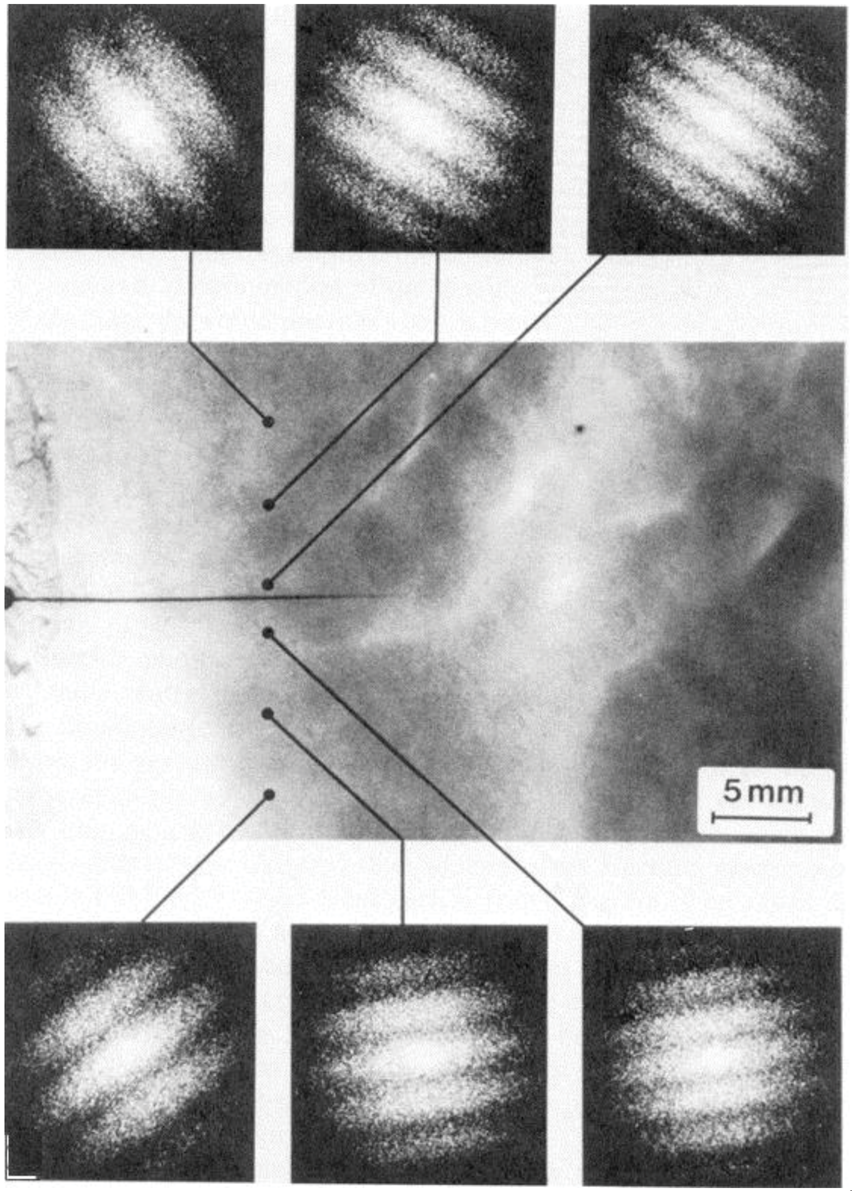

Fourier analysis of specklegram

Placing specklegram in an optical Fourier processor

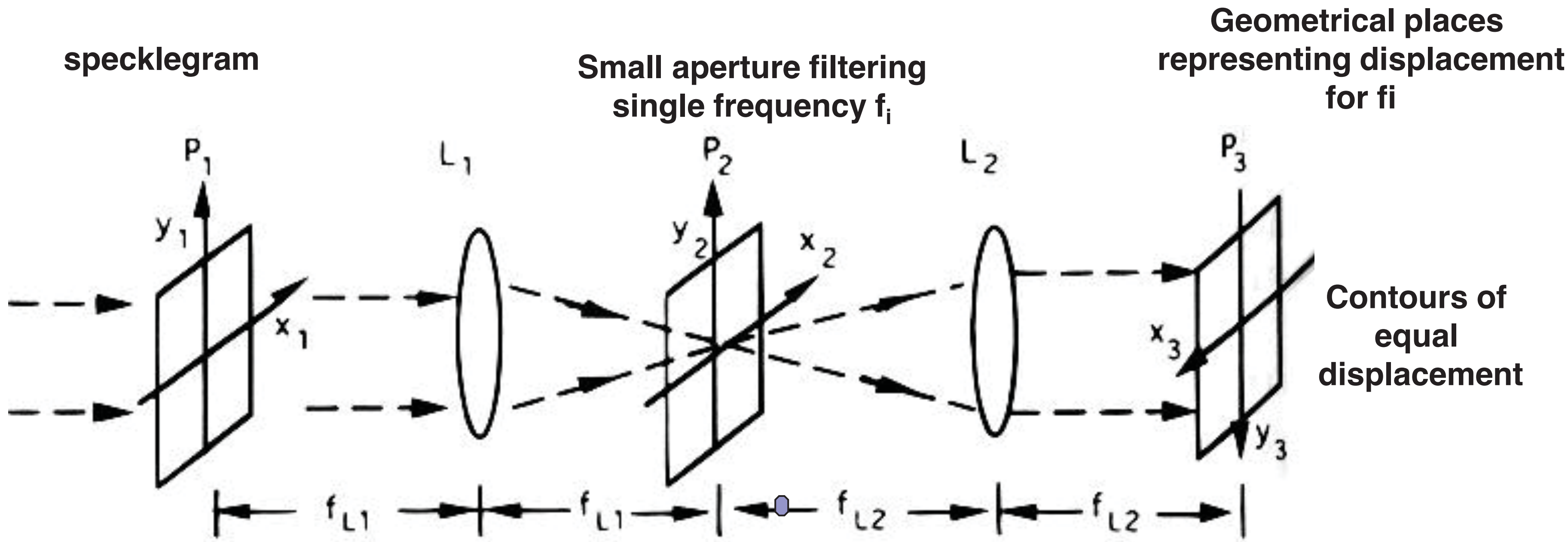

Digital Image Correlation technique

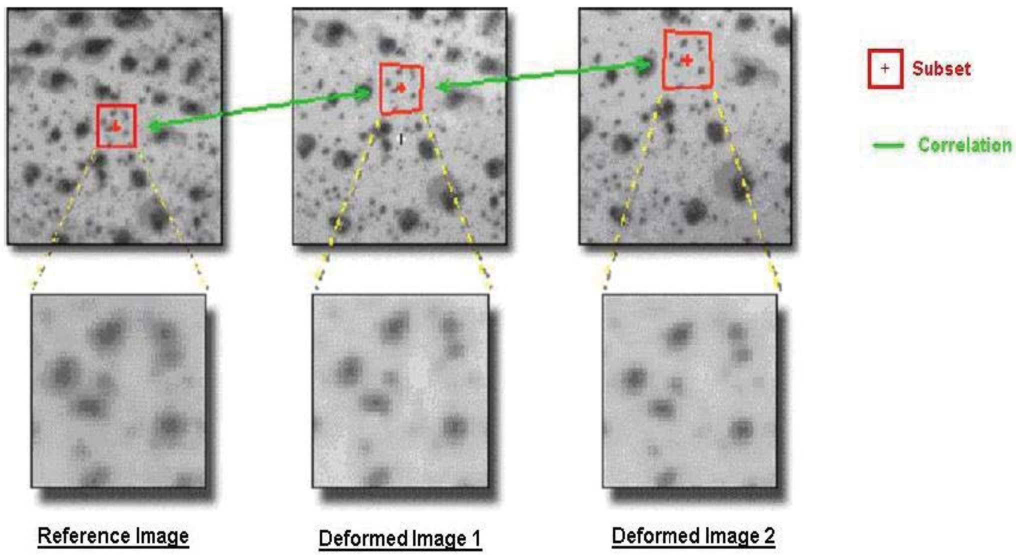

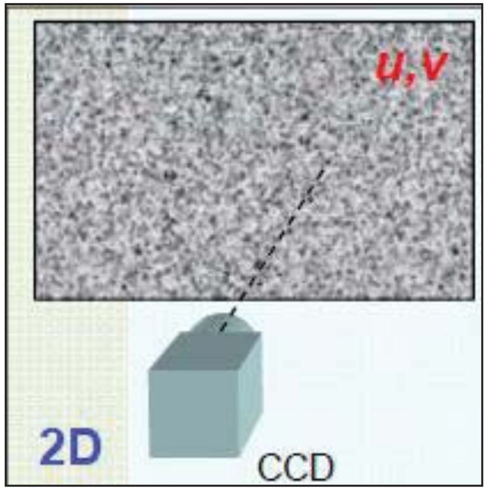

$$C_{normfg} = \frac{\sum_{i=1,j=1}^{n,m} f(i,j)\,g(i,j)}{\sqrt{\sum_{i=1,j=1}^{n,m} f(i,j)^2}\,\sqrt{\sum_{i=1,j=1}^{n,m} g(i,j)^2}}$$

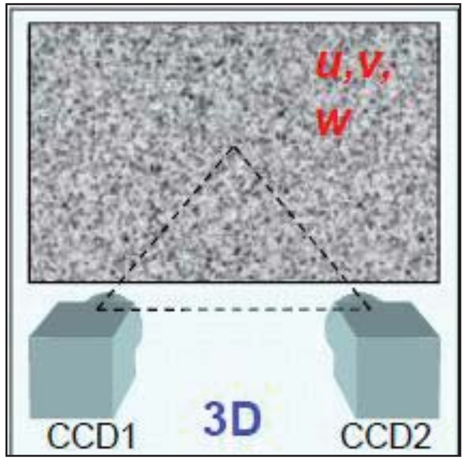

Digital Image Correlation technique

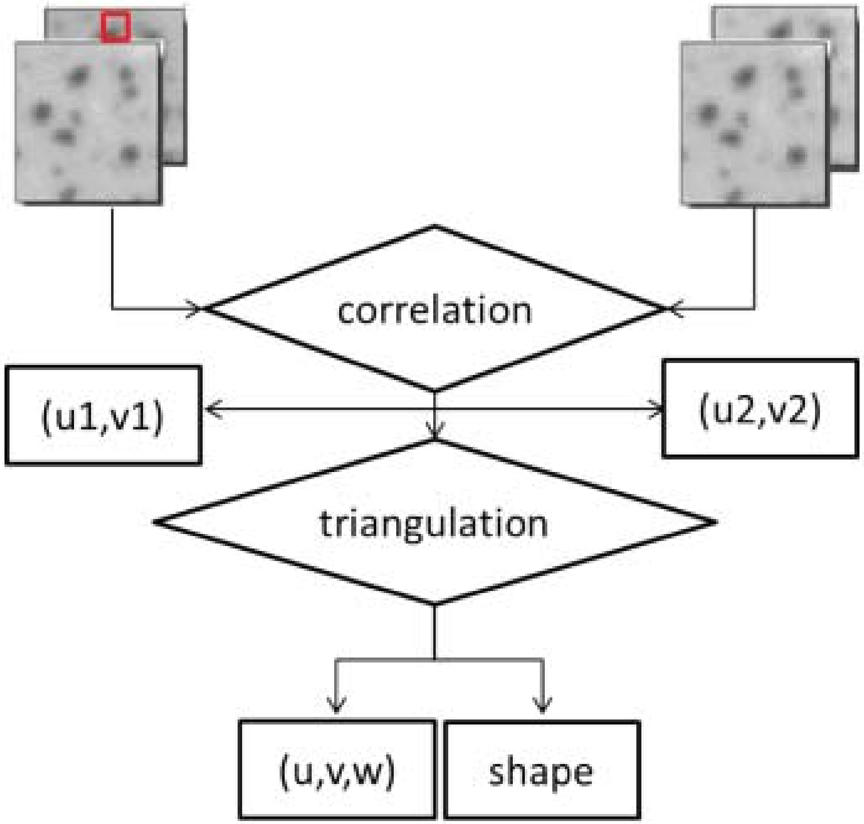

DIC data processing flow-chart

features of the DIC:

- full-filed non-contact measurements
- scalable field of view
- scalable and high accuracy
- relatively cheap hardware configuration
- flexibility with data acquisition frequency

Digital Image Correlation technique

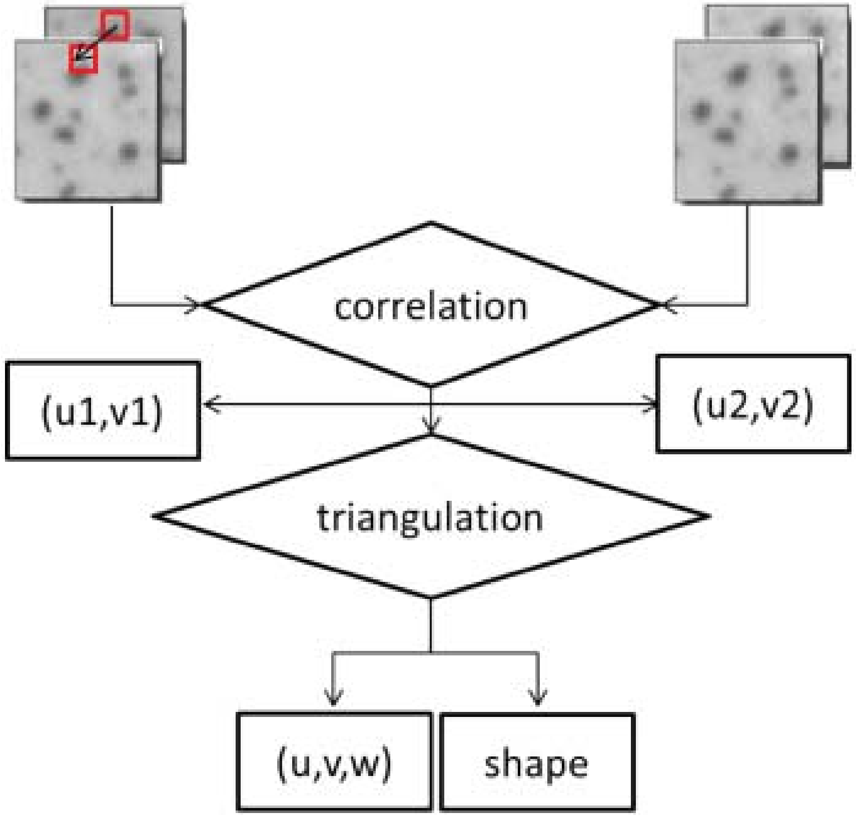

DIC data processing flow-chart

features of the DIC:

- full-filed non-contact measurements
- scalable field of view
- scalable and high accuracy
- relatively cheap hardware configuration
- flexibility with data acquisition frequency

Digital Image Correlation technique

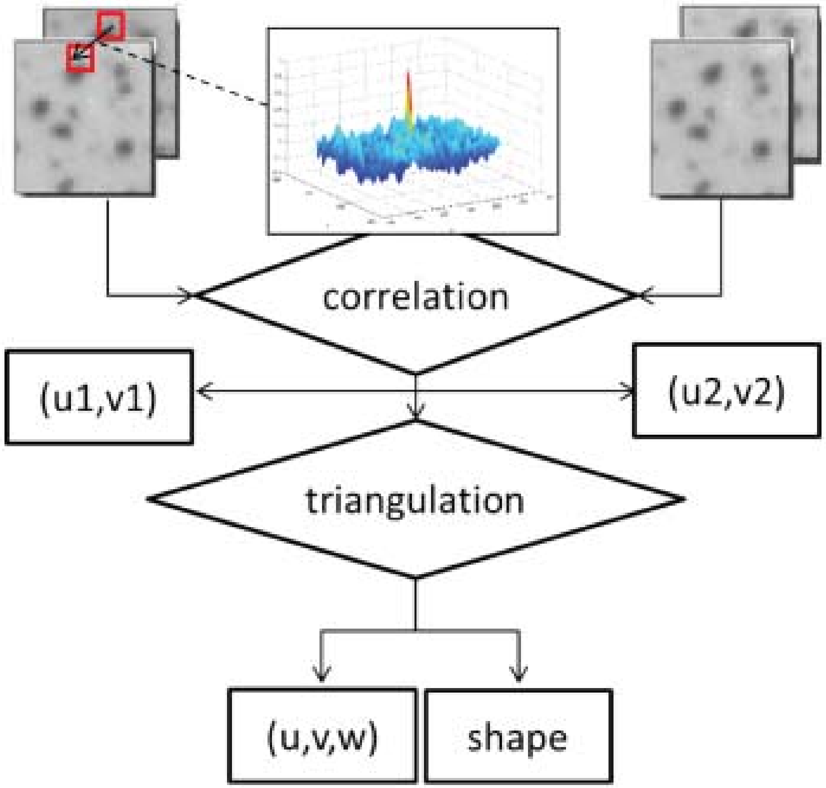

DIC data processing flow-chart

features of the DIC:

- full-filed non-contact measurements
- scalable field of view
- scalable and high accuracy
- relatively cheap hardware configuration
- flexibility with data acquisition frequency

Digital Image Correlation technique

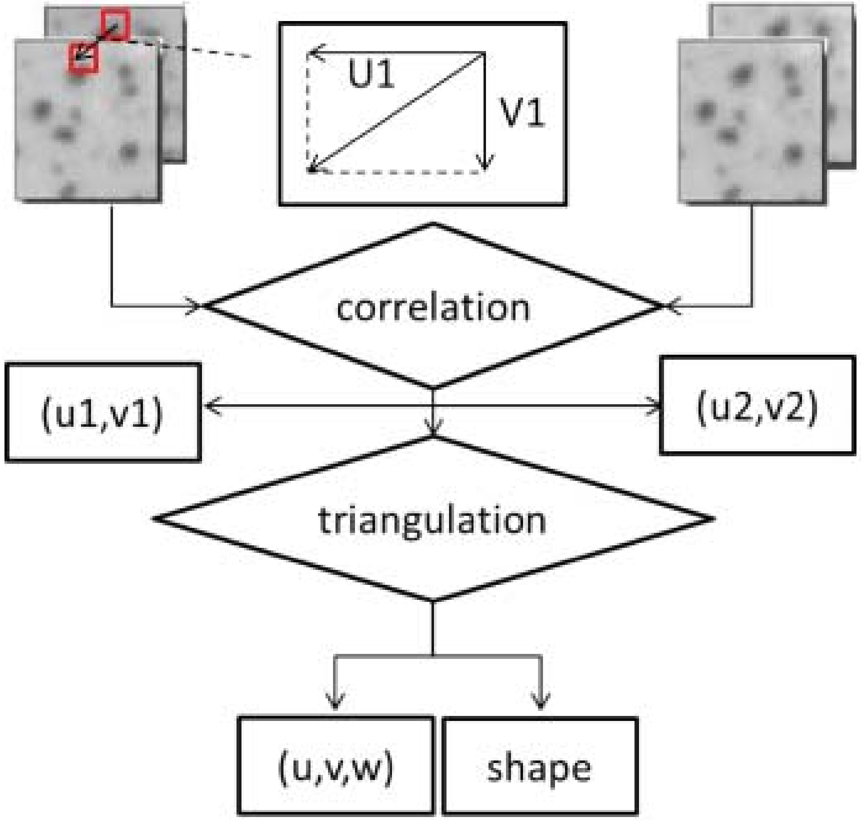

DIC data processing flow-chart

features of the DIC:

- full-filed non-contact measurements
- scalable field of view
- scalable and high accuracy
- relatively cheap hardware configuration
- flexibility with data acquisition frequency

Low-cost civil engineering structures

real object - part of a warehouse complex, 12m span and 45m length

physical representation - fragment of the metal-plate arch, 4 individual modules, 12m span

Measurements

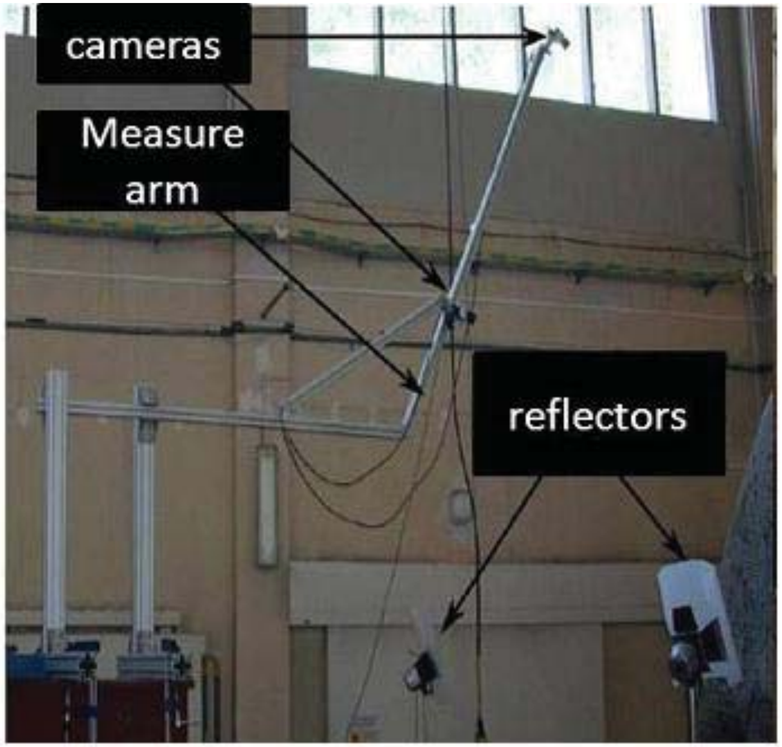

3D DIC setup on aluminium scaffold

- 2x 2Mpx AVT cameras equiped with 8mm focal lenght lenses
- 2x 650W halogen reflectors
- 2m x 2m FOV
- 1Hz acquisition frequency
- 0.05mm in-plane accuracy
- 0.07mm out-of-plane accuracy

3D DIC results

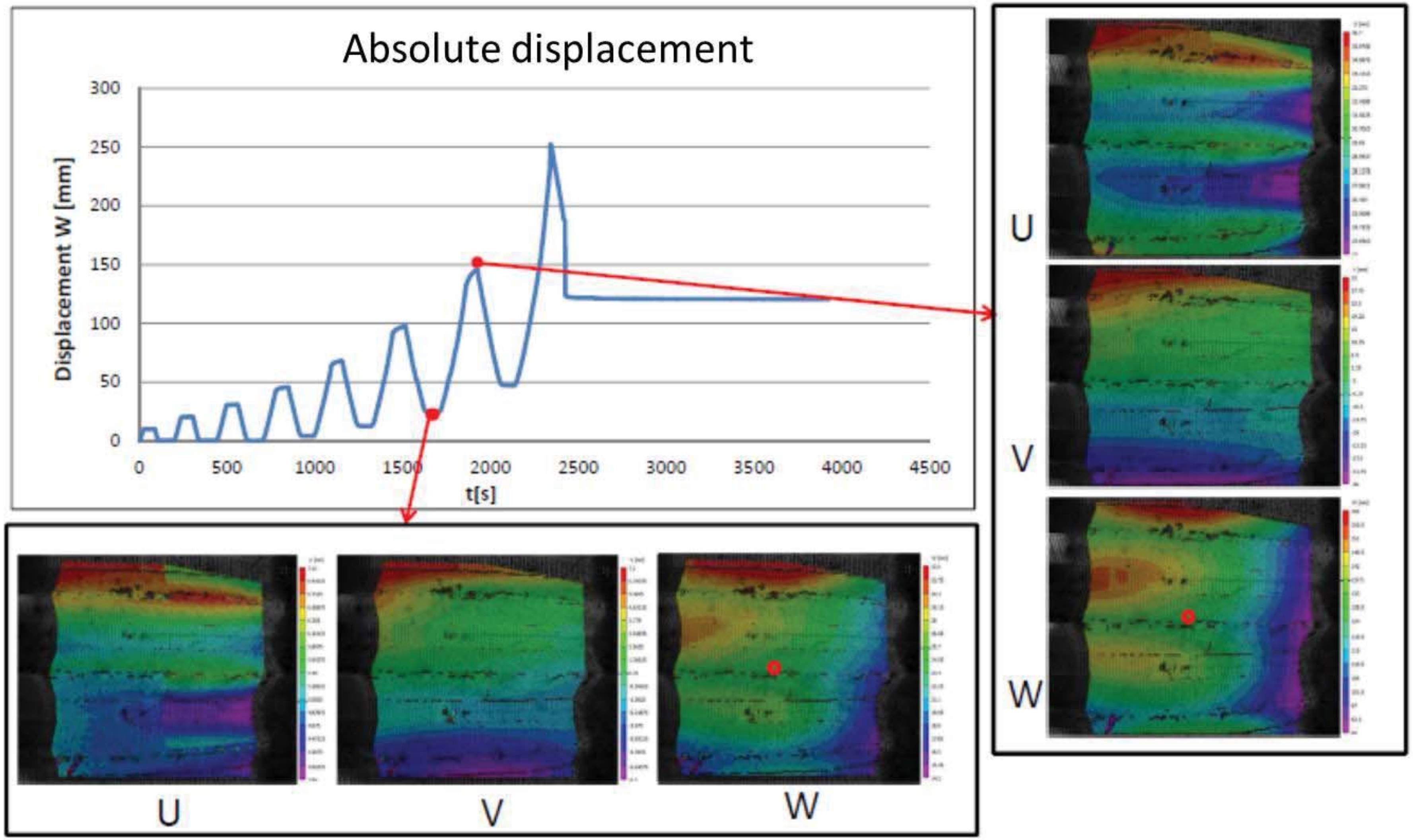

Canvas paintings measurements in changing environmental conditions

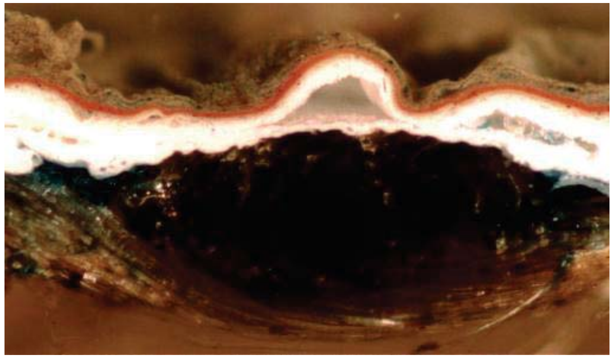

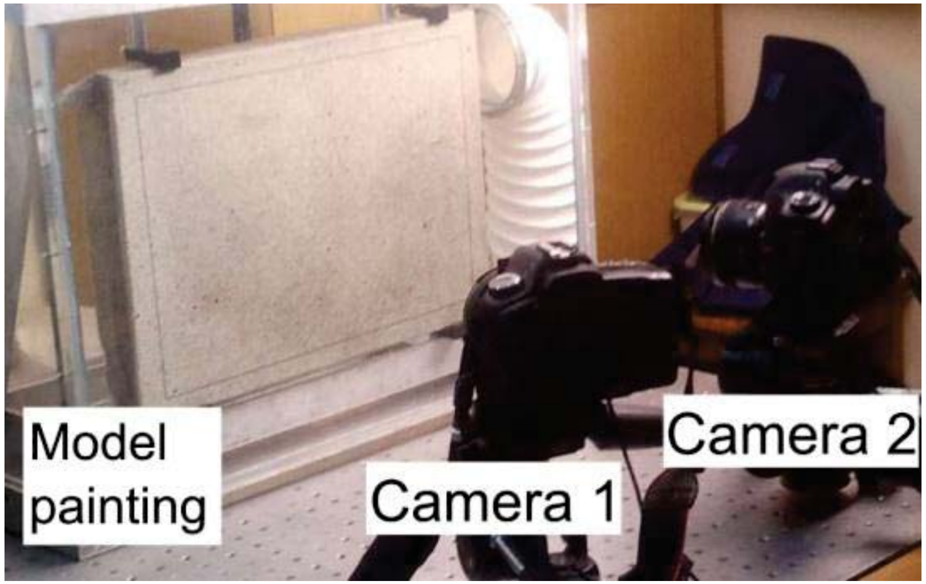

parametry:

- Cameras: 2x AVT Stingray 2Mpx
- Objectives : 2x Schneider Kreuznach 8mm
- Illumination: halogen lamp 650W
- fps: 1/20
- FOV: 0.4m x 0.3m
- accuracy: 0.02mm

Influence of a local repair of painting

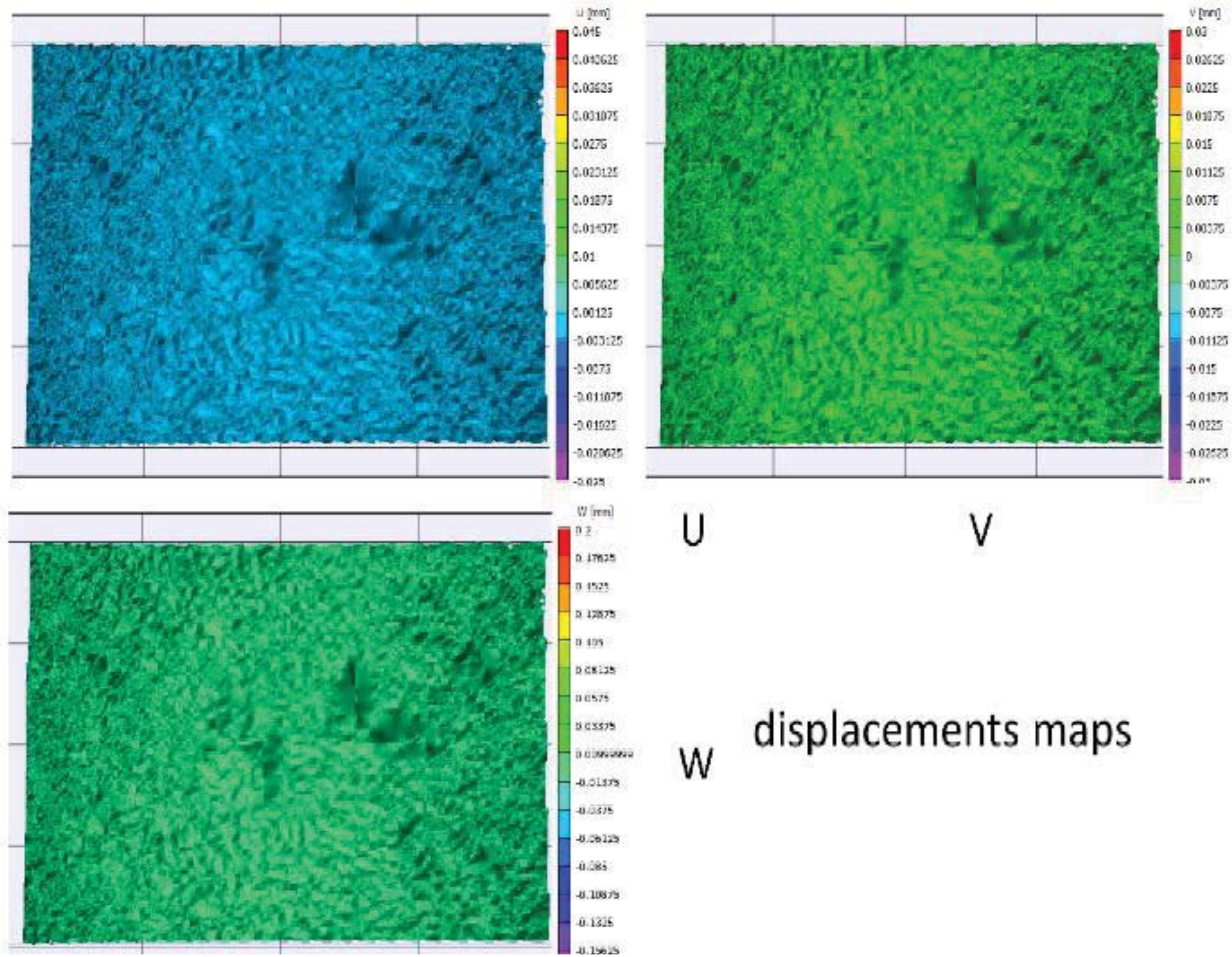

3D DIC Using natural texture

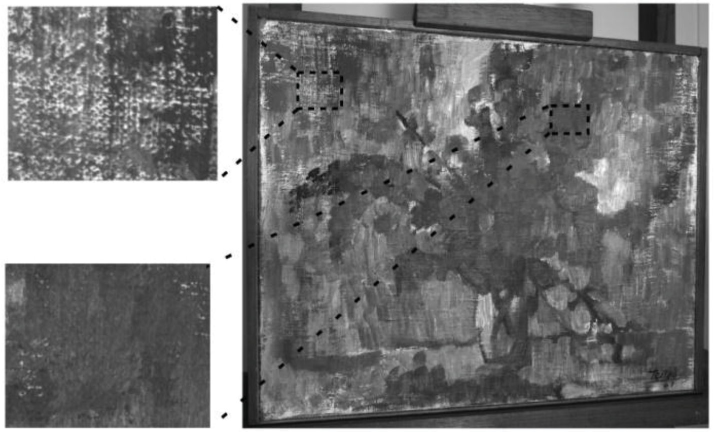

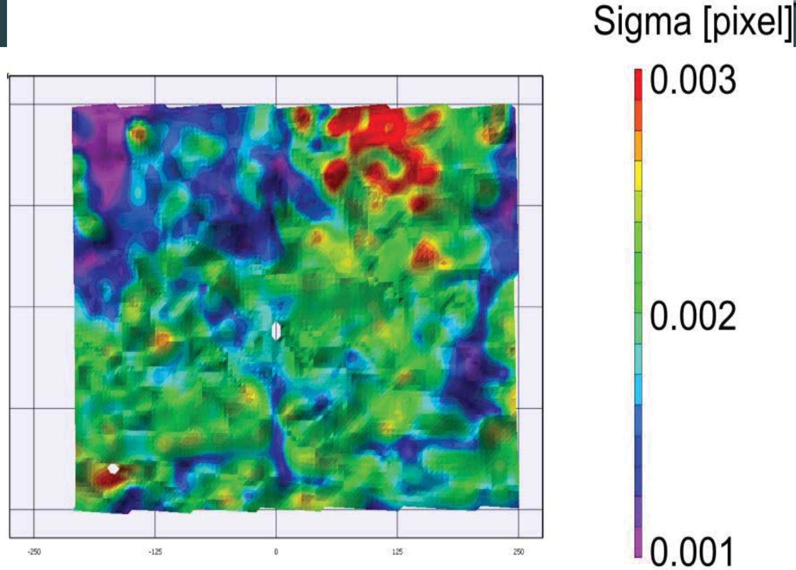

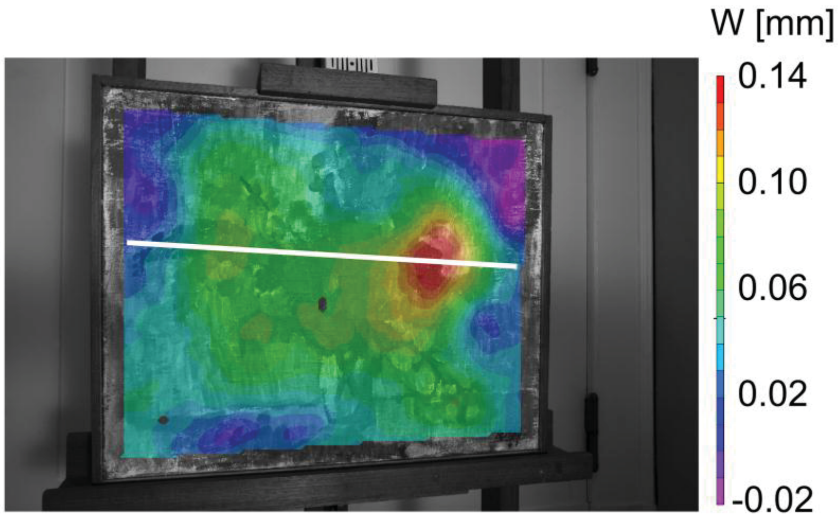

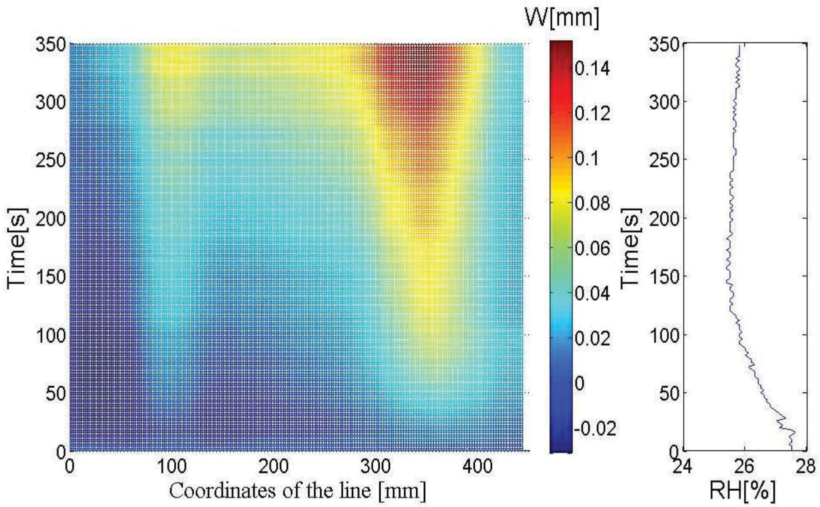

3D metrology of microobjects

Gathering data for tomographic reconstruction:

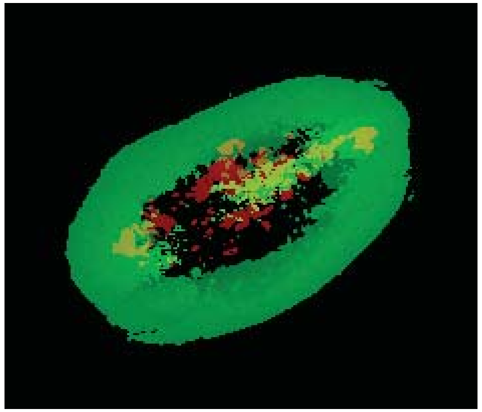

phase contrast microscopy – qualitative

interferometry - quantitaive

digital holography - quantitative

Can we convert optical microscope into quantitative phase measuring device???

Can we get 3D information about phase (refractive index distribution??

How We Usually Measure Phase

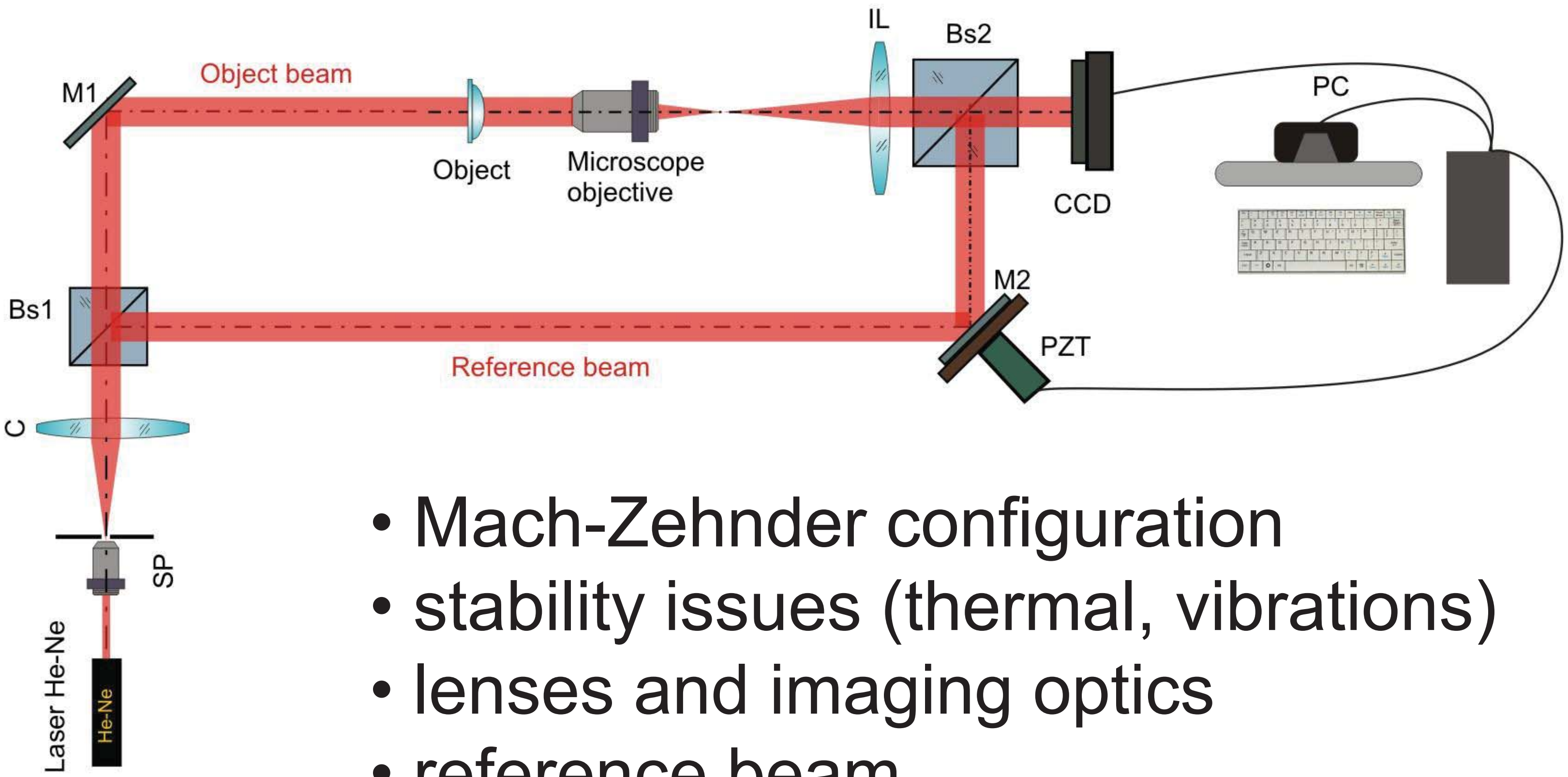

- Mach-Zehnder configuration
- stability issues (thermal, vibrations)
- lenses and imaging optics
- reference beam
- interference pattern

What we need

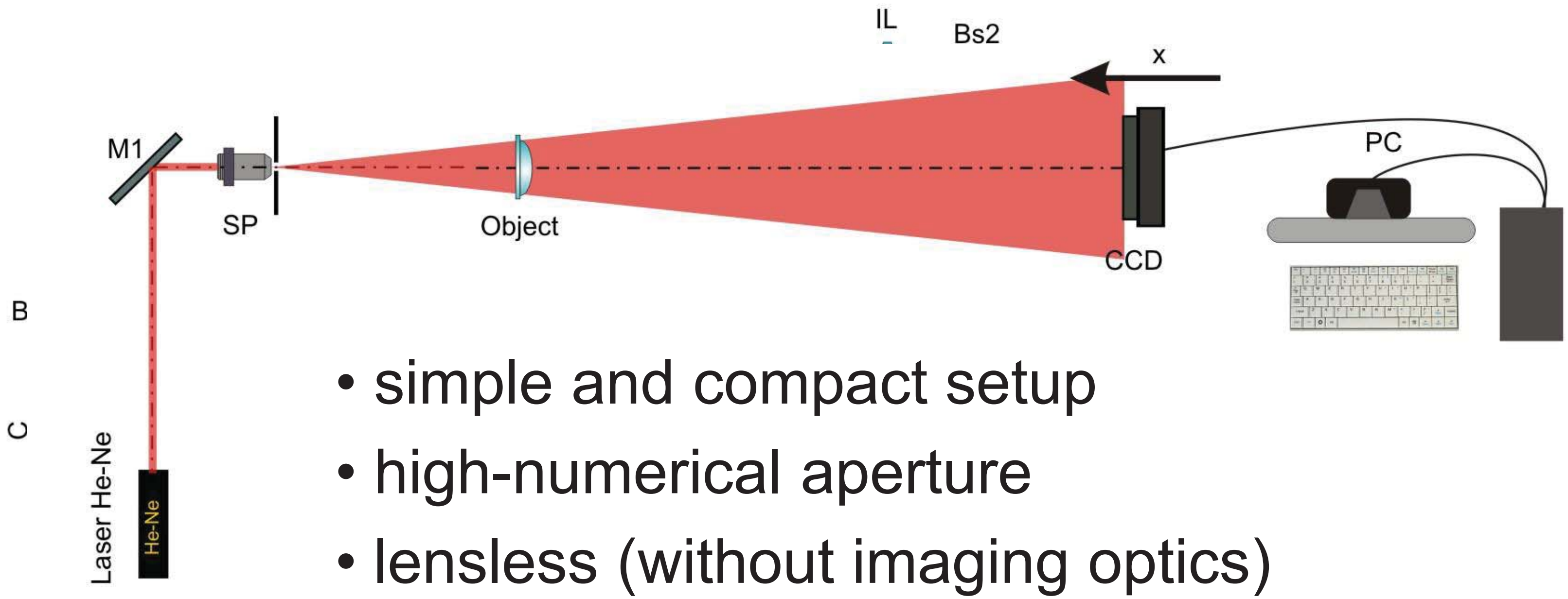

- simple and compact setup
- high-numerical aperture
- lensless (without imaging optics)
- no reference beam
- intensity distribution

Are there methods of object phase recovery that would enable design and development of quantitative phase object imaging and thereby **bridge a conventional microscope with a digital holographic microscope**

Single beam phase retrieval algorithms

- In-line digital hologram

• Transport of Intensity Equation
• Itrerative algorithms based on wave propagation

Digital In-Line Holographic Microscope

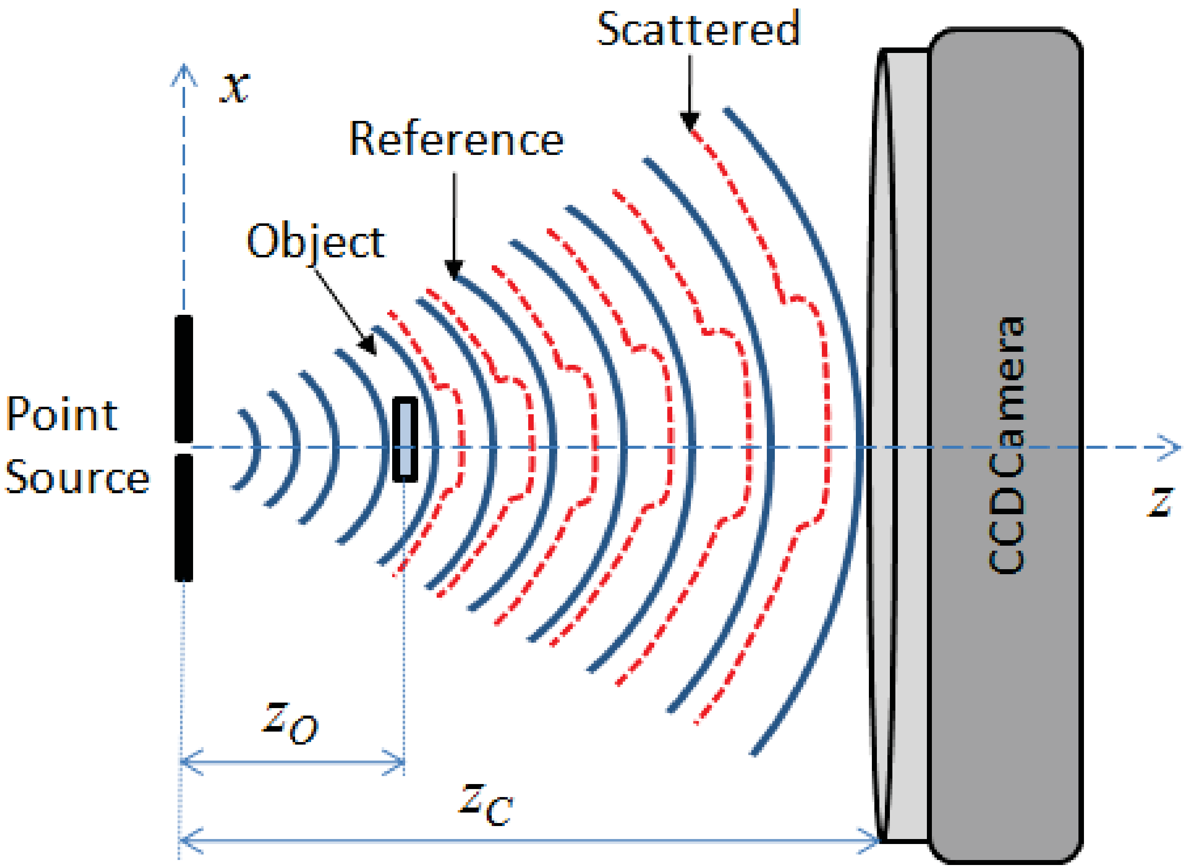

<u>final idea:</u>

- single beam
  - high-NA
- nonlin. magnification
- lensless
- no reference arm
- partial coherent light

1.) Phase Retrieval Algorithms

2.) Wave Propagation Techniques

3.) Image Formation System & Sampling Issues

State of the Art (1)

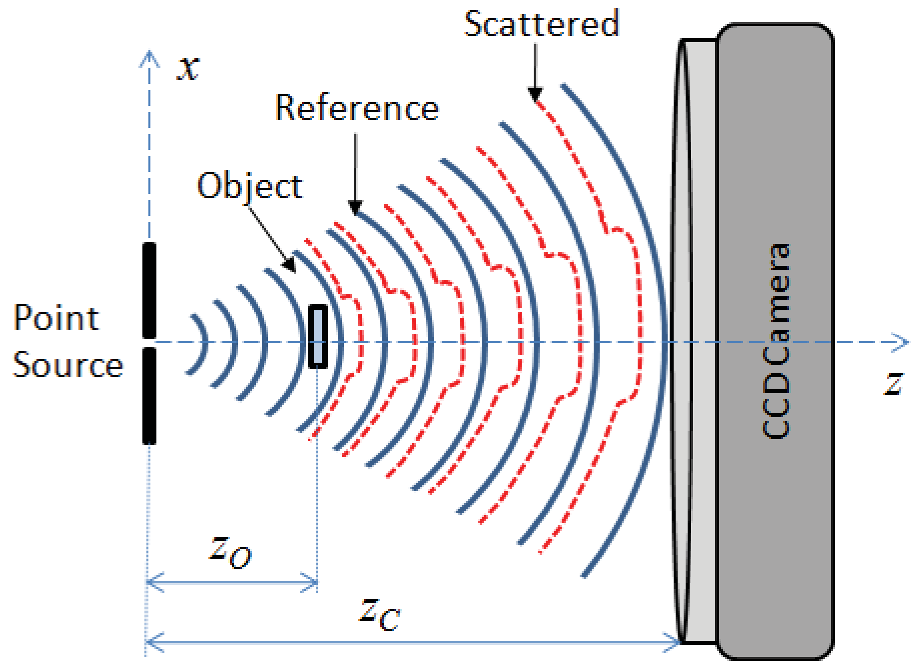

$$I = |A_{ref} + A_{obj}|^2 = A_{obj}A_{obj}^* + A_{ref}A_{ref}^* + A_{obj}A_{ref}^* + A_{ref}A_{obj}^*$$

$$\tilde{I} = |A_{ref} + A_{obj}|^2 - A_{ref}A_{ref}^* = A_{obj}A_{obj}^* + A_{obj}A_{ref}^* + A_{ref}A_{obj}^*$$

$$H = A_{ref}\tilde{I} = A_{ref}(A_{obj}A_{obj}^* + A_{obj}A_{ref}^* + A_{ref}A_{obj}^*)$$
$$= A_{ref}I_{obj} + A_{obj}I_{ref} + (A_{ref})^2 A_{obj}^*$$
$$\sim A_{ref}I_{obj} + A_{obj}I_{ref} + I_{ref}A_{obj}^* \quad (A_{ref} = A_0 e^{-jkz}, z \to 0)$$

wave propagation techniques needs to be applied

State of the Art (2)

Centre for International Cooperation

Phase Retrieval

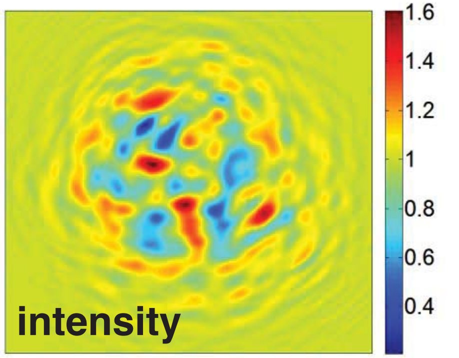

wave propagation

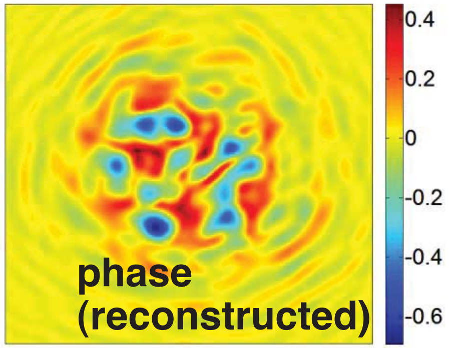

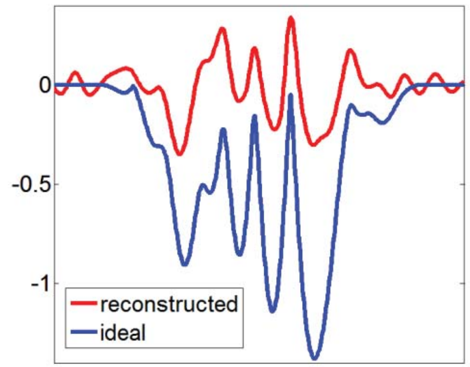

camera plane

object plane

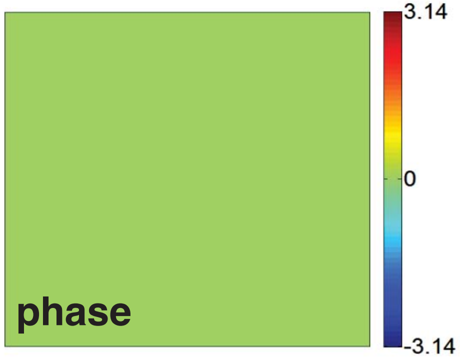

$$|\Delta\varphi| \leq \frac{\pi}{2}$$

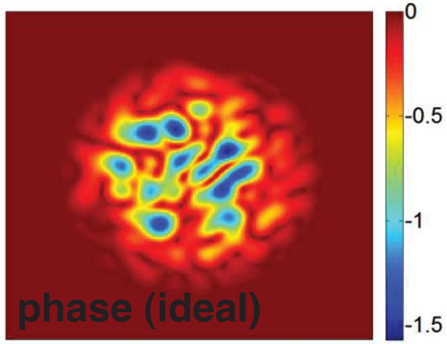

state of the art does not allow accurate object reconstruction.

1 Plane, z=6.33mm, N = 512, λ = 0.633um, Δx = 3.45um, SNR = 25dB (=256:15)

Commercial Microscope

Phase Retrieval

Centre for International Cooperation

Resolution Optics Microscope with <u>HoloSuite 3D Software:</u>

- produces high contrast images
- good qualitative results
- very poor quantitative results

HoloSuite3D Software ®

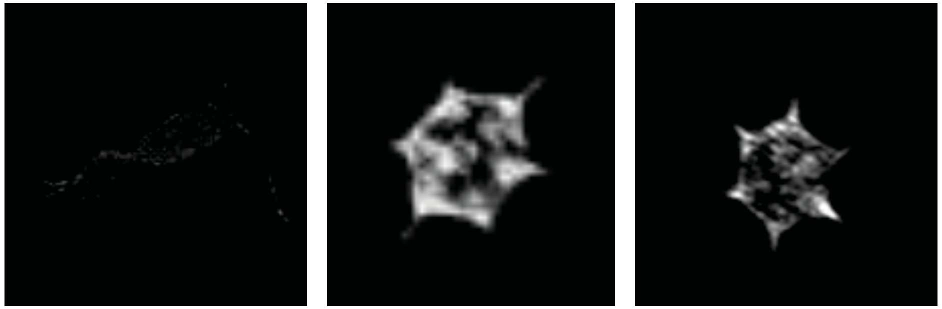

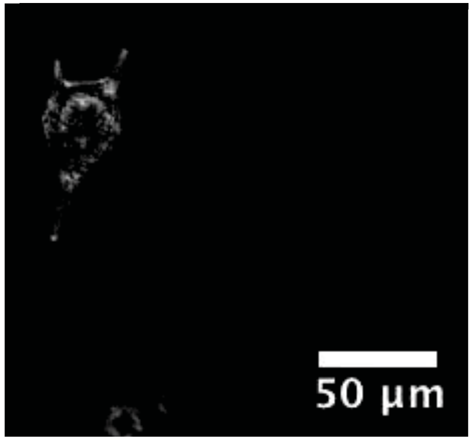

- Jericho, M. H., Kreuzer, H. J., et. al., (2010). Planetary and Space Science, 58(4), 701–705.
- Xu, W., Kreuzer, H. J., et. al., (2001). Proc. of the National Academy of Sciences of USA98(20), 11301–5.
- Xu, W., Kreuzer, H. J., et. al., (2002). Appl. Opt. 41(25), 5367–75.

3D phase – Phase Retrieval from multiple planes

Experimental setup:

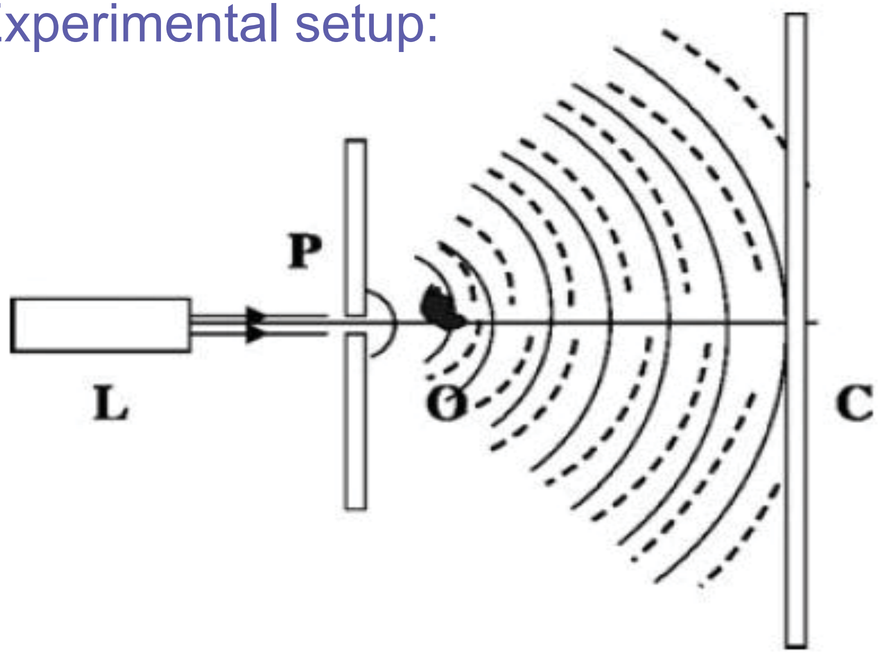

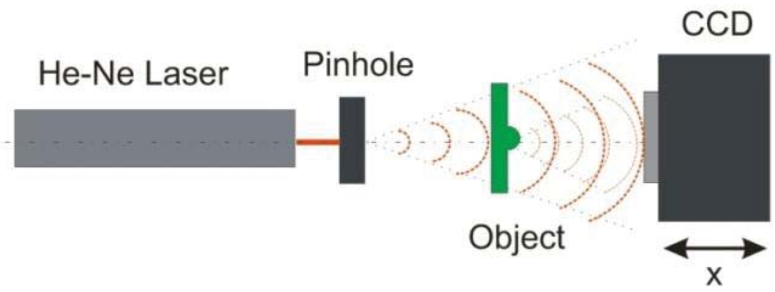

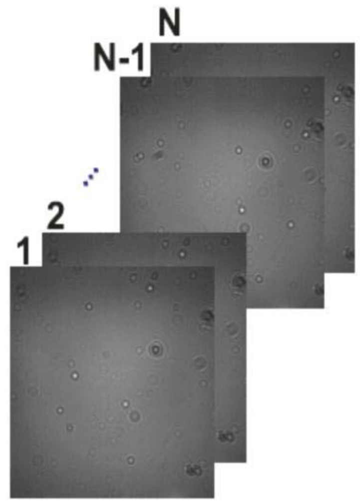

- high-numerical aperture
- high-phase difference
- high-phase gradient
- 2D / 3D technique
- lensless
- no reference
- partial coherent light

Transport of Intensity Equation (1)

Phase Retrieval

$$(\Delta + k^2)\,U(r) = 0$$

$$(\partial_x^2 + \partial_y^2 + \partial_z^2 + k^2)\,U(r) = 0$$

$$U(r) = U(r_\perp, z) = u(r_\perp, z)\,e^{jkz}$$

$$\partial_z^2 u(r_\perp, z) \approx 0$$

$$\nabla_\perp[I(r_\perp, z)\nabla_\perp \phi(r_\perp, z)] = \partial_z I(r_\perp, z)$$

$$\nabla_\perp I(r_\perp, z)\nabla_\perp \phi(r_\perp, z) + \Delta_\perp \phi(r_\perp, z) = \partial_z I(r_\perp, z)$$

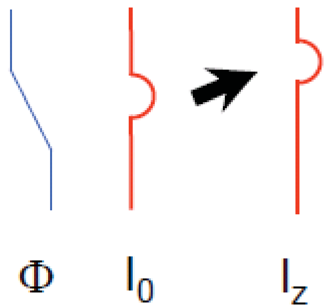

- Prism term -

- Hartman & variations
- lateral shearing
- deflectometry

- ombroscopie
- curvature sensor

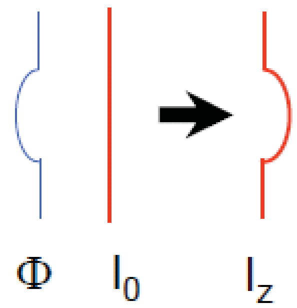

- Lens term -

bridge between
geometric and **interferometric sensing**

Transport of Intensity Equation (2)

Quantities that Affect the Accuracy of the TIE Solver

$\nabla_\perp I(r_\perp, z)$

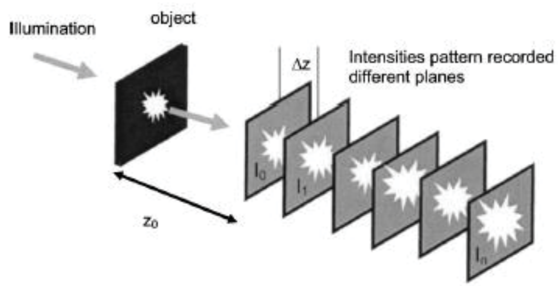

$\partial_z I(r_\perp, z)$

(from multiple planes)

- Nugent, K. A., et al. (2001). A Phase Odyssey. Physics Today, 54(8), 27.
- Huang, et.al. (2012). *Journal of Modern Optics*, *59*(1), 35-41.
- Waller, L., Tian, L., & Barbastathis, G. (2010). Optics express, 18(12), 12552–61.

Transport of Intensity Equation (3)

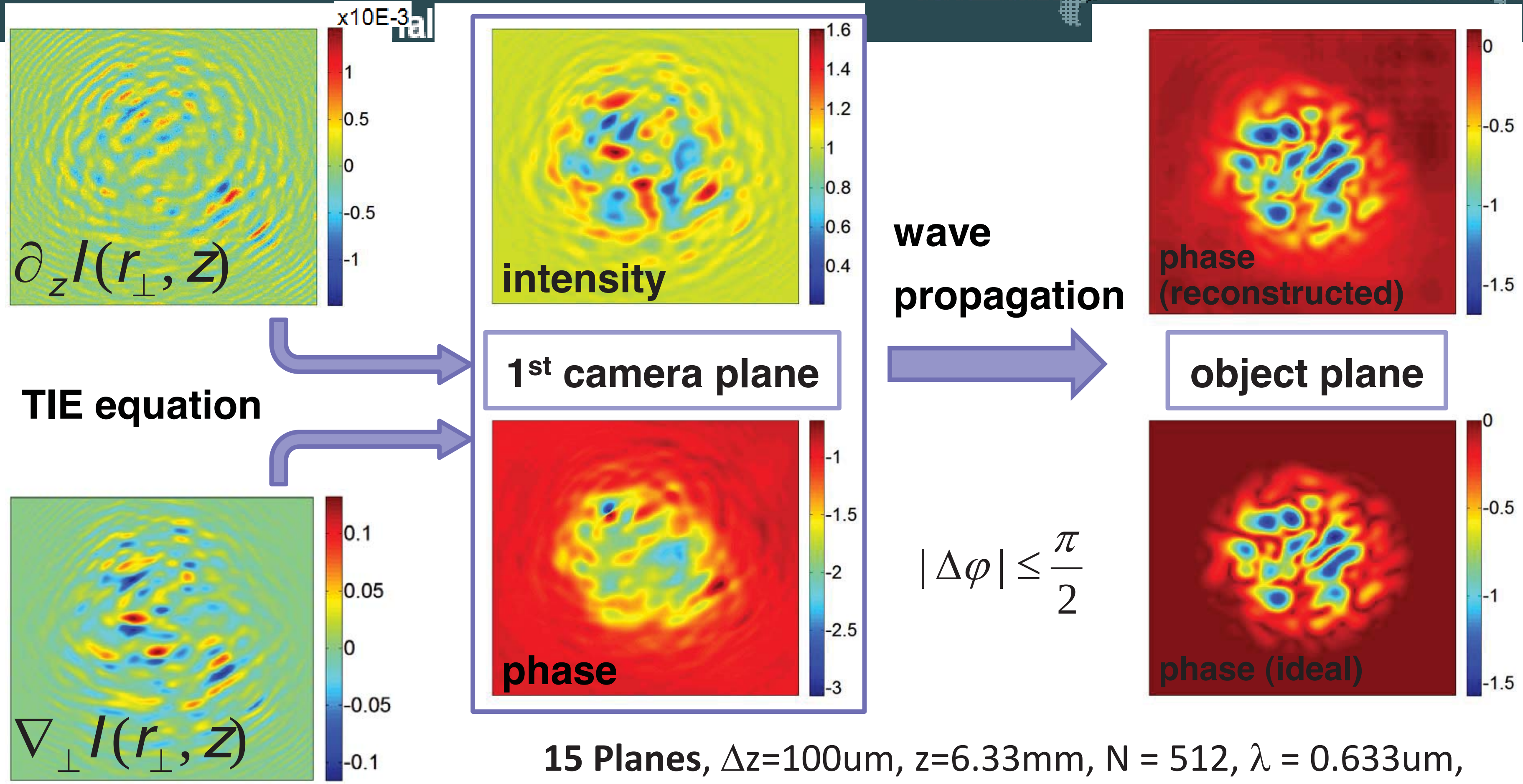

15 Planes, Δz=100um, z=6.33mm, N = 512, λ = 0.633um,
Δx = 3.45um, SNR = 25dB (=256:15), **Dirichlet BC**

Transport of Intensity Equation

Phase Retrieval

1.) Numerical methods (PDA solvers)

$$\nabla_\perp \left(I(r_\perp, z) \nabla_\perp \phi(r_\perp, z) \right) = \partial_z I(r_\perp, z)$$

(Multi-grid, Poisson Solver, etc)
→ Dirichlet, Neumann, or Periodic BC.

$$\nabla_\perp I(r_\perp, z) \nabla_\perp \phi(r_\perp, z) + \Delta_\perp \phi(r_\perp, z) = \partial_z I(r_\perp, z)$$

2.) Fourier Transform methods

$$\nabla_\perp^2 \psi(r_\perp, z) = F^{-1}\{(q_x^2 + q_y^2)\, F\{k \partial_z I(r_\perp, z)\}\}$$

approximate solution → (Green Function Approach or FT)

$$I(r_\perp, z) \nabla_\perp \phi(r_\perp, z) = \nabla_\perp \psi(r_\perp, z) + [\nabla \times A(r_\perp, z)]$$

$$\phi(r_\perp, z) = -F^{-1}\{(q_x^2 + q_y^2)\, F\{\nabla_\perp [\frac{\nabla_\perp \psi(r_\perp, z)}{I(r_\perp, z)}]\}\}$$

→ division by small intensity values, ill-conditioned Regularization techniques may be needed
→ Implicit Periodic boundary conditions, inaccurate at the edges

3.) Wave propagation (iterative)

(robust against noise, higher sampling, computational expensive)
→ No boundary conditions assumed

$$u(r_\perp, \Delta z) = u(r_\perp, z=0)\; e^{j \frac{\Delta z}{2k} \nabla_\perp^2}$$

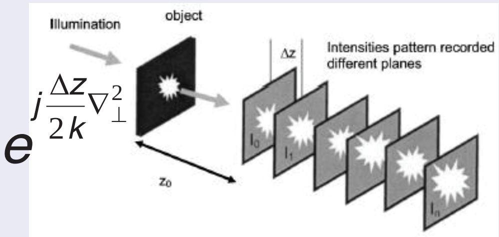

Transport of Intensity Equation

Properties of TIE solver:

- TIE Solver very sensitive to errors in the axial derivative
  - ➔ Higher order derivatives TIE
  - ➔ Robustness against noise
  - ➔ Non-equally spaced planes

- TIE applicable only for rather low spatial frequencies
  - ➔ Slowly varying object, small phase difference
  - ➔ Small intensity values problematic
  - ➔ not applicable: stronger phase objects, high spatial frequencies, non-paraxial case

other phase retrieval technique

Single-Beam Multiple-Intensity Reconstruction (SBMIR)

Wave propagation Methods (iterative)

$$(\Delta + k^2)U(r) = 0$$

$$(\partial_x^2 + \partial_y^2 + \partial_z^2 + k^2)U(r) = 0$$

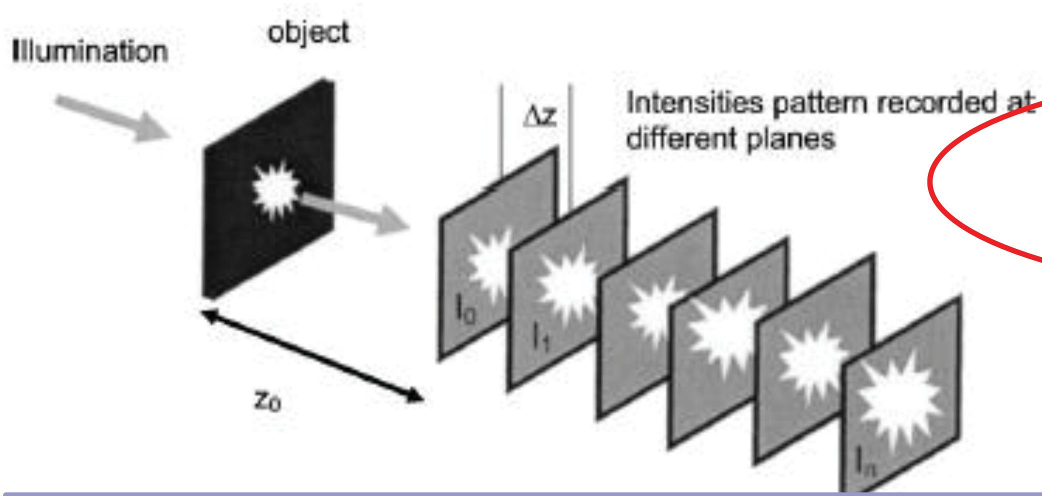

Angular Spectrum Method
➔ exact, high NA, iterative

- high-numerical aperture
- high-phase difference
- high-phase gradient
- lensless
- no reference
- partial coherent light

Eliminates effectively high frequency error components

- Giancarlo **Pedrini**, Wolfgang **Osten**, and Yan Zhang, "Wave-front reconstruction from a sequence of interferograms recorded at different planes," Opt. Lett. 30, 833-835 (2005)

Single-Beam Multiple-Intensity Reconstruction (SBMIR)

Wave propagation Methods (iterative)

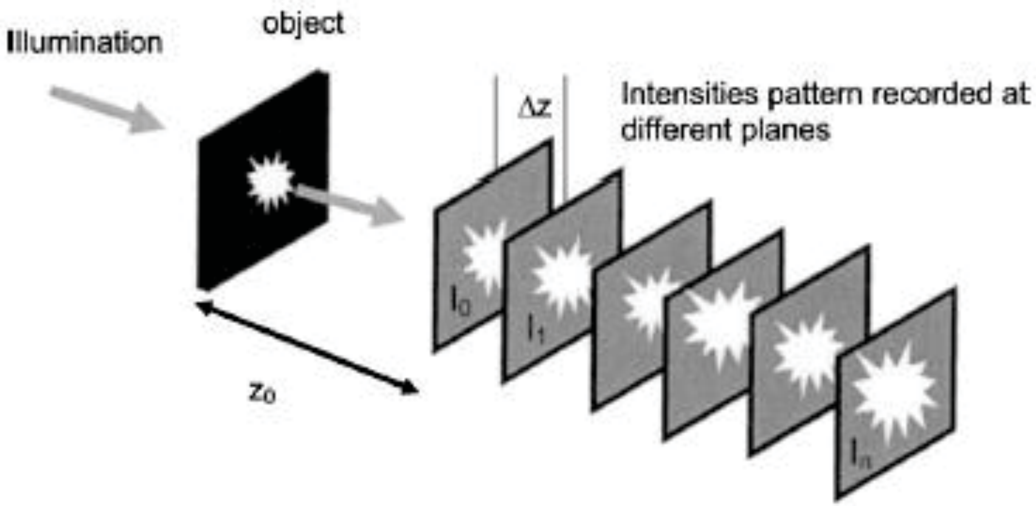

- high-numerical aperture
- high-phase difference
- high-phase gradient
- lensless
- no reference
- partial coherent light

Relaxation Parameter, feed information slowly

$$U_{n+1} = (1-\beta) L^{+}\{U_n\} + \beta A_{n+1} \exp[i\angle L^{+}(U_n)]\}$$

$$U_n = (1-\beta) L^{-}\{U_{n+1}\} + \beta A_n \exp[i\angle L^{-}(U_{n+1})]\}$$

β = 1, conventional approach

overestimate solution present at a given iteration step

Summary

- Main phase retrieval techniques based on fringe pattern analysis: spatial and temporal (interferometric/grid based methods)
- Recent development of single beam phase retrieval algorithms (refrieval from diffraction field)
- Image processing algorithms (DIC) support noncoherent methods of phase difference retrieval

Overview of Available Techniques

Centre for International Cooperation

	Digital Holography Interferometry	DIHM using a single Hologram	Iterative Phase Reconstruction Using Wave Propagation Methods	Transport of Intensity Equation	Inversion of the OTF (standard)	Inversion of the OTF (advanced)	Optical Diffraction Tomography	Inverse scattering problems
High NA, high $\Delta\varphi$	□		□/?			□		
High grad(φ)	□		□			□		
2D / 3D	2D	2D	2D	2D	2.X D	2.X D	3D	2.X D
No lenses/mirrors		□	□	□	□	□	n.a.	□
No reference arm		□	□	□	□	□	n.a.	□
Partial coherent light		□		□	□	□	n.a.	□
Theoretical Complexity	low	low	med.	low	Low	high	med.	high

References -1

Robinson D.W., Reid G.T (eds): *Interferogram Analysis: Digital Fringe Pattern Measurement Techniques*, Institute of Physics Publ., Bristol and Philadelphia, 1993.

Heijden F.: Image based measurement systems, J.Wiley & Sons

Osten W., Kujawińska M.: *Active phase measuring metrology* w Trends in Optical Nondestructive Testing, P.K.Rastogi, D.Inaudi (eds), Elsevier Science, 2000, 45-69., Chichester, 1994

Osten W.: *Digital processing and evaluation of fringe patterns*, w “Optical methods in experimental solid mechanics”, K-H.Laerman (ed), 289-422, Springer, Wien-New York, 2000

Malacara D., Servin M., Malacara Z.: Interferogram analysis for optical testing, Marcel Dekker Inc., New York, 1998

Dyson J.: *The rapid measurement of photographic records of interference fringes*, Appl. Opt., 1993, **2**, 487-489.

Jones R.A., Kadakia P.L.: *An automated interferogram analysis technique*, Applied Optics, 1998, **7,** 1477-1482.

Bruning J.H. et al.: *Digital wavefront measurement interferometer for testing optical surfaces and lenses*, Applied Optics, 13, 2693-2703, 1974

Schwider J.: *Automated evaluation techniques in interferometer* in Wolf E. (Ed), Progress in Optics, XXVIII, Amsterdam, Elsevier Science Publ., 1990

Freischlad K., Koliopoulos C.L.: *Fourier description of digital phase-measuring interferometer*, JOSA A, 7, 542-551, 1990

Creath K., Schmit J.*: N-point spatial phase measurement technique for nondestructive testing*, Opt. Lasers Eng., 24, 365-379, 1996

References - 2

Pirga M., Kujawińska M.: *Two-directional spatial-carrier phase shifting method for analysis of crossed and closed fringe pattren*, Opt. Eng., 34, 2459-2466, 1995

Massie N.A., Nelson R.D., Holly S.: *High performance real-time heterodyne interferometry,* Appl. Opt., 18, 1797-1803, 1979

Takeda M., Ina H., Kobayashi S.: *Fourier-transform method of fringe pattern analysis for computer based topography and interferometry*, J. Opt., Am., 72, 156-160, 1982

Bone D.J., Bachor R., Sandeman J.: *Fringe pattern analysis using a 2-D Fourier transform*, Appl. Opt., 23, 1760-1764, 1984

Kreis T.M., Jüptner W.P., Geldmacher J.: *Principles of digital holographic interferometry*, Proc. SPIE, 3478, 45-54, 1998

K. Patorski, Z. Sienicki, A. Styk „*The phase shifting method contrast calculations in time average interferometry: error analysis*", Optical Engineering 44 (6), 1- 14, 065601, published online June 7, 2005;

K. Patorski, A. Styk „*Interferogram intensity modulation calculations using temporal phase shifting: error analysis*", Optical Engineering 45 (8), 085602,1-16, published online August 2, 2006;

Osten W., Nadeborn W., Andra P.*: General hierarchical approach in absolute phase measurement*, Proc. SPIE, v. 2860, 2-13, 1996

Huntley J.M.: *New methods for unwrapping noisy phase maps*, Proc. SPIE, 2340, 110-123, 1994

Takeda M.: *Recent progress in phase-unwrapping techniques*, Proc. SPIE, 2782, 334-343, 1996

Kujawińska M., Pawłowski M.: *Spatio-temporal approach to shape and motion measurements of 3D objects*, Proc. SPIE, 4101, 21-28, 2000